TABLE OF CONTENTS

Page

LIST OF TABLES

Page

LIST OF FIGURES

Page

LIST OF ABREVIATIONS, INITIALS AND ACRONYMS

AFM	Ambiguity Function Method
AFSCN	Air Force Satellite Control Network
C-LAMBDA	Constrained Least-Square AMBiguity Decorrelation Adjustment
BPSK	Binary Phase Shift Keying
CDMA	Code Division Multiple Access
CS	Control Segment
DD	Double Difference
DGPS	Differential GPS
DOP	Dilution Of Precision
E	East
ECEF	Earth Centered Earth Fixed
EKF	Extended Kalman Filter
FARA	Fast Ambiguity Resolution Approach
FASF	Fast Ambiguity Search Filter
FDMA	Frequency Division Multiple Access
FIR	Finite Impulse Response
FOAM	Fast Optimal Attitude Matrix
FOC	Full-Operational-Capability
FRQNT	Fonds de Recherche du Québec – Nature et Technologies
FT	Fourier Transform
GDOP	Geometry Dilution Of Precision
GLONASS	GLObal NAvigation Satellite System
GLONASST	GLONASS Time
GNSS	Global Navigation Satellite System
GPS	Global Positioning System
GPST	GPS Time
HDOP	Horizontal Dilution Of Precision
IERS	International Earth Rotation and reference systems Service

IID	Identically Independently Distributed
ILS	Integer Least-Squares
IMU	Inertial Measurement Unit
INS	Inertial Navigation System
LAMBDA	Least-squares AMBiguity Decorrelation Adjustment
LOS	Line Of Sight
LSAST	Least-Squares Ambiguity Search Technique
MILS	Mixed Integer Least -Squares
N	North
NGA	National Geospatial-intelligence Agency
OTF	On The Fly
PCV	Phase Center Variation
PDOP	Position Dilution Of Precision
PNT	Positioning, Navigation, and Timing
PZ90	Parametry Zemli 1990
OUEST	QUaternion ESTimator
RINEX	Receiver INdependent EXchange format
RLS	Recursive Least-Squares
RMSE	Root Mean Square Error
SBAS	Satellite Based Augmentation System
SD	Single Difference
SNR	Signal to Noise Ratio
SPP	Single Point Positioning
SS	Space Segment
SVD	Singular Value Decomposition
TD	Triple Difference
US	User Segment
USAF	United State Air Force
USG	United State Government
USNO	United States Naval Observatory

UTC	Universal Time Coordinated
UTC-SU	Universal Time Coordinated, Soviet Union standard
WGS84	World Geodetic System 84
WT	Wavelet Transformation

CHAPTER 1

INTRODUCTION

A simple definition of navigation can be described as the best possible estimate of the position, velocity, and attitude of a moving object. Historically, navigation has been associated with guiding ships through the desired route using compass. However, nowadays navigation is an extensive field which can be found everywhere from cell phones and wristwatches to aviation, mapping, surveying and search and rescue. The most effective way to achieve a robust and consistent navigation system is through the technology of the Global Positioning System (GPS). The GPS offers an accurate, free, continues, weather-proof, and globally available satellite-based navigation services, which makes it a seamless tool to satisfy many of needs for navigation purposes. The accurate determination of position, velocity, acceleration, and time, in both relative and absolute sense, construct the main applications of this technology.

Among recent applications of such a system is to determine the orientation of the object's body frame with respect to a known reference frame. This is called attitude determination. By using high-cost receivers and antennas, as well as high-frequency signal transmission rates (e.g., P-code), this technology provides highly precise measurements, and has been used in high sensitivity applications such as military applications. Nevertheless, these systems are commonly expensive and large in size and the use of such systems may be restricted by governments. For example, the P-code is only available for the USA armed forces.

The overall objective of this thesis is to provide an inexpensive and light-weight alternative to conventional attitude determination systems using the GPS technology. In particular, we are interested in low-cost and light-weight receivers and antennas in a compact configuration with civil frequency ranges (i.e. L1 frequency).

This work tries to answer the following questions: What are the limitations of such a system? How much precision can be obtained? Is it possible to replace those expensive and heavy systems with such a low-cost and light-weight system? Such an attitude determination system is an opening window to a wide range of applications from smartphones in civil applications to military purposes and precise applications.

Our industrial partner Numerica.Inc searches for a low-cost and light weight system to measure the position of an object[1]. This object is located within about 1 km distance from the observer and it needs to be located within an error of 1m. Such a system needs two measuring systems, one of them is to measure the distance between the object and the observer, and the other one to measure the 3-D attitude of the observer pointing system aiming the object. The focus of this work is to determine the attitude of the observer pointing system with precision of about 0.05° for the yaw, pitch, and roll angles so the object can be located within 1m error, Figure 1.1.

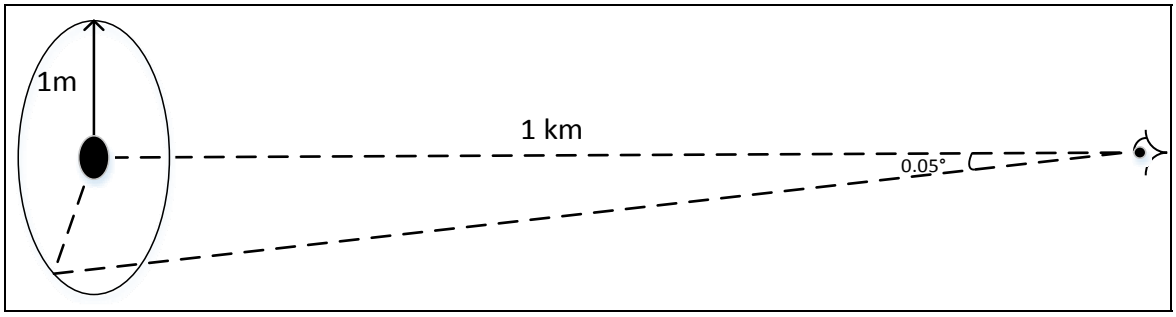

Figure 1.1 Geometry of the defined project

This thesis has the following structure. This chapter present an overview of the research problem, objectives and methodology. Chapter 2 presents an overview of GPS constellation and signals, GPS segments and its data characteristics. This chapter also outlines the

[1] This project is funded by Fonds de Recherche du Québec – Nature et Technologies (FRQNT) and our industrial partner Numerica.Inc.

mathematical modelling of GPS measurements and their associated errors as well as error cancelling techniques.
Chapter 3 provides a detailed literature review on the most challenging problems of the project, namely ambiguity resolution and attitude determination methods. Chapter 4 is dedicated to the proposed methodology for the Attitude Determination System (ADS), its mathematical procedure and algorithm. The details of the proposed ADS developments are explained extensively in this chapter.

Chapter 5 is dedicated to result presentation, comparison and discussion. In order to analyse the performance of the ADS, we designed different test cases with different configurations, receivers, antennas and record locations. Some concluding remarks as well as some future works to improve the proposed ADS are presented in chapter 6.

1.1 Research problems

The research problems of this project can be expressed as follows:

1. GPS has two main types of observables: pseudorange measurements which are the range between the receiver and the satellite, and carrier phase measurements which are measured as the phase difference of received signal and the replica in the receiver. In order to obtain a precise solution for attitude determination, using phase measurement that is about 100 times more precise than the code measurement is necessary. The main problem of using this measurement is its ambiguity resolution that needs to be solved and fixed. Ambiguity resolution will be explained in details in the next chapter;

2. A computational time reduction strategy needs to be applied in order to be able to use the designed ADS system real time;

3. To increase accuracy and availability of GNSS satellites, it is advantageous to incorporate other GNSS signals into the ADS algorithm. This needs to overcome the difference between GNSS constellation which needs to be studied.

In this research, the main research problematic is consist of solving ambiguity parameters of several low-cost GPS receivers which are synchronized together and to develop an attitude determination algorithm in order to compute the 3-D attitude angles precisely. The raw measurements are limited to GPS L1 and can be affected by noises as well as errors namely multipath error. Those effects will need to be processed according to the state-of-the-art processing techniques.

1.2 Research objectives

The main objective of this thesis is to determine the 3D attitude angles of a moving platform using four low-cost GPS receivers attached to the platform with an attitude resolution better than 50m degrees. This resolution is necessary to secure the localization of an object at 1km within an error of 1 meter. In accordance with and to fulfill the main objective of this research, there are 4 defined specific objectives. The first one is to fix the ambiguity parameters as an integer. The second one is to synchronize several receivers by hardware or software algorithm. The third one is to investigate the processing load of the designed system in order to use the developed attitude determination system in real-time applications. The last objective is to investigate theoretically how to incorporate measurements of the Global Navigation Satellite System (GLONASS) of the Russian federation into the system.

1.3 Research methodology

In order to fulfil the research objectives, we conduct our work in four algorithm modules which are:

1. **Data selection:** An algorithm is designed to filter the data based on satellites elevation angle and Carrier to Noise ratio (C/N_0). This algorithm has the capability

of compromising between number of satellites and duration of satellite visibility depends on the user's choice in order to get a proper period of data for analysis;

2. **Single point positioning:** We calculate the master antenna position with Single Point Positioning (SPP) algorithm. This algorithm uses only pseudorange measurements in order to have an approximate position of the master antenna. In this module, we also calculate satellite positions as well as calculating receiver and satellite's clock errors;

3. **Baseline estimation:** In order to estimate the baseline vectors, a Recursive Least-Squares (RLS) method is designed and developed by combining both code and carrier measurements. By taking advantage of the structure of the problem, we try to decrease the computational cost of the algorithm as well as preserving the accuracy. All the three aspects of computer implementation, namely numerical reliability, computational, and storage efficiency have been considered in this method. We also use the configuration information, baseline length, and fix the ambiguity with Least-squares AMBiguity Decorrelation Adjustment (LAMBDA) method;

4. **Attitude determination:** In this module we developed Singular Value Decomposition (SVD) method which is an estimator for Wahba's loss function. This algorithm does not need a-priori information for dynamic applications.

Along with the mentioned methodology for the designed algorithm, the research methodology is as follows:

1. Development a complete attitude determination system consisting 4 main mentioned modules of the algorithm in Matlab. The inputs are GPS L1 raw measurements and the outputs are the 3-D attitude angles;

2. Test the complete designed system using simulated data (in Matlab and with GPS simulator). This step is designed to validate the developed algorithms;

3. Build a platform and mounting four low-cost receivers and antennas to acquire sufficient GPS raw measurements. In order to compare the results, two pairs of low-cost receivers and high-cost antennas are mounted on the platform as well;

4. Analyze the performance of the ADS algorithm using real GPS L1 measurements for all the test cases.

Furthermore, a detailed theoretical research is done to incorporate GLONASS measurements into this system in order to achieve much precise and reliable system even without a suitable visibility for GPS constellation.

1.4 Contributions

The contributions of this research can be summarized as follows:

1. Designing an ADS algorithm and system combining four main modules:

   - to read, to filter and to synchronize the incoming raw measurements from 4 GPS L1 receivers. The input of this module is raw measurements from 4 GPS L1 receivers and the outputs are four set of filtered data based on the chosen criteria by the user, which are synchronized together in ms precision. The user can choose the analysis duration, the minimum used satellites, minimum C/N_0 and the mask angle;

   - to estimate the position of GPS satellites using the SPP algorithm proposed by (Borre, 2003) and to compute the best geolocation position of the master antenna. The input of this module is the filtered data from previous step and the output is satellite positions and master antenna position;

- to compute precise baseline vectors by the RLS algorithm. By having the master antenna position and satellite position, now we can compute the baseline vectors;

- to compute precise Euler angles using the SVD method. The input of this module is 3 baseline vectors and the output is 3-D attitude angles.

2. Combining the RLS algorithm with the LAMBDA method according to (Joosten, 2001) in order to fix the float solution. Constrain the solution by using the prior configuration information. In this work we used baseline length to constrain the baseline estimation solution.

This research allows the publication of the following conference paper:

Oliazadeh, Nasim; Landry, Rene Jr; Yeste-Ojeda, Omar A; Gagnon, Eric and Wong, Franklin 2015. «GPS-based attitude determination using RLS and LAMBDA methods». In *Localization and GNSS (ICL-GNSS), 2015 International Conference on*. p. 1-7. IEEE. doi: 10.1109/ICL-GNSS.2015.7217146.

CHAPTER 2

GPS OVERVIEW

In this chapter, we present an overview of GPS and navigation principals in order to give the reader a better understanding of the rest of thesis.

In the first section, we present a brief review on GPS constellation and segments. Then a comprehensive introduction on GPS measurements, common techniques and errors will be presented. Afterwards, we go through the most commonly used navigation frames and transformation matrices followed by a discussion about the satellite geometry in space and its impact on the solution accuracy.

2.1 GPS segments

Navstar Global Positioning System known as GPS, owned by the United States Government (USG) and operated by the United States Air Force (USAF), is the earliest and the most accurate space-based radio-navigation system of the world. This project, which has been started in 1973 and completed in 1994, provides accurate Positioning, Navigation, and Timing (PNT) 24 hours a day, in all weather and all over the world. GPS consists of three main segments: Space, Control and User segments.

The Space Segment:

The Space Segment (SS) consists of six orbital planes at an altitude of about 20,200 km above the earth's surface at an inclination angle of 55° with respect to the equatorial plane. Each orbit has four equally-spaced slots for satellites, which is covered by at least one operational satellite all the time. For global coverage, USAF ensures availability of at least 24 satellites for 95% of the time. With this arrangement we always have at least 4 visible satellites, which is the minimum required number of satellites to calculate 3D position and time. GPS satellites carry atomic clocks with nanosecond accuracy and broadcast continues

radio frequency signals on the two carrier frequencies of L1 (1575.42 MHz) and L2 (1227.6 MHz).

The Control Segment:

The Control Segment (CS) is a ground-based global network to track and monitor GPS satellites consisting two master control stations, 16 monitoring stations including six from the Air Force and 10 from the National Geospatial-Intelligence Agency (NGA), 4 ground antennas and 8 Air Force Satellite Control Network (AFSCN).

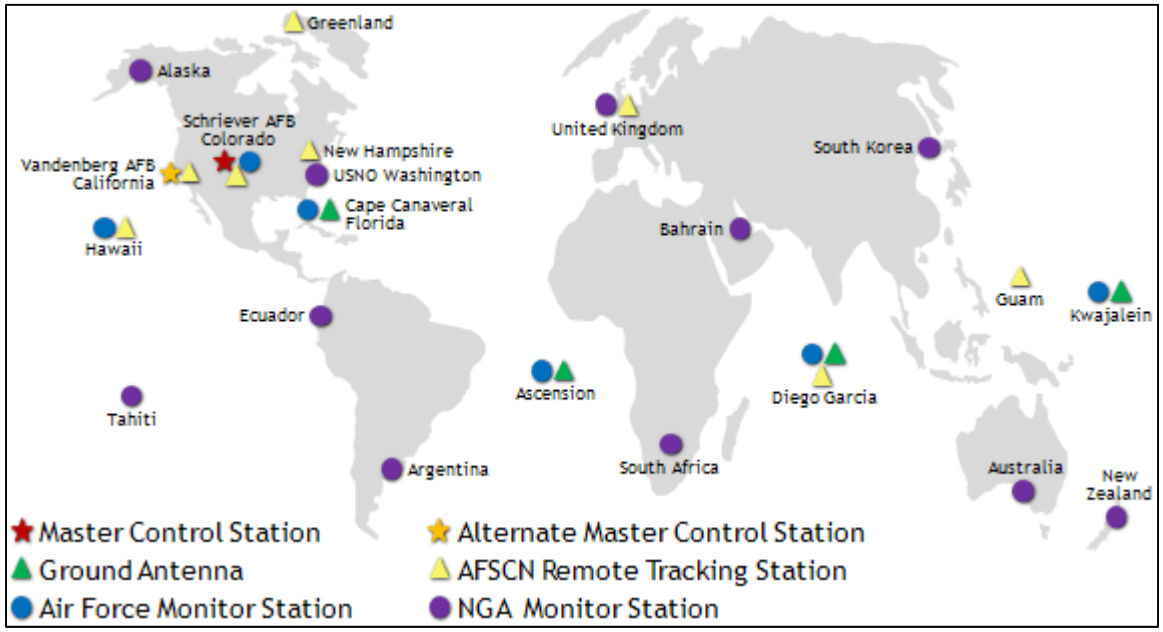

Figure 2.1 Control segment
Taken from Force (2015)

The monitoring stations collect data from each visible satellite and send them to the master control stations. The master control stations are responsible for computing extremely precise satellite orbits and send them, as an updated navigation massages, to the ground antennas. Then the ground antennas send updated navigation massage to each visible satellite. Finally in order to increase tracking robustness, the control segment is tracked by eight AFSCN remote tracking stations.

The User Segment:

User Segment (US) consists of all GPS receivers which receive and process GPS signals in order to calculate position and time.

2.2 GPS signal and data characteristics

The GPS signals are transmitted on two radio frequencies, L1 and L2 in L band. L1 and L2 are both derived from a common frequency called f_0:

$$f_0 = 10.23\ MHz \tag{2.1}$$

$$f_{L1} = 150\ f_0 = 1575.42\ \text{MHz} \tag{2.2}$$

$$f_{L2} = 120\ f_0 = 1227.60\ \text{MHz} \tag{2.3}$$

Each of these signals is consist of three parts:

- **carrier:** The carrier wave with f_{L1} and f_{L2} frequency;

- **navigation message:** This message is about satellite orbits and clock errors, which are uploaded from the ground base control segment with 50 bps rate;

- **spreading sequence:** Each satellite has two unique spreading sequences. The first one is Coarse Acquisition (C/A) code with 1.023 MHz frequency, and encrypted Precision (P(Y)) code with 10.23 MHz frequency. The C/A code is only modulated on L1 frequency while P(Y) is modulated on both L1 and L2.

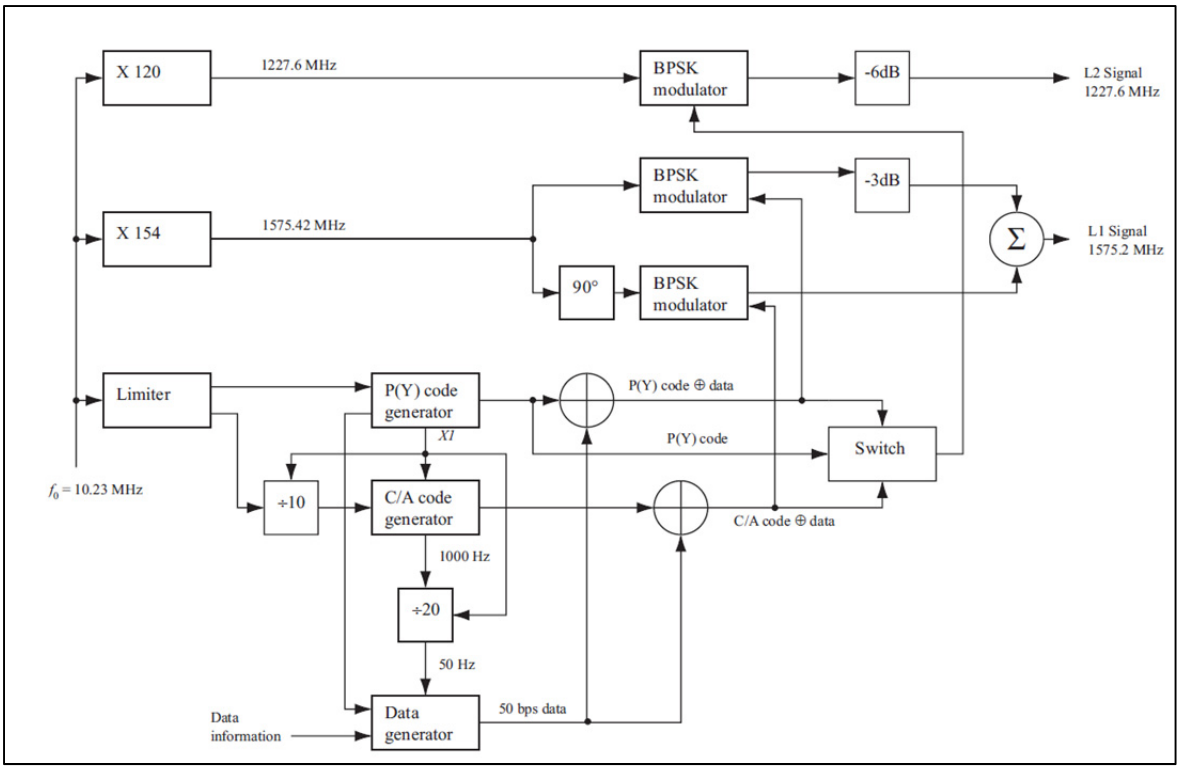

Figure 2.2 GPS signals generation
Adapted from Benedetto et al. (2013)

Figure 2.2 is a detailed description of signal generation. At the left the main clock is supplied to three blocks which generate f_{L1}, f_{L2} and to the limiter to stabilize the clock signal. At the very bottom, the data generator generates the navigation data that is synchronized with code generators by X1 supplied by P(Y) generator. Afterwards, the generated codes through an exclusive OR operation, are combined with the navigation data. The resulted signals are modulated onto the carrier signal by Binary Phase Shift Keying (BPSK) method and with 90° shift between two codes. As summary, the transmitted signal from satellite k can be described as follows:

$$s^k(t) = \sqrt{2P_C}\Big(C^k(t)\oplus D^k(t)\Big)\cos(2\pi f_{L1}t) + \sqrt{2P_{P_{L1}}}\Big(P^k(t)\oplus D^k(t)\Big)\sin(2\pi f_{L1}t) \quad (2.4)$$

$$+\sqrt{2P_{P_{L2}}}\left(P^k(t)\oplus D^k(t)\right)\sin(2\pi f_{L2}t)$$

where P_C, $P_{P_{L1}}$, and $P_{P_{L2}}$ are the powers of the signals, $C^k(t)$ is the C/A code of satellite k, and $D^k(t)$ is the navigation message.

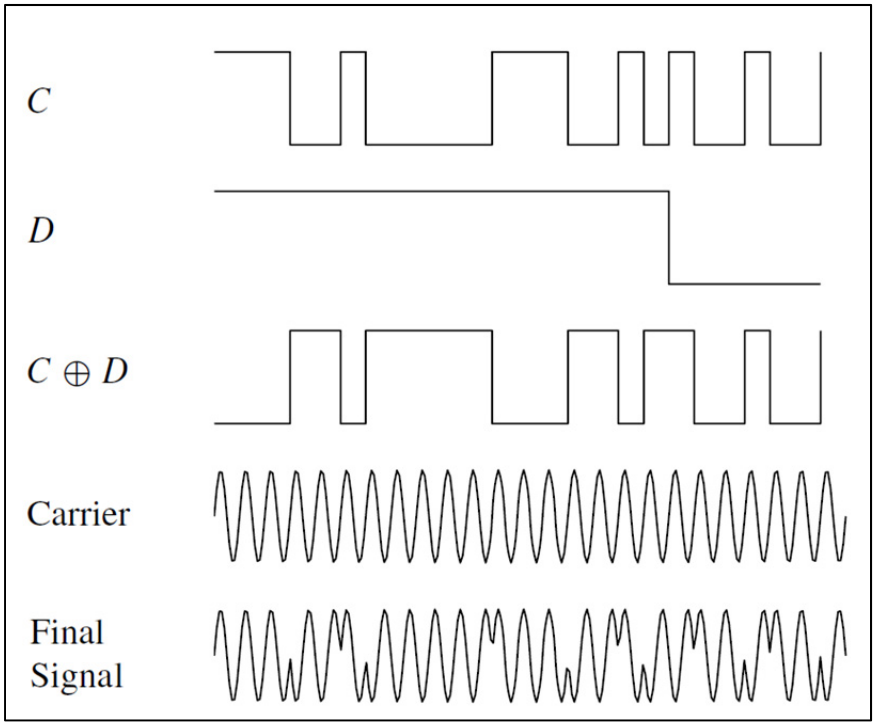

Figure 2.3 BPSK modulation with C/A code and navigation message
Adapted from Benedetto et al. (2013)

Figure 2.3 shows the final signal modulation with BPSK after C/A code and navigation addition. Phase is shifted by 180° when the chip changes.

2.2.1 Navigation data structure

Navigation data with 50 bps rate is a 1500 bit-long frame which is consists of 5 subframes and each 300 bits long. Each subframe contains 10 words and each of them has 30 bits length. By 50 bps rate, a transmitted subframe lasts 6 s, one frame lasts 30 s and one entire navigation massage lasts for 12.5 minutes, Figure 2.4.

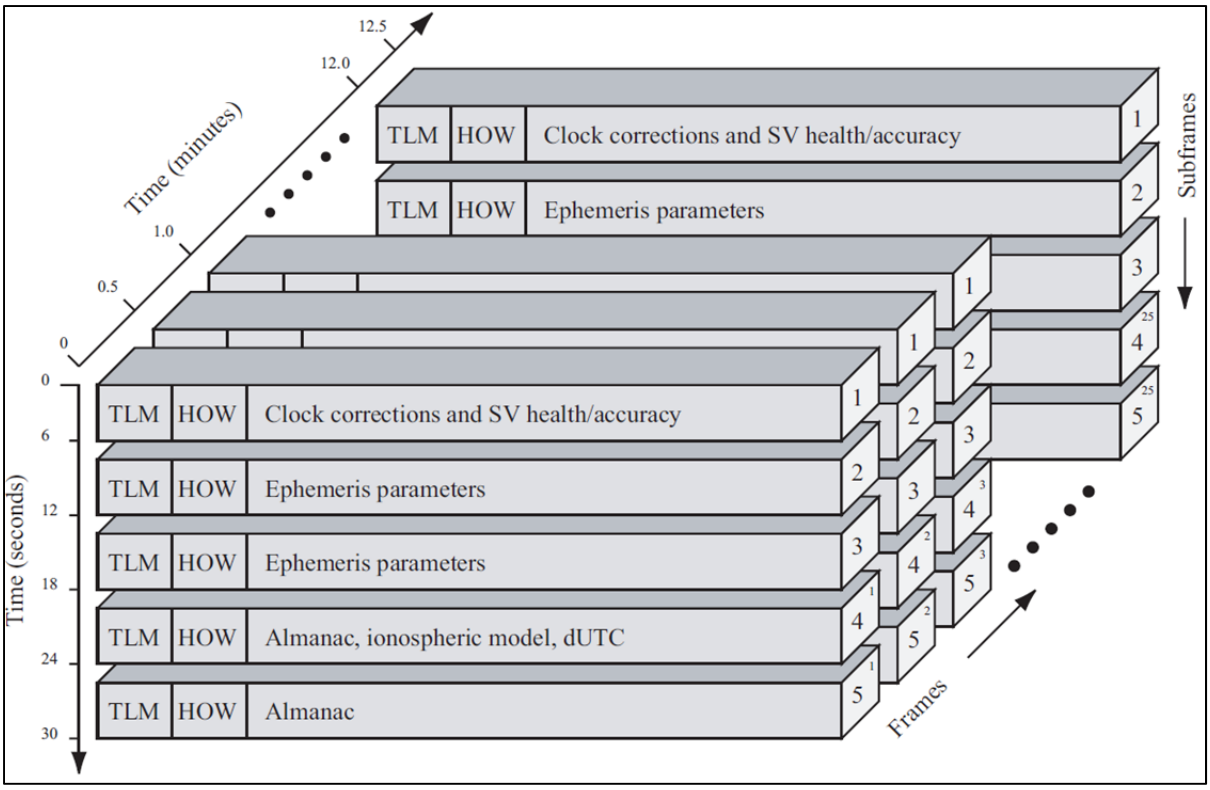

Figure 2.4 GPS navigation data structure
Adapted from Benedetto et al. (2013)

Each subframe contains 10 words which always starts with two words, the *telemetry* and *handover word* followed by 5 subframes as follows:

- **telemetry (**TML) is the first word that is repeated every 6 s. TML contains 8-bit preamble and 16 reserved bit and parity which are used for frame synchronization;

- **handover** (HOW) contains of 17-bit of time of week and antispoofing flag followed by the subframe ID;

- **satellite clock and health** is used to calculate navigation message transmission time and satellite information is used to inform whether the data can be trusted or not;

- **satellite ephemeris data** subframe is used for satellite position calculation;

- **support data** subframe is contained almanac, ionospheric model, UTC parameters, etc. The almanac data is the ephemeris data with reduced precision. Each satellite send almanac data for all GPS satellites while each satellite only transmits ephemeris data for itself.

2.3 Mathematical modelling of GPS measurements and errors

This section presents the GPS measurements and their mathematical modelling briefly. Then three kinds of differential techniques and their equations will be presented. In the last section, the most common errors in these measurements will be discussed.

2.3.1 GPS measurement and associated errors

Most of the GPS receivers provide three types of measurements: Pseudorange, Carrier phase, and Doppler. These measurements can be used either directly or using differential techniques to calculate Position, Navigation and Timing (PNT) parameters, (Scaccia, 2011).

2.3.1.1 Code measurement and associated errors

The earliest and the easiest GPS positioning method is based on the code measurement. Receiver counts the amount of chips of the received C/A code and the one which is generated by its oscillator. Then it can calculate time difference of the corresponding GPS satellite and itself. By multiplying the radio signal's speed in vacuum, the distance between the receiver and the GPS satellite (pseudorange) can be computed. Each satellite transmits its Keplerian elements in the World Geodetic System established in 1984 (WGS-84) reference system to calculate its position in the orbit. So we have a sphere with the center of satellite and the radius of pseudorange. Therefore by using a least-squares method or Kalman filter, with at least four satellites a 3D position and the receiver clock error can be computed, (Delaporte, 2009; Lu, 1995; Scaccia, 2011).

The code measurement modelling can be written as follows:

$$\rho_i^j = r_i^j - c\,t^j + c\,t_i + I_i^j + T_i^j + \varepsilon_\rho \quad (2.5)$$

where r is geometric range between receiver position and satellite position (m), ρ is the measured range (m), j is the j^{th} satellite, i is the i^{th} receiver, c is the speed of light $(^m/_s)$, t is the clock error (s), I is the ionospheric error (m), T is the tropospheric error (m), and ε_ρ is the code measurement noise and other errors (m).

2.3.1.2 Carrier phase measurement

The GPS satellites have two constant carrier frequencies which are centered at 1575.42 and 1227.60 MHz. In order to track satellite signals, a receiver first establishes a carrier and code phase lock so that it can measure the range difference over time. Then not only the receiver can measure difference between the received phase signal and the generated one, but also it can measure the phase difference over time as long as it does not lose the lock. By this way, the receiver can track the range changing with respect to the satellite, however, it contains environmental errors. As a result, the true range between the receiver and the satellite must be estimated or inferred. Since this method use pure carrier frequency, and all cycles are the same, there is no way for receiver to distinguish one cycle to another and in order to count the number of travelled signal cycles. This ambiguous number is known as integer ambiguity, which is needed to be solved in a quick and reliable method for each epoch.
Carrier phase measurement can be modelled as:

$$\lambda\,\phi_i^j = r_i^j - c\,t^j + c\,t_i + \lambda\,N_i^j - I_i^j + T_i^j + \varepsilon_\phi \quad (2.6)$$

where ϕ is the measured phase $(cycle)$, j is the j^{th} satellite, i is the i^{th} receiver, c is the speed of light $(^m/_s)$, t is the clock error (s), λ is GPS signal wavelength (m), N is the integer ambiguity (cycle), I is ionospheric error (m), T is Tropospheric error (m), and ε_ϕ is the carrier phase measurement noise and other noises (m).

2.3.1.3 Doppler

The phase rate or the Doppler frequency is another GPS observable, which is the time derivative of phase and measures the relative motion between the receiver and the satellite. This is based on the frequency shift of the electromagnetic signals caused by relative motion, as the familiar acoustics version. The radial velocity of the satellite with respect to the receiver can be modelled as, (Xu, 2007):

$$V = \vec{V}.\vec{U}_\rho = |\vec{V}|\cos(\alpha) \tag{2.7}$$

where $\vec{V}$ is the velocity of the satellite related to the receiver, $\vec{U}_\rho$ is the unit vector in the direction from the receiver to the satellite, α is the projection angle of $\vec{V}$ to $\vec{U}_\rho$ and subscript ρ is the distance from the receiver to the satellite, Figure 2.5.

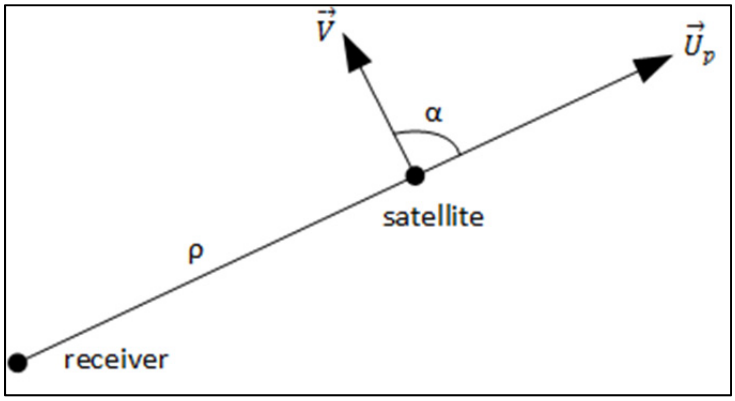

Figure 2.5 Doppler effect
Adapted from Xu (2007)

The frequency of the received signal is:

$$f_r = f\left(1 + \frac{V_p}{c}\right)^{-1} \simeq \left(1 - \frac{V_p}{c}\right) \tag{2.8}$$

where c is the speed of light. The Doppler frequency shift is:

$$D = \frac{d\phi}{dt} = f - f_r \simeq f\frac{V_p}{c} = \frac{V_p}{\lambda} \tag{2.9}$$

where f is the nominal frequency, ϕ is the phase of the received signal, and λ is the signal wavelength. This measurement can be used in the following model (Delaporte, 2009):

$$\dot{\varphi} = \dot{\rho}_i^j - c\,\dot{t}^j + c\,\dot{t}_i - \dot{I}_i^j + \dot{T}_i^j + \dot{\varepsilon}_\phi \tag{2.10}$$

where φ is the Doppler measurements ($^m/_s$), $\dot{\rho}_i^j$ is the relative velocity between satellite j and receiver i, $\dot{t}^j$ is the satellite clock drift, $\dot{t}_i$ is the receiver clock drift, $\dot{I}_i^j$ and $\dot{T}_i^j$ are the ionospheric and tropospheric drift respectively, and $\dot{\varepsilon}_\phi$ is the carrier phase noise drift ($^m/_s$).

2.3.2 Differential GPS

One of the most effective ways to remove or reduce common errors in GPS measurements is to use Differential GPS (DGPS) method. By differencing two GPS measurements with respect to a common error source, the common error sources can be removed without extra computation.

For both code and carrier phase measurements, there are three types of DGPS methodologies: single, double and triple.

2.3.2.1 Single difference

Single Difference (SD) involves two receivers which are usually called Station (reference) and Rover (slave) receivers. This naming does not necessarily mean that one of them is moving and the other one is static, but it only means that the relative position with respect to the reference one is interested, (Zheng, 2010).

This method takes one common visible satellite measurement from two receivers at the same epoch. In order to eliminate common errors such as satellite clock errors and orbital errors, measurements can be modelled as a differential method known as single difference.
Single difference of the code measurement can be modelled as:

$$\begin{aligned} \Delta\rho_{r,s}^{j} &= \rho_r^j - \rho_s^j \\ &= r_r^j - r_s^j + c\,(t_r - t_s) + I_r^j - I_s^j + T_r^j - T_s^j + \varepsilon_{r,\rho}^j - \varepsilon_{s,\rho}^i \\ &= \Delta r_{r,s}^j + c\,(t_r - t_s) + \Delta I_{r,s}^j + \Delta T_{r,s}^j + \Delta\varepsilon_{rs,\rho}^j \end{aligned} \tag{2.11}$$

By neglecting the ionospheric and tropospheric errors in ultra-short baseline applications, which is our application, the simplified model can be written as:

$$\Delta\rho_{r,s}^{j} \simeq \Delta r_{r,s}^j + c\,(t_r - t_s) + \Delta\varepsilon_{rs,\rho}^j \tag{2.12}$$

and the carrier phase single difference can be written as:

$$\begin{aligned} \lambda\Delta\phi_{r,s}^{j} &= \phi_r^j - \phi_s^j \\ &= r_r^j - r_s^j + c\,(t_r - t_s) + \lambda\left(N_r^j - N_s^j\right) - I_r^j + I_s^j + T_r^j - T_s^j + \varepsilon_{r,\phi}^j - \varepsilon_{s,\phi}^i \\ &= \Delta r_{r,s}^j + c\,(t_r - t_s) + \lambda\Delta N_{r,s}^j + \Delta I_{s,r}^j + \Delta T_{r,s}^j + \Delta\varepsilon_{rs,\phi}^j \end{aligned} \tag{2.13}$$

$$\lambda\Delta\phi_{r,s}^{j} \simeq \Delta r_{r,s}^j + c\,(t_r - t_s) + \lambda\Delta N_{r,s}^j + \Delta\varepsilon_{rs,\phi}^j \tag{2.14}$$

where the term Δ represents differential parameter between the stationary and the rover receiver.

Even though ionospheric, tropospheric, and, satellite clock error will be eliminated or greatly reduced in SD method, receiver clock error is one of the main error that is still remaining in this method. Double difference can eliminate this error.

2.3.2.2 Double difference

The standard Double Difference (DD) involves two receivers and two satellites. This will be done by taking two receivers measurements with respect to a common satellite and repeating this procedure for another common satellite. By taking a difference between the results, common errors between receivers can also be eliminated or greatly reduced. In other words, this method is a second difference of the SD method with respect to two satellites which eliminates the common errors between two receivers namely the receiver clock error.
The mathematical model of DD pseudorange can be written as:

$$\begin{aligned}\nabla\Delta\rho_{r,s}^{j,i} = {} & \Delta r_{r,s}^{j} - \Delta r_{r,s}^{i} + \Delta I_{r,s}^{j} - \Delta I_{r,s}^{i} + \Delta T_{r,s}^{j} - \Delta T_{r,s}^{i} + \Delta\varepsilon_{rs,\rho}^{j} - \Delta\varepsilon_{rs,\rho}^{i} \\ = {} & \nabla\Delta r_{r,s}^{j,i} + \nabla\Delta I_{r,s}^{j,i} + \nabla\Delta T_{r,s}^{j,i} + \nabla\Delta\varepsilon_{rs,\rho}^{j,i}\end{aligned} \tag{2.15}$$

Where Δ is the single difference and the ∇ is the double difference operator.

In the case of short baseline applications such as attitude determination applications, the differential ionospheric and tropospheric errors are negligible. This assumption is based on having approximately the same atmospheric conditions over a short distance.
The final equation is then:

$$\nabla\Delta\rho_{r,s}^{j,i} \simeq \nabla\Delta r_{r,s}^{j,i} + \nabla\Delta\varepsilon_{rs,\rho}^{j,i} \tag{2.16}$$

The DD of carrier phase measurement can be modelled as:

$$\begin{aligned}\lambda\nabla\Delta\phi_{r,s}^{j,i} = {} & \Delta r_{r,s}^{j} - \Delta r_{r,s}^{i} + \lambda\left(\Delta N_{r,s}^{j} - \Delta N_{r,s}^{i}\right) - \Delta I_{r,s}^{j} + \Delta I_{r,s}^{i} \\ & + \Delta T_{r,s}^{j} - \Delta T_{r,s}^{i} + \Delta\varepsilon_{rs,\phi}^{j} - \Delta\varepsilon_{rs,\phi}^{i} \\ = {} & \nabla\Delta r_{r,s}^{j,i} + \lambda\nabla\Delta N_{r,s}^{j,i} + \nabla\Delta I_{r,s}^{i,j} + \nabla\Delta T_{r,s}^{j,i} + \nabla\Delta\varepsilon_{rs,\phi}^{j,i}\end{aligned} \tag{2.17}$$

and the final equation is:

$$\lambda \nabla \Delta \phi_{r,s}^{j,i} \simeq \nabla \Delta r_{r,s}^{j,i} + \lambda \nabla \Delta N_{r,s}^{j,i} + \nabla \Delta \varepsilon_{rs,\phi}^{j,i} \quad (2.18)$$

2.3.2.3 Triple difference

The Triple Difference (TD) technique is actually the difference of two double differences at two adjacent epochs. This method is mainly used for the elimination of ambiguity parameters and consequently the cycle slip. From the equation (2.18), we have:

$$\nabla \Delta \phi_{r,s}^{j,i}(t_2) - \nabla \Delta \phi_{r,s}^{j,i}(t_1) = \nabla \Delta r_{r,s}^{j,i}(t_2) - \nabla \Delta r_{r,s}^{j,i}(t_1) = \nabla \Delta r_{r,s}^{j,i}(t_2 - t_1) \quad (2.19)$$

2.3.3 Other residual errors

Study of the carrier phase measurement characteristics and errors can lead us to specifically define, model, and finally correct the errors. In this section, other errors that cannot be canceled out using any differential methods will be discussed.

2.3.3.1 Phase center variation

The exact point on the antenna in which carrier phase measurement is received, is known as the phase center. The Phase Center Variation (PCV) is an important error source in ultra-short baseline (less than 1 meter), as even one centimeter error in baseline estimation can cause several degree of error in attitude determination, (Zheng, 2010). The baseline vector is actually a vector between phase centers of two antennas. The problem is that the geometric antenna center is not necessarily at the antenna phase center. This problem will be more complicated to solve with the fact that the phase center is a function of the direction of received signal, its power density, and frequency. This is not only different in different types of antennas but it is also different in antennas of the same model from the same company as well (Zheng, 2010).

There are two methods to deal with this error:

- **experimental approach:** this method can be done by isolating the antenna from all errors and putting it in an exactly predefined position. Then the phase center error can be modelled using spherical harmonics or polynomial function of elevation and azimuth angle. This method is mainly used for relative calibration between two antennas;

- **laboratory approach:** in this approach the antenna is placed in an anechoic table which rotates the antenna to change received signal direction. Despite the other approach, the absolute PCV can be modelled in this method;

Comparison of these two method showed that these two approaches have approximately the same results, less than 2 mm difference, (Zheng, 2010).

2.3.3.2 Multipath

This phenomenon that distorts the signal with one or more replicas (depends on the environment) from nearby objects such as walls, buildings, vehicles, trees, water or ground surfaces, etc is called multipath. This means that, the receiver receives a sum of the original signal with other replicas with a different amplitude and phase. Because the multipath error depends on the antenna environment, this error is not consider as common source error and cannot be cancelled with the differential techniques. So this error is still a dominant error source in the precise GNSS based applications.

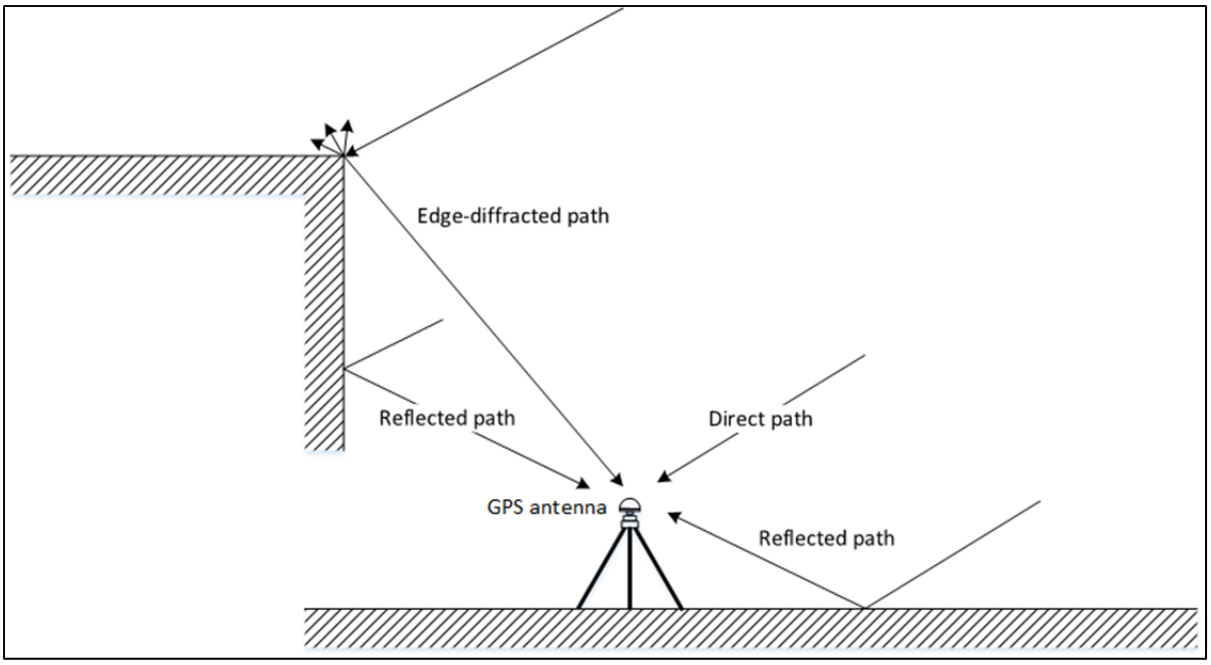

Figure 2.6 Multipath effect
Adapted from Hannah (2001)

Multipath causes inaccurate measurement and even loss of lock on the signal. Two of the earliest methods in multipath elimination which are not always feasible, are the installation of antennas away from buildings, and using choke ring antennas, (Vaillon et al., 2000).

Apart from these two general methods which can be used in both static and dynamic modes, in this work we categorized solutions in two groups, stationary receiver and dynamic receiver. Some of previous works are as follows:

Stationary receiver:

- due to the repetition of geometry between GNSS satellites and receiver every sidereal day, the multipath pattern is also repeated in the same way. This fact can be used to mapping multipath error based on elevation and azimuth satellite angles. Another factor that helps to formulate and recognize this kind of error is that the replicated

signals always have a delay with respect to the Line Of Sight (LOS) signal. This is because of the longer path due to the reflection;

- another method is to use an adaptive filter to extract multipath error base on the GNSS repetition noise factor, (Ge, Han et Rizos, 2002).

Dynamic receiver:

- Excluding invisible satellites from the positioning computation is one way to mitigate the multipath error. Invisible satellite means a satellite that has been detected by the receiver but without LOS. This technique calculate the geometrical relation between satellites and the receiver by observing satellite positions using a satellite orbit simulator, (Marais, Berbineau et Heddebaut, 2005; Meguro et al., 2009). Additionally by calculating body frame heading angle with gyro or Inertial Measurement Unit (IMU) and observing obstruction position for example with an omnidirectional camera one can achieve a more accurate solution, (Meguro et al., 2009);

- Using a bandpass Finite Impulse Response (FIR) to extract multipath from the LOS signal is another method to mitigate the multipath error, (Han, Dai et Rizos, 1999);

- another method is based on signal to noise ratio value analysis, because not only the phase, but also the amplitude of the carrier phase signal is affected by multipath. So the SNR and the known antenna gain can be used for multipath mitigation, (Axelrad, Comp et Macdoran, 1996);

- another method is to use of Wavelet Transformation (WT), which is the transformation for non-stationary signals like GPS instead of Fourier Transform (FT). This method is close to the time-frequency analysis based on the Wigner-Ville distribution, (Chui, 2014; Satirapod et Rizos, 2005);

- various correlator techniques like narrow correlator can also reduce multipath errors, (Dierendonck, Fenton et Ford, 1992; Fenton et al., 1991).

2.4 Important parameters in satellite geometry

Apart from GPS measurements errors, satellite geometry and its associated parameters, is another important factor in the positioning solution accuracy. In this section, we discuss how to calculate satellite elevation and azimuth angle and quality metrics in the GPS constellation.

2.4.1 Elevation and azimuth

The azimuth and elevation angles are describe as the orientation of the line of sight vector with respect to the north, east and down of the user.

$$\mathbf{u} = [u_N \quad u_E \quad u_D] \tag{2.20}$$

where $\mathbf{u}$ is the line of sight unit vector. Then:

$$\theta = -\arcsin(u_D) \tag{2.21}$$

$$\Psi = \arctan2(u_E, u_N) \tag{2.22}$$

where θ is the elevation angle and Ψ is the azimuth angle.

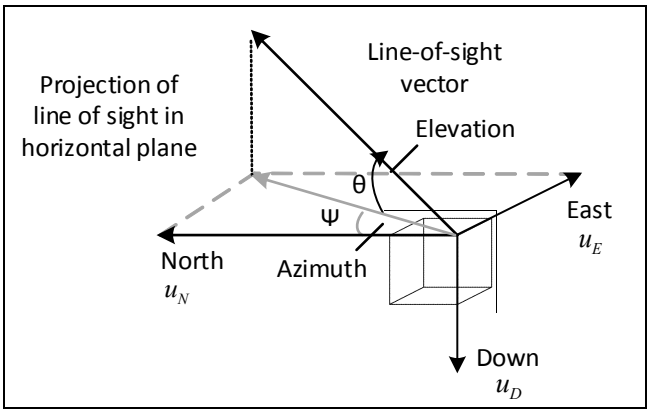

Figure 2.7 Azimuth and elevation angles
Adapted from Groves (2008)

2.4.2 Quality metrics of GNSS constellation

The position accuracy not only depends on the measurement accuracy and receiver quality but also depends on the satellite geometry. Figure 2.8 and Figure 2.9 clearly show the meaning of satellite geometry.

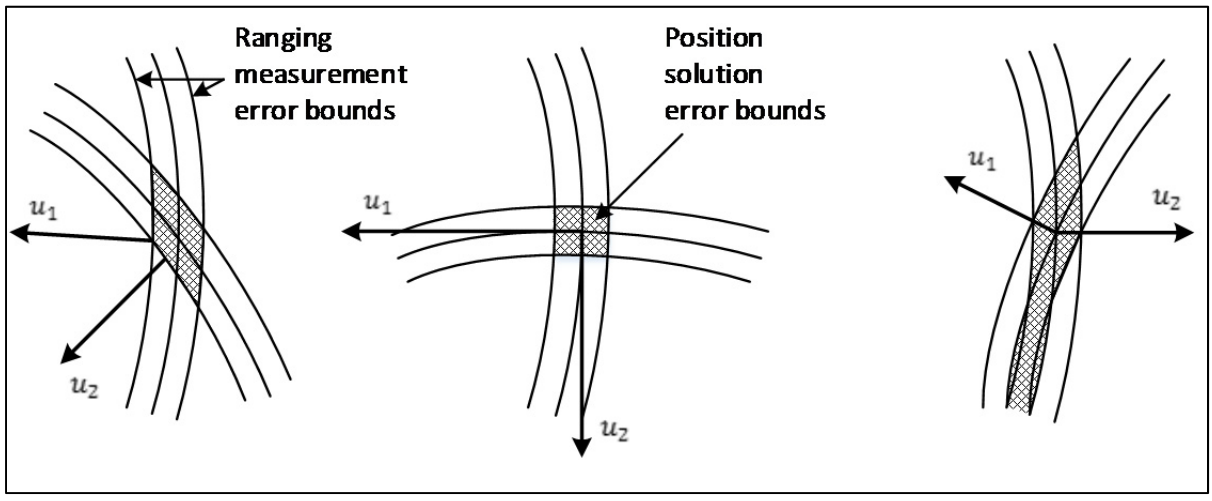

Figure 2.8 Effect of signal geometry on the position accuracy
Adapted from Groves (2008)

In Figure 2.8, arcs show the average and the error bound for each ranging measurement, the shaded areas show the uncertainty bounds for the position solution and the vectors are the

line of sight vectors from user to satellites. The position solution is optimum when lines of sights are perpendicular. This effect is called Dilution Of Precision (DOP). Figure 2.9 shows the position of satellites in a poor and a good geometry.

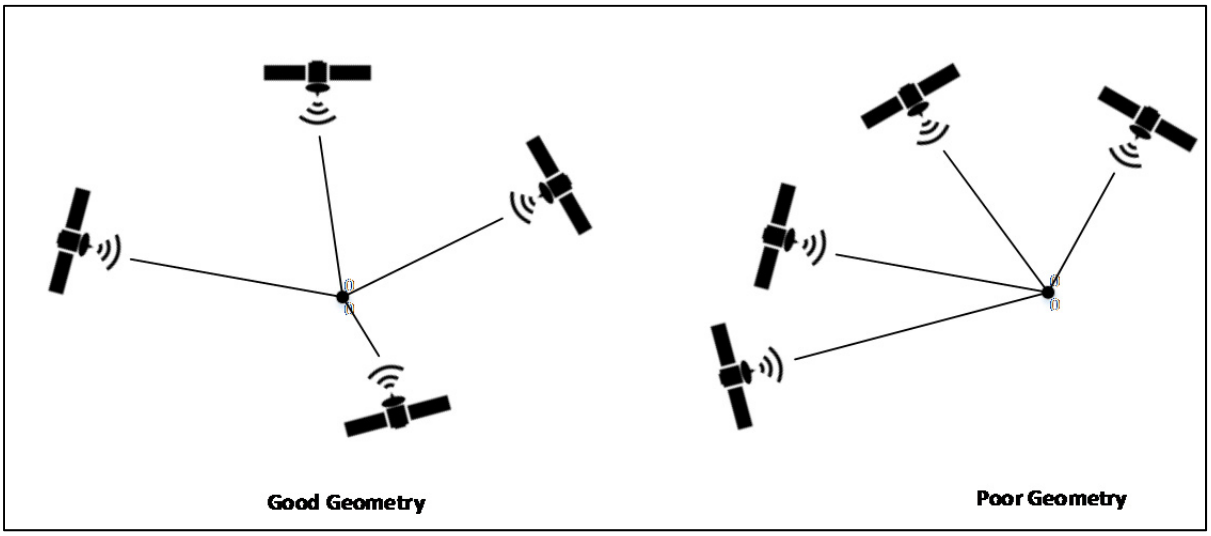

Figure 2.9 Satellite geometry
Adapted from Groves (2008)

In order to calculate DOP, a matrix of unit vectors line of sights for each satellite is created as follows:

$$A = \begin{bmatrix} \mathbf{u}_{x_1} & \mathbf{u}_{y_1} & \mathbf{u}_{z_1} & -1 \\ \mathbf{u}_{x_2} & \mathbf{u}_{y_2} & \mathbf{u}_{z_2} & -1 \\ \mathbf{u}_{x_3} & \mathbf{u}_{y_3} & \mathbf{u}_{z_3} & -1 \\ \mathbf{u}_{x_4} & \mathbf{u}_{y_4} & \mathbf{u}_{z_4} & -1 \end{bmatrix} \tag{2.23}$$

$$\mathrm{Q} = (\mathrm{A}^{\mathrm{T}}\mathrm{A})^{-1} = \begin{bmatrix} \sigma_{\mathrm{x}}^2 & \sigma_{\mathrm{xy}} & \sigma_{\mathrm{xz}} & \sigma_{\mathrm{xt}} \\ \sigma_{\mathrm{xy}} & \sigma_{\mathrm{y}}^2 & \sigma_{\mathrm{yz}} & \sigma_{\mathrm{yt}} \\ \sigma_{\mathrm{xz}} & \sigma_{\mathrm{yz}} & \sigma_{\mathrm{z}}^2 & \sigma_{\mathrm{zt}} \\ \sigma_{\mathrm{xt}} & \sigma_{\mathrm{yt}} & \sigma_{\mathrm{zt}} & \sigma_{\mathrm{t}}^2 \end{bmatrix} \tag{2.24}$$

From the diagonal parameters of the Q matrix, different DOP can be calculated as follows:

- Horizontal Dilution of Precision (HDOP):

$$D_H = \sqrt{\sigma_x^2 + \sigma_y^2} \tag{2.25}$$

- Position Dilution of Precision (PDOP):

$$D_P = \sqrt{\sigma_x^2 + \sigma_y^2 + \sigma_z^2} \tag{2.26}$$

- Geometry Dilution of Precision (GDOP):

$$D_G = \sqrt{\sigma_x^2 + \sigma_y^2 + \sigma_z^2 + \sigma_t^2} \tag{2.27}$$

The GDOP lower than 1 is considered as a high level of confidence of data. Considering the calculated DOP values can help to interpret the achieved result.

2.5 Important references for GNSS navigation

Navigation in science terminology has two different meanings; the first one is to determination position or velocity of a moving object with respect to a known reference. The second one is to lead a moving user, a car, vessel or an airplane, from one location to another which is known as autopilot or guidance. In order to understand clearly the implementation part of this work, the more important navigation basics that have been used in this project is presented in this section.

Due to the importance of comparison between two frames in navigation, it is important to have a good understating of each frame. Some of important frames in navigation are as follows:

2.5.1 Earth centred earth fixed reference frame

The Earth Centred Earth Fixed (ECEF) reference frame is a commonly used navigation frame, on which their axis are fixed with respect to the earth and its origin is the mass center of the earth. The z axis is pointing toward true North Pole (not the magnetic pole). The x axis points toward the intersection of the equator and International Earth Rotation and Reference Systems Service (IERS) reference meridian which defines the zero degree longitude. The y axis completes the right handed orthogonal set. This is an important reference frame in navigation because the axis is fixed with respect to the earth.

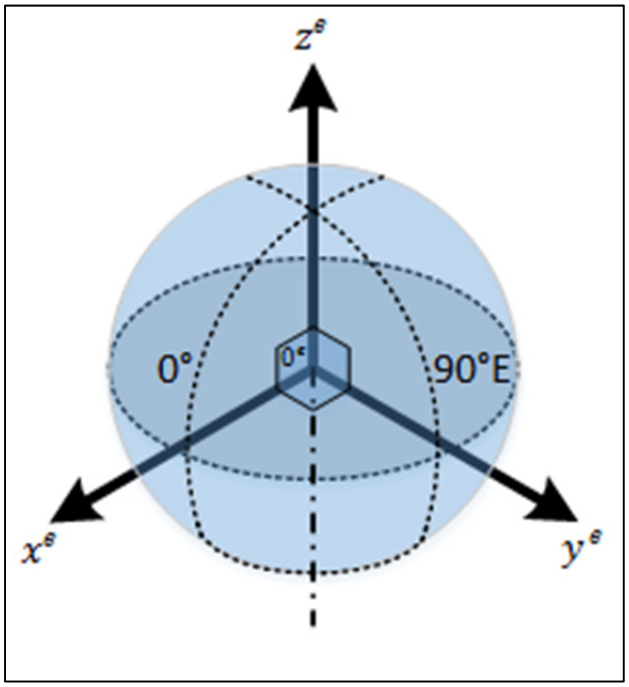

Figure 2.10 ECEF frame axis
Adapted from Groves, 2008

2.5.2 Local frame

The local frame is a frame that is fixed with respect to a chosen position and its origin is the desired position (i.e. navigation system position or user position or the mass center of an object). The x axis is always pointing toward the East and it is known as E axis. The y axis is

the projection of the vector pointing to the North Pole into the orthogonal plane to the earth surface and it is known as North (N) axis. The z axis completes the right handed rule and it is known as Up (U) axis. This frame is an important frame in navigation because it is convenient to know the user's position with respect to the East, North, and Up.

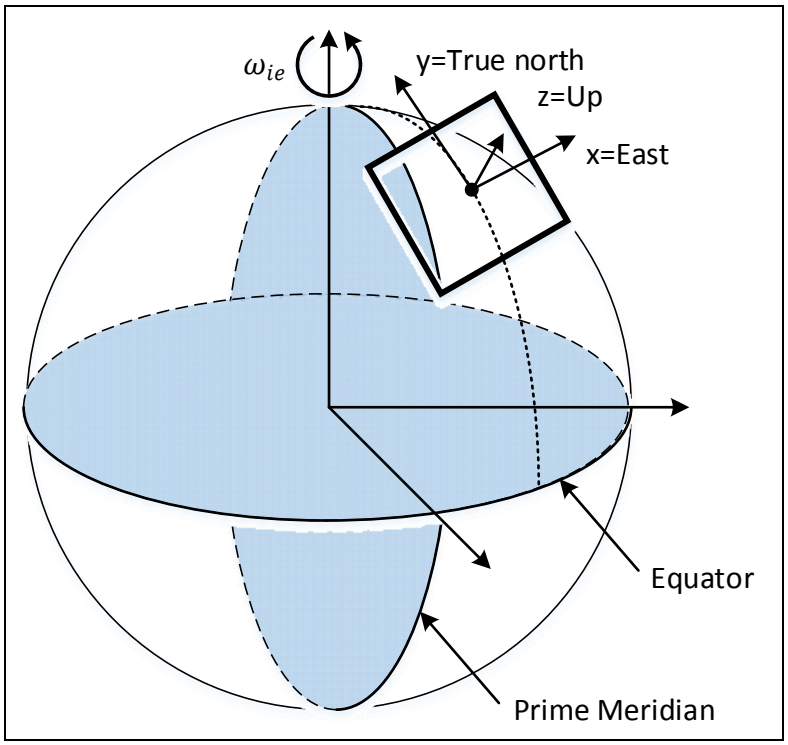

Figure 2.11 Local frame, ENU
Adapted from Groves (2008)

2.5.3 Body frame and Euler angles

This frame remains fixed with respect to the object body and its origin is at the mass origin of the object. The x axis is in the direction of movement. The z axis is the direction of gravity vector and the y axis is the right handed orthogonal set. For the Euler angles, rotation about the x axis is roll, the rotation about the y axis is pitch and the rotation about the z axis is yaw angle, Figure 2.12.

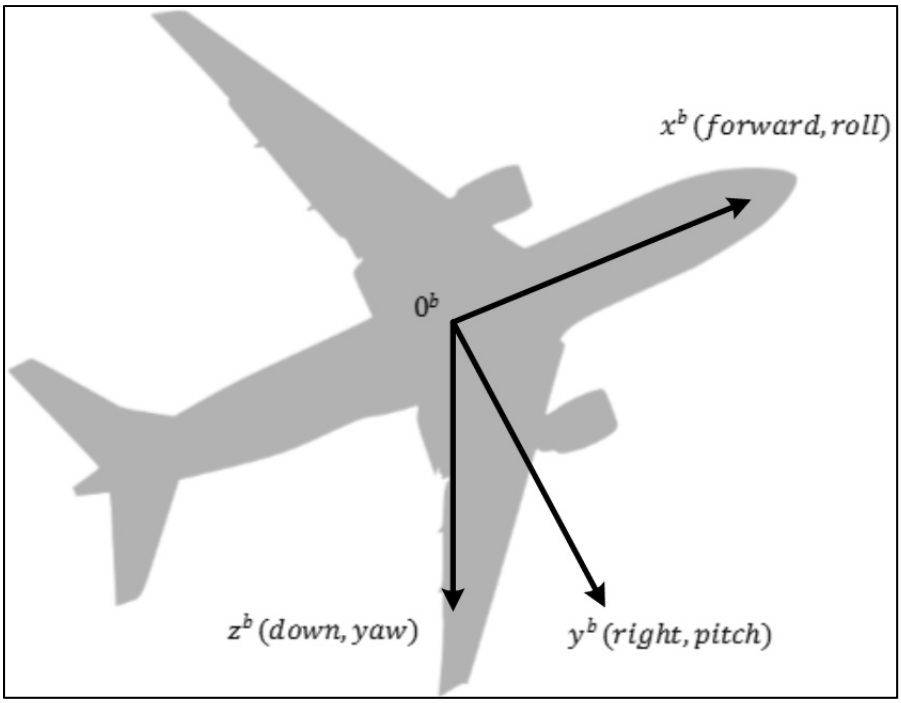

Figure 2.12 Body frame

2.6 Rotation Matrix

Rotation matrix is a 3×3 matrix which transforms a vector from a frame to another. In navigation this matrix defines a rotation from the body frame to the reference frame or vice versa which contains Euler angles as well.

A rotation matrix in general is called *R* matrix and is defined as follow:

$$R_{\alpha}^{\beta} = \begin{bmatrix} \mathbf{u}_{\beta_x}.\mathbf{u}_{\alpha_x} & \mathbf{u}_{\beta_x}.\mathbf{u}_{\alpha_y} & \mathbf{u}_{\beta_x}.\mathbf{u}_{\alpha_z} \\ \mathbf{u}_{\beta_y}.\mathbf{u}_{\alpha_x} & \mathbf{u}_{\beta_y}.\mathbf{u}_{\alpha_y} & \mathbf{u}_{\beta_y}.\mathbf{u}_{\alpha_z} \\ \mathbf{u}_{\beta_z}.\mathbf{u}_{\alpha_x} & \mathbf{u}_{\beta_z}.\mathbf{u}_{\alpha_y} & \mathbf{u}_{\beta_z}.\mathbf{u}_{\alpha_z} \end{bmatrix} \tag{2.28}$$

$$= \begin{bmatrix} \cos(\mu_{\beta_x\alpha_x}) & \cos\left(\mu_{\beta_x\alpha_y}\right) & \cos(\mu_{\beta_x\alpha_z}) \\ \cos\left(\mu_{\beta_y\alpha_x}\right) & \cos\left(\mu_{\beta_y\alpha_y}\right) & \cos\left(\mu_{\beta_y\alpha_z}\right) \\ \cos(\mu_{\beta_z\alpha_x}) & \cos\left(\mu_{\beta_z\alpha_y}\right) & \cos(\mu_{\beta_z\alpha_z}) \end{bmatrix}$$

where the upper index refers as "To" and the lower case refers to "From". $\mathbf{u_i}$ is the unit vector of different axis $[x, \quad y, \quad z]^T$ and $\mu_{i,j}$ is the angle between axis i and j.

For example the rotation matrix between ECEF and local navigation frame is as follows:

$$R_e^n = \begin{bmatrix} -\sin L_b \cos\lambda_b & -\sin L_b \sin\lambda_b & \cos L_b \\ -\sin\lambda_b & \cos\lambda_b & 0 \\ -\cos L_b \cos\lambda_b & -\cos L_b \sin\lambda_b & -\sin L_b \end{bmatrix} \tag{2.29}$$

In this thesis the rotation matrix will be frequently used in order to convert the baseline vectors from the ECEF frame to the local frame, from the local frame to the body frame and vice versa.

Now that an overview of the GPS, its measurements and associated errors, as well as the important references are presented, we go through different methods in the literature in order to choose the appropriate method. The next chapter presents an extensive literature review on the main challenging problems of this project namely ambiguity resolution and attitude determination.

CHAPTER 3

LITERATURE REVIEW

As we need a high precision solution for attitude determination, using carrier phase measurement which is more precise than the code measurements is necessary. The first important aspect to be able to use this measurement is to estimate the ambiguity parameter. The carrier phase measurement is ambiguous by an integer number of cycles from the satellite to receiver which remains constant until loss of lock. The section 3.1 presents the evolution of the GPS ambiguity resolution methods, as it is the first challenging problem in this scope. Then in the section 3.2, in order to find an appropriate method to estimate the attitude angles, a survey of attitude determination methods and comparison is presented. Finally, in the section 3.3, for increasing the solution accuracy and system reliability, a detailed study on how to incorporate the GLONASS measurements into the system is explained. For each module, first we go through the literature review of different methods and approaches then, summary for all the studied methods will be presented. At the end, a conclusion is provided for the findings of the entire chapter in the section 3.4.

3.1 Methods of GPS ambiguity resolution

Carrier phase measurement is the result of the phase difference of the received signal relative to the replica that is generated by the receiver. Therefore the fractional part of the phase difference can be measured within a millimetre accuracy (Verhagen et Teunissen, 2006), which is the reason why carrier phase measurement is much more accurate than code measurement. However the initial number of wavelengths from satellite to receiver is unknown and needs to be estimated for each satellite in view.

Since calculating the ambiguity of the carrier phase measurement is the key to use in high accuracy applications, we review here the most commonly used methods in literature.
Based on the literature, there are two main categories of ambiguity resolution methods consisting of (Crassidis, Lightsey et Markley, 1999; Teunissen, Giorgi et Buist, 2011):

- dynamic or motion-based;

- search-based, motionless or instantaneous.

The first category is dynamic or motion-based which uses a collected data set in a certain period in which the ambiguity remains constant and provides a batch solution. These methods are based on the satellite and body frame motion. These methods are not fast and they need high amount of memory to save the collected data and non-coplanar baselines, (Wang et al., 2009b). Despite these disadvantages, this method is highly reliable because of several criteria to accept the solution. Statistical checks of the error and considering the closeness of the floating point solution and the actual integers are among those criteria (Crassidis, Lightsey et Markley, 1999).

The second category which is usually called motionless or instantaneous or search-based methods are based on estimating a set of integers of one epoch and search for the best solution, (Hatch, 1991; Park et Teunissen, 2003). Due to the high convergence speed, this method is a suitable method for real time applications, (Li et al., 2004; Park et Teunissen, 2003), but since it can converge to an incorrect solution in the presence of noise especially multipath, all solutions should be checked several times before selecting the final solution, (Teunissen, 1997; Yoon et Lundberg, 2002). The instantaneous category, consists of three steps: *float solution*, *integer ambiguity resolution* and *integer ambiguity validation*. The first step usually is the result of an estimation process consisting of estimation the ambiguity in real numbers. The second step can be done with three types of methods: *Simply rounding*, *integer bootstrapping* and *Integer Least-Squares (ILS) estimator*, (Zheng, 2010). The instantaneous category can be divided into three types of search domains, (Kim et Langley, 1999):

1. The measurement domain: It uses the C/A code or P-code directly to calculate the integer ambiguity of the corresponding carrier phase measurement. In order to

achieve this ambiguity with a proper accuracy, usually observation combination of L1 and L2 is needed, (Cocard et Geiger, 1992; Collins, 1999);

2. The coordinate domain: The coordinate domain is the biggest subcategory in the instantaneous category. Many ambiguity search methods are in this category such as: Least-Squares Ambiguity Search Technique (LSAST), Fast Ambiguity Search Filter (FASF), Ambiguity Function Method (AFM), Fast Ambiguity Resolution Approach (FARA), (Kim et Langley, 2000);

3. The ambiguity domain: The ambiguity domain is known as an efficient with high success rate method and has recently received lots of attention. This method is based on the original search domain transformation in ambiguity domain which is easier and faster to solve, (Teunissen, Giorgi et Buist, 2011). LAMBDA is the most important and well known method in the ambiguity domain.

The different methods of ambiguity resolution are not comparable and even is not always feasible, (Kim et Langley, 2000). We describe all these methods briefly as follows:

3.1.1 Ambiguity function method

(Counselman et Gourevitch, 1981) has proposed this technique and (Remondi, 1991) has improved it. Since the Ambiguity Function Method (AFM) uses the fractional value of the carrier phase, and triad positions are searched instead of triad ambiguity set, it is insensitive to cycle slip which makes it different from other methods, (Hofmann-Wellenhof, Lichtenegger et Collins, 2013; Kim et Langley, 2000; Park et al., 1996).

This technique is based on geometric change between satellite and receiver, (Hofmann-Wellenhof, Lichtenegger et Collins, 2013). In case of cycle slip, despite other methods, AFM can continue the calculation without any interruption or reinitialisation. As a result, this feature significantly improves the computational time of this method.

It is proved that the effectiveness and accuracy of the solution barely changes with loss of lock and even when data is absent for a long time, which means a few minutes of data at any time plus a few minutes one hour later is almost the same with one hour data without interruption, (Lu, 1995). However, this method takes high computational time, 1 to 2 minutes and consequently it is not a suitable method for real time applications, (Lu, 1995).

3.1.2 Least-squares ambiguity search technique

The early studies in this method is done by (Beutler et al., 1984) and (Wei, 1986). In this method, each double difference ambiguity term from each satellite is considered as an independent parameter. All these unknown parameters, take time for finding a search space and the fixed number.

One of the main disadvantages of this method is its heavy computational burden, which makes it unusable method for On-The-Fly (OTF) ambiguity resolution. (Hatch, 1989) and (Hatch, 1991) proposed a method to overcome this inconvenience by limiting the number of independent parameters to three and adding one check before acceptance of the solution. For n satellite, there are $n-1$ double difference ambiguity parameters, so for example, for having three independent ambiguities, four satellites have to be chosen based on the PDOP value. The search space cube is calculated by theses four satellites which are known as primary satellites. The rest of satellites which are called secondary satellites are usually used as to check on each potential ambiguity set in the search space. Chi-square test usually is applied for each ambiguity set. If more than one ambiguity set is passed, due to the noise or bad geometry of satellites, this test can help to approve the solution for the next epoch. Gaussian error distribution is assumed in this method. Due to 3 dimensional ambiguity search space regardless of the number of tracked satellites, this method is fast in computational time, thus it is suitable for real time application, (Lu, 1995).

3.1.3 Fast ambiguity resolution approach

This technique is proposed by (Frei et Beutler, 1989) and it consists of four steps to obtain the solution:

1. **First Step** is to estimate the ambiguity based on the carrier phase measurement and by an adjustment procedure with corresponding covariance matrix of the unknown parameters and the standard deviation of the ambiguity numbers,
   (Landau et Euler, 1992);

2. **Second Step** is to determine the search space based on standard deviation and ambiguity correlation. This means by having δN as standard deviation of ambiguity N, $\pm k\delta N$ is the search range for this ambiguity where k is statistically calculated from Student's t-distribution;

3. **Third step** is to perform a least-squares adjustment for each ambiguity set that is accepted statistically;

4. **Final step** is to pick the solution with smallest variance and compare it with the float solution. If the solution is compatible, this set will be accepted.

3.1.4 Fast ambiguity search filter

(Chen, 1993) proposed this method and further investigations were made by (Chen et Lachapelle, 1995). This method uses Kalman filter as an estimator with the ambiguity parameters in the state vector. As soon as the ambiguity parameters are set with a proper level of confidence, they are treated as fix known integers. After that, in order to determine the search space, for example for the second ambiguity parameter, the first ambiguity is considered as known integer and removed from the state vector. For determining the third ambiguity search space, the first and the second ambiguities are considered known and fix integers. This procedure will be performed for all the ambiguities, one by one, and because of that, it is called a recursive method.

After fixing all the ambiguities, they are treated as known parameters and they will be removed from the state vector. Other unknown parameters, which are the coordinates of the receivers, will be replaced then into the state vector, unknown parameter. So the receiver's coordinates can be calculated more precisely.

This technique uses full information of satellite geometry and the ambiguity search space for each satellite is calculated not only recursively but also based on other integer ambiguities. Consequently, two important factors to OTF ambiguity resolution which are computational and observational time, are significantly reduced compare to the least-squares method, (Chen et Lachapelle, 1995).

3.1.5 Least-squares ambiguity decorrelation adjustment

One of the most powerful ambiguity resolution method is LAMBDA, which was proposed by (Teunissen, 1995). This method is different from FASF, FARA, and AFM in search space transformation and it is known as an efficient method with maximum success rate, (Teunissen, 1995; Zheng, 2010).

In this method, each baseline can be written in a linearized model as, (Wang et al., 2009a):

$$Y = Aa + Bb + e \tag{3.1}$$

where Y is the measured minus computed double difference GPS carrier phase measurement, a is the double difference ambiguity vector, b is the baseline component, e is the noise vector, and A and B are the design matrices.

First a and b with their covariance matrices should be estimated with least-squares method as:

$$\begin{bmatrix} \hat{a} \\ \hat{b} \end{bmatrix} \begin{bmatrix} Q_{\hat{b}} & Q_{\hat{b}\hat{a}} \\ Q_{\hat{a}\hat{b}} & Q_{\hat{a}} \end{bmatrix} \tag{3.2}$$

Then the optimal solution of the Equation (3.1) will be:

$$\min\|\hat{a} - a\|^2_{Q_{\hat{a}}^{-1}}, \qquad a \in \mathbb{Z}^n \tag{3.3}$$

Due to the cross-correlation of the ambiguities in the original search space, the search space is extremely elongated and it takes a long time to determine the ambiguity with high level of accuracy. This dependency can be seen as a discontinuity in the spectrum of ambiguity conditional variances, and it will be far more problematic in the short observation time span and in the absence of the P-code, (Teunissen, 1995).

LAMBDA overcomes this problem by performing a Z-transformation in order to decorrelate the cross-correlation between ambiguities while preserving the integer nature of the problem. This method reformulates the original search space by decorrelating via a Z-transformation into another search space, which is easier to solve and it is faster. LAMBDA converts the elongated space to a round (spherical) space, the search space then will be aligned to the grid axes and can be simply estimated by rounding to the nearest integer, (Teunissen, 1995). The transformed search space of Equation (3.3) can be written as:

$$(\hat{z} - z)^T Q_{\hat{z}}^{-1} (\hat{z} - z) \leq \chi^2 \tag{3.4}$$

where $\hat{z} = Z^T \hat{a}$ and the $Q_{\hat{z}} = Z^T Q_{\hat{a}} Z$ and the χ^2 is the size of the search ellipsoid. The size of χ^2 is determined by $z_i = [z_i]$. The boundary of the search space is an ellipsoid centered at $\hat{z}$, its shape is defined by covariance matrix $Q_{\hat{z}}$ and its size is determined by χ^2, (Zheng, 2010).

The idea of the search strategy is the same with other search-based methods but it is different in integer ambiguity resolution (second step). After the transformation, a sequential conditional least-squares is then performed.

Size of the search space is a critical issue because the small one may not contains the correct integer ambiguity and the large one takes a long time to converge. However, this method has been developed for unconstrained or linearly constrained, which is not necessarily optimal for GNSS attitude determination specially for those with rigid platform, (Teunissen, Giorgi et Buist, 2011).

Some notes about ambiguity resolution methods:

- according to (Kim et Langley, 2000), there is another way to categorize the ambiguity resolution method. We can split up the problem into all ambiguity search method like FARA, FASF, LAMBDA, modified Cheloskey decomposition method and independent ambiguity search method like LSAST. In the first category, all the ambiguity parameters will be searched but in the second category, first independent ambiguities should be fixed and dependent ambiguities will be fixed after based on independent parameters;

- a long time span is usually needed to converge the ambiguity solution especially in single frequency and low-cost system because the observations are taken at low rate and errors are highly correlated, (Zheng, 2010);

- there are three fundamental properties that should be targeted, in order to select a suitable method, (Campo-Cossio et al., 2009):

  - initial attitude independent;

  - high success rate estimation;

  - high correction ability of the incorrect ambiguities.

3.1.6 Summary

As summary, all of these methods need three steps to determine the integer as fixed and correct number.

First step consist of solving an ordinary least-squares or an Extended Kalman Filter (EKF) in order to estimate the integers as a real number. Since this step does not guarantee to converge to integer numbers, it is known as float solution.

Second step and the core one is about to calculate the best integer ambiguity guess from the real numbers, float solution, which is known as integer ambiguity resolution and can be done by different methods. Three of the most popular methods are as following:

- **simply rounding,** which rounds off the solution to the nearest integer. Not only this method can simply be applied, but also it is an optimal solution if the integers are uncorrelated. In other words, it minimizes the following cost function if only $Q_{\widehat{N}\widehat{N}}$ is a diagonal matrix:

$$C = \min\left(\widehat{N} - N\right)^T Q_{\widehat{N}\widehat{N}}^{-1}\left(\widehat{N} - N\right) \tag{3.5}$$

- **integer bootstrapping** is based on the rounding estimator which takes the correlation and partially cross-correlation into account and it is known as sequential rounding. For this reason, one can start with the integer with a smallest variance. However because using just one part of the cross-correlation and not all of them, the accumulated product of them may not give a high success rate, but this method is still an optimal method, because we can partially fix the integer with a high success rate, (Teunissen, 2004; Teunissen, 1995);

- **Integer Least-Squares (ILS) estimator** is based on search strategy which searches in a predefined search space and choose the solution that minimizes the cost function.

Like all other search-based methods, the problem is that because of cross-correlation between ambiguity numbers, this search mandates a high computational burden and time. By decorrelating the cross-correlation between ambiguity numbers with z-transformation, a high success rate can be achieved. (Teunissen, 1999) proved the efficiency of this method and its high success rate. This is the method that is applied to the LAMBDA and C-LAMBDA methods. In C-LAMBDA the solution requires the computation of a nonlinear constrained least-squares problem and unlike the LAMBDA the search space is non-ellipsoidal (Nadarajah et al., 2012).

Although all of these three methods can be performed in the Z space and get a higher success rate (number of correct guess in the total processed samples), but as it is proved by (Teunissen, 1999), highest success rate can be achieved by Z transformation of the ILS estimator. In (Zheng, 2010), 1.34 % success rate improvement compared to the simple rounding and 1.92 % with respect to the integer bootstrapping was achieved. The assumption in this test is a float solution with the Gaussian distribution and zero mean.

Third step consists of determining a confidence level of the given integer ambiguity of the previous step and perform a selection based on that.

A summary of integer validation tests and performance comparison can be found in (Verhagen, 2004; Wang, Stewart et Tsakiri, 2000).

3.2 Attitude determination methods

Attitude determination typically means to search a least-squares estimate of a rotation matrix which brings a vector or a set of vectors from one coordinate frame to another. Traditionally, differential positioning and attitude determination systems have been solved separately. However, these two systems can be combined in one system in a way that the attitude parameters are estimated directly without the baseline estimation. This section presents a

survey on two categories of attitude determination methods, direct method and baseline method. Then a detailed review on the baseline method will be presented.

The baseline method is a bigger category compared to the direct method and got more attention in the literature. This method is applied by different techniques in the literature which are namely Quaternion, QUEST, SVD, FOAM, ESOQ and ESOQ2. . These methods are the most commonly used method in the attitude determination literature and we present them in this chapter in order to choose the most appropriate method for our application. At the end, all the presented methods will be compared and a method will be selected in order to implement.

3.2.1 Direct method for attitude determination

As it is mentioned earlier the attitude parameters can be estimated directly without baseline vector estimation. Attitude parameters can be estimated directly from carrier phase measurements equation as follows (Scaccia, 2011):

$$A\mathbf{b}^L = \mathbf{b}^B \tag{3.6}$$

where A is the rotation matrix, b^L is the baseline vector in local frame, and b^B is the baseline vector in body frame. The range difference (as shown in Figure 3.1) can be expressed as:

$$\Delta\rho = (\mathbf{b}^l)^T\mathbf{e} = \|\mathbf{b}\|\cos(\theta) \tag{3.7}$$

By substituting $\mathbf{b}^L$ from the Equation (3.6) into the Equation (3.7), we have:

$$\Delta\rho = (\mathbf{b}^L)^T\mathbf{e} = (\mathbf{b}^B)^T A\,\mathbf{e} \tag{3.8}$$

The final model using directly attitude rotation matrix can be written as:

$$\lambda\,\Delta\phi^{j}_{r,s} = (\mathbf{b}^{B})^{T} A\mathbf{e} + c(t_r - t_s) + \lambda\Delta N^{j}_{r,s} + \Delta\varepsilon^{j}_{rs,\phi} \tag{3.9}$$

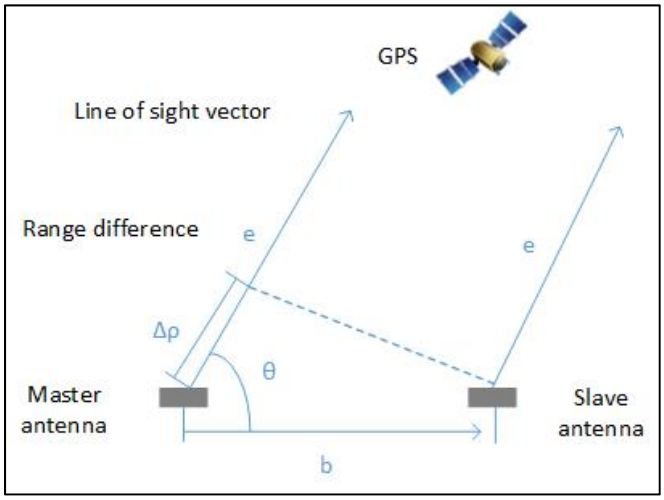

Figure 3.1 GPS phase difference geometry
Adapted from Scaccia (2011)

In (Axelrad et Ward, 1996), an Extended Kalman Filter (EKF) has been used to estimate the attitude quaternion matrix. In this method the attitude quaternion parameters are incorporated directly into the Kalman Filter state vector. The error associated with the initial guess is the biggest challenge of this method. If this error would be too large to be correctly modelled in linearization step, the solution may not converge. This effect is called the linearization limitation.

Another example is proposed in (Psiaki, 2006). This method is a batch algorithm which simultaneously solves attitude quaternion and ambiguity resolution. The algorithm can work using data from only two satellites and three receivers excluding the master receiver's estimation. The contribution of the mentioned work can be considered as the ability to solve a mixed-integer nonlinear least-squares problem. The direct method can be divided in two phases:

The first phase of the direct method solves a Recursive Least-squares (RLS) problem. This method simplifies the problem by using a Taylor series approximation and taking real ambiguities values instead of integers.

In the second phase of the direct method, a Mixed Integer Least -Square (MILS) algorithm is applied which minimizes the full cost function subjects. It takes the initial guess and uses Taylor series to solve the cost function. Then it increments the guess and solve the approximate problem again. At each step the improvement will be added into the initial guess.

All attitude parameters will be obtained through these two steps. This method is not recursive and it does not use the new data and neither the previous one.

3.2.2 Baseline method for attitude determination

Suppose we have several antennas whose positions are fixed in the body frame, and their relative positions are known in the body frame as well as shown in the Figure 3.2. By estimating the position of each of them at each epoch, the baseline vectors in the local frame can be calculated. Then, the rotation matrix, which converts a set of vectors from one frame into another one can be estimated based on these two baseline sets in two frames, Figure 3.2. This is one of the most common ways to represent the attitude and it is called the Wahba's problem.

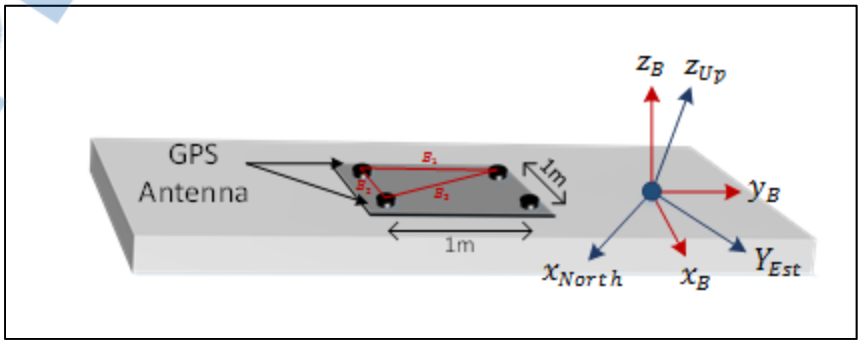

Figure 3.2 Baseline vectors of our defined project in body frame and local frame

In order to estimate the optimal rotation matrix, a least-squares estimation of the rotation matrix is performed to minimize the Wahba's cost function:

$$J(A) = \sum_{i=1}^{n} W_i \left\| \mathbf{b}_i^B - A\mathbf{b}_i^R \right\|^2 \tag{3.10}$$

where b_i^B is the i^{th} vector in the body frame, b_i^R is the i^{th} vector in reference frame, A is a rotation matrix, and W_i is a set of positive weight, and n is the number of epochs. From the Equation 2.14 and the Figure 3.1 we can write:

$$\lambda\Delta\phi_{r,s}^{j} = (\mathbf{b}_{rs})^T \mathbf{e}_s + c(t_r - t_s) + \lambda\Delta N_{r,s}^{j} + \Delta\varepsilon_{rs,\phi}^{j} \tag{3.11}$$

where b_{rs} is the baseline vector from the stationary receiver (Master antenna) to the rover (Slave antenna) and e_s is the line of sight from the antenna to the satellite .The cost function based on Wahba's problem can be modelled as:

$$J(A_k) = \sum_{i=1}^{n} W_{r,s}^{j} \|\mathbf{b}_{rs}^B - A_k \mathbf{b}_{rs}^R\|^2 \tag{3.12}$$

where k is the number of observation, n is the number of satellite, and $W_{r,s}^{j}$ is a weight associated to each measurement.

In order to find the minimum point of function $f(x)$, the following equation needs to be solved:

$$F(x) = f'(x) = 0 \tag{3.13}$$

One of the most common approach to solve the Equation (3.13) is Newton's method which is based on Taylor series. It is assumed that the x_{n+1} is close to the solution, then we have:

$$F(x_{n+1}) = F(x_n + \Delta x) = F(x_n) + \frac{\partial F}{\partial x}(x_n)\Delta x \tag{3.14}$$

In this method we want to find where $F(x_{n+1})$ is equal to zero, so we put $F(x_{n+1})$ then we have:

$$\Delta x = -\left[\frac{\partial F}{\partial x}\right]^{-1} F(x_n) \tag{3.15}$$

$$x_{n+1} = x_n - \left[\frac{\partial F}{\partial x}\right]^{-1} F(x_n) \tag{3.16}$$

This process needs to be continued until $\Delta x \to 0$ and $F \to 0$, where in GPS applications, F is a matrix.

3.2.2.1 Quaternion method for attitude determination

For introducing the Quaternion method, we start with expanding the Wahba's loss function, (Scaccia, 2011):

$$\begin{aligned} \mathrm{J}(A) &= \sum_{i=1}^{n} W_i(\mathbf{b}_i^B - A\mathbf{b}_i^R)^T(\mathbf{b}_i^B - A\mathbf{b}_i^R) \\ &= \sum_{i=1}^{n} W_i\left(\mathbf{b}_i^{B^T}\mathbf{b}_i^B + \mathbf{b}_i^{R^T}\mathbf{b}_i^R - 2\mathbf{b}_i^{B^T}A\mathbf{b}_i^R\right) \end{aligned} \tag{3.17}$$

The vectors are normalized so the two first parts are equal to 1 and the loss function can be written as:

$$J = \sum_{i=1}^{n} W_i(1 - \mathbf{b}_i^{B^T}A\mathbf{b}_i^R) \tag{3.18}$$

Minimizing the Equation (3.18) is equal to maximizing the gain function:

$$g = \sum_{i=1}^{n} W_i \mathbf{b}_i^{B^T} A \mathbf{b}_i^R \tag{3.19}$$

After reformulating the rotation matrix in terms of quaternion $\overline{\mathbf{q}} = [\mathbf{q}^T q_4]^T$ we have:

$$A = q_4^2 - \mathbf{q}^T\mathbf{q} + 2\mathbf{q}\mathbf{q}^T - 2q_4\mathbf{q}^T \tag{3.20}$$

$$\overline{\mathbf{q}}^T\overline{\mathbf{q}} = 1 \tag{3.21}$$

and the gain function can be written:

$$g(\overline{\mathbf{q}}) = \overline{\mathbf{q}}^T K \overline{\mathbf{q}} \tag{3.22}$$

$$K = \begin{bmatrix} S - \sigma I & Z \\ Z^T & \sigma \end{bmatrix} \tag{3.23}$$

By defining *B* as follows, elements of the *K* matrix can be defined as:

$$B = \sum_{i=1}^{n} W_i \left[\mathbf{b}_i^{R^T} A \mathbf{b}_i^B\right] \tag{3.24}$$

$$S = B + B^T \tag{3.25}$$

$$Z = [B_{23} - B_{32} \quad B_{31} - B_{13} \quad B_{12} - B_{21}]^T \tag{3.26}$$

$$\sigma = tr[B] \tag{3.27}$$

For maximizing the gain function (Equation (3.19)), the derivative of the gain function with respect to the $\bar{q}$ is calculated, then we add the constrain:

$$g'(\overline{\mathbf{q}}) = \overline{\mathbf{q}}^T K \overline{\mathbf{q}} - \lambda \overline{\mathbf{q}}^T \overline{\mathbf{q}} \tag{3.28}$$

By putting Equation (3.28) equal to zero we get Equation (3.29) which is an eigenvalue problem and the optimal solution in an eigenvector of matrix K:

$$K\overline{\mathbf{q}} = \lambda\overline{\mathbf{q}} \tag{3.29}$$

By substitution Equation (3.29) into the gain function, Equation (3.22), we get:

$$g(\overline{\mathbf{q}}) = \overline{\mathbf{q}}^T K\overline{\mathbf{q}} = \overline{\mathbf{q}}^T\lambda\overline{\mathbf{q}} = \lambda\,\overline{\mathbf{q}}^T\overline{\mathbf{q}} = \lambda \tag{3.30}$$

So the largest eigenvalue maximizes the gain function and the eigenvector corresponding to this eigenvalue is the least-squares solution of the attitude as well.

The quaternion method is the most commonly used method to solve Wahba's problem however an additional step needs to calculate the quaternion parameters, (Markley, 1993; Zanetti et al., 2012). There are several methods to calculate the attitude parameters directly such as QUEST, SVD, FOAM, ESOQ and ESOQ-2 which we present them in the next sections.

3.2.2.2 QUEST method for attitude determination

The QUaternion ESTimator (QUEST) method uses a cheaper way compare to quaternion method to estimate the eigenvalue and eigenvector, (Scaccia, 2011). Recall the gain function, Equation (3.29) and its optimal solution:

$$g = \sum_{i=1}^{n} W_i \mathbf{b}_i^{B^T} A \mathbf{b}_i^R \tag{3.31}$$

$$g = \lambda_{opt} \tag{3.32}$$

Then we get,

$$\lambda_{opt} = \sum W_i - J \tag{3.33}$$

In order to maximizing λ, the following approximation is used which is enough for most of the applications:

$$\lambda_{opt} \simeq \sum W_i \tag{3.34}$$

After calculating the optimal eigenvalue, the eigenvector needs to be calculated. Then the quaternion vector is converted in eigenproblem to Rodriguez parameters as follows, (Markley et Mortari, 1999; Zanetti et al., 2012):

$$P = \frac{\bar{q}}{q_4} = \text{atan}\left(\frac{\Phi}{2}\right) \tag{3.35}$$

$$P = \left[\left(\lambda_{opt} + \sigma\right) - S\right]^{-1} Z \tag{3.36}$$

After that the quaternion can be calculated as:

$$\bar{q} = \frac{1}{\sqrt{1 + P^T P}} \begin{bmatrix} P \\ 1 \end{bmatrix} \tag{3.37}$$

OUEST is the optimal numerical implantation of the Quaternion method and it is one of the most frequently used algorithm for 3-axis attitude determination. However, recently a robustness problem of this method is raised in the literature. One problem with this method is that the Rodriguez parameters become singular when the rotation angle is π
(Cheng et Shuster, 2013).

3.2.2.3 SVD method for attitude determination

For introducing Singular Value Decomposition (SVD) method, we start with Wahba's loss function again (Markley et Mortari, 1999):

$$\frac{1}{2}\sum_{i} a_i |\mathbf{b}_i - A\mathbf{r_i}|^2 \tag{3.38}$$

where $\mathbf{b}_i$ are unit vectors in a body frame, $\mathbf{r}_i$ are unit vectors in a reference frame, and a_i are non-negative weights. SVD method which is one of the most robust algorithms in the literature is as following:

$$B = U\Sigma V^T = U\text{diag}[\Sigma_{11}\Sigma_{22}\Sigma_{33}]V^T \tag{3.39}$$

where U and V are orthogonal and $\Sigma_{11} > \Sigma_{22} > \Sigma_{33} \geq 0$ then we have,

$$tr(AB^T) = \text{tr}(A\ V\ \text{diag}[\Sigma_{11}\Sigma_{22}\Sigma_{33}]\ U^T) = \text{tr}(U^T\ A\ V\ \text{diag}[\Sigma_{11}\Sigma_{22}\Sigma_{33}]) \tag{3.40}$$

The trace is maximized with the constraint of $\det(A) = 1$:

$$U^T A_{opt} V = \text{diag}[1\ \det(U)\ \det(V)] \tag{3.41}$$

And the optimal attitude matrix is:

$$A_{opt} = U\ \text{diag}[1\ \det(U)\ \det(V)]\ V^T \tag{3.42}$$

The SVD method compute the attitude parameters directly rather than the quaternion. This method requires no initial guess and it is numerically stable as well (Zanetti et al., 2012). This method has also the advantage of calculating eigenvalue and eigenvectors of the covariance matrix which can be used for the analysis. The eigenvalue and its eigenvector represent the magnitude and the direction of the largest component of the attitude uncertainty (Markley, 1988).

3.2.2.4 FOAM method for attitude determination

In the Fast Optimal Attitude Matrix (FOAM) (Markley et Mortari, 1999), the optimal attitude matrix can be written as:

$$A_{opt} = (k\lambda_{max} - detB)^{-1}[(k + \|B\|_F^2)B + \lambda_{max} adjB^T - BB^T B] \tag{3.43}$$

where

$$k = \frac{1}{2}(\lambda_{max}^2 - \|B\|_F^2) \tag{3.44}$$

In this method the λ_{max} is computed as follows:

$$\lambda_{max} = tr(A_{opt}B^T) \tag{3.45}$$

The advantage of this method is that, the FOAM algorithm is less sensitive to error raising compared to other methods and it is fast
(Crassidis et Markley, 1997; Markley et Mortari, 1999).

3.2.2.5 ESOQ method for attitude determination

In EStimator of the Optimal Quaternion (ESOQ) method, (Markley et Mortari, 1999), the proposed approach is based on orthogonalization. Based on Equation (3.29), the optimal quaternion is orthogonal to all columns of $K - \lambda_{max} I$ matrix.

$$adj(K - \lambda \mathbf{I}) = adj\left[\sum_{i=1}^{4}(\lambda_i - \lambda)\mathbf{q}_i\mathbf{q}_i^T\right] = \sum_{i=1}^{4}(\lambda_j - \lambda)(\lambda_k - \lambda)(\lambda_l - \lambda)\mathbf{q}_i\mathbf{q}_i^T \tag{3.46}$$

where λ is any scalar value and i, j, k, l is permutation of 1,2,3,4 respectively. By getting

$$\lambda = \lambda_{max} = \lambda_1 \tag{3.47}$$

we have,

$$adj(K - \lambda_{max} I) = (\lambda_2 - \lambda_{max})(\lambda_3 - \lambda_{max})(\lambda_4 - \lambda_{max})\mathbf{q}_{opt}\mathbf{q}_{opt}^T \tag{3.48}$$

Then $\mathbf{q}_{opt}$ can be computed as,

$$\left(\mathbf{q}_{opt}\right)_i = c\,(-1)^{k+i} det[(k - \lambda_{max} I)_{ki}]\,, \qquad i = 1,2,3,4 \tag{3.49}$$

where $(k - \lambda_{max} I)_{ki}$ is the obtained matrix from deleting k^{th} row and i^{th} column from the matrix $k - \lambda_{max} I$.

The ESOQ is validated as the fastest optimal attitude estimation algorithm as it requires a small number of floating point operations. This method does not show any singularity problem as well (Mortari, 1997b).

3.2.2.6 ESOQ2 method for attitude determination

The second version of the ESOQ (Markley et Mortari, 1999), starts with relation of the optimal quaternion with associated rotation angle ϕ and the rotation axis *e* as follows :

$$\mathbf{q}_{opt} = \begin{bmatrix} e \sin\left(\phi/2\right) \\ cos\left(\phi/2\right) \end{bmatrix} \tag{3.50}$$

Also by substituting Equation (3.50) into Equation (3.36) we get:

$$M = (\lambda_{max} - trB)[(\lambda_{max} + trB)\mathbf{I} - S] - zz^T \tag{3.51}$$

Because M is singular and all its columns are parallel, it can be written as,

$$\mathbf{e} = \frac{\mathbf{y}}{|\mathbf{y}|} \tag{3.52}$$

where $\mathbf{y}$ is the column of $adjM$ which has the maximum norm, and we have:

$$\cos\left(\frac{\phi}{2}\right) = h(z.y) \tag{3.53}$$

$$\sin\left(\frac{\phi}{2}\right) = h(\lambda_{max} - \mathrm{tr}B)|\mathbf{y}| \tag{3.54}$$

and the optimal quaternion can be calculated as:

$$\mathbf{q}_{opt} = \frac{1}{\sqrt{|(\lambda_{max} - trB)\mathbf{y}|^2 + (z.\mathbf{y})^2}} \begin{pmatrix} (\lambda_{max} - trB)\mathbf{y} \\ z.\mathbf{y} \end{pmatrix} \tag{3.55}$$

In the case of zero rotation angle and if M has rank less than two, ESOQ2 does not define the rotation axis uniquely. Both ESOQ and ESOQ-2 are optimal, because they fully satisfy Wahba's problem, and nonsingular, due to the use of sequential rotations. The only difference is that ESOQ-2 computes the solution faster (Mortari, 1997a).

3.2.3 Summary of attitude determination algorithms

Overall comparison of all mentioned method result shows that the SVD method and the q method are the most robust and reliable approaches, (Markley et Mortari, 1999). Using FOAM with more iterations gives the same accuracy, however, it does not guaranty the same confidence level in the literature. In terms of speed, QUEST seems to require more time to converge, as it needs the sequential iteration. However, with a good approximation of attitude, the computational time can be reduced significantly. QUEST with good initial estimation, ESOQ and ESOQ2 are the fastest algorithms with nearly similar accuracy.

FOAM seems to be the slowest method however it has the most robustness among all the other.

SVD method is the most robust estimator which minimizes Wahba's loss function. Other methods such as FOAM, QUEST, ESOQ and ESOQ2 are less robust due to solve characteristic polynomial equation to find the maximum eigenvalue. However, they are faster than the SVD method which is only preferable when the number of baseline is numerous (more than 10) like star sensor applications. All the presented method have approximately the same accuracy while the speed of them can differ (Mortari, 1997a). In our application, we have only 4 baselines, the SVD method can perform fast enough while it is the most robust method among other methods. AS a result, the SVD method is selected for our application. A summary of the presented attitude determination methods performance based on the study in the literature is presented in Table 3.1.

Table 3.1 Attitude determination methods comparison

	Quaternion	**QUEST**	**SVD**	**FOAM**	**ESOQ**	**ESOQ2**
Speed	Average	High	Average	High	High	High
Numerical stability	Average	Low	High	High	Low	Low
Initial guess needed?	No	Yes	No	No	No	No

3.3 GPS and GLONASS integration

The Russian GNSS constellation, called Global Navigation Satellite System (GLONASS), was fully operational in 1997 with 24 satellites. However, due to the government economic

problem in 1991, this number has been reduced to 7 operational satellites in the orbits. This constellation reached again its Full-Operational-Capability (FOC) in late 2011 with 24 satellites, (Tamazin, 2011). After the GLONASS recovery, the idea of integrating these two measurements of the GPS and the GLONASS constellations, their problems and errors got more attention in the literature.

Due to the military purposes of GPS and GLONASS, they were not originally designed to be combined to each other, so the integration is not a straightforward process and they are different from several aspects. Three of the major differences that should be taken into account are: different time, coordinates reference frames, and signal modulation techniques.

Time reference frame: The GLONASS time (GLONASST) is the time standard of the system which has a three hours offset with its time reference frame, (Tamazin, 2011). GLONASS time reference is the Universal Coordinate Time, Soviet Union standard (UTC-SU). While GPS time (GPST) uses UTC time reference frame maintained by the United States Naval Observatory (UTC-USNO). GPST is accurate within a nanosecond level of accuracy with respect to the UTC-USNO. GLONASS broadcasts the difference of the GLONASST and UTC-SU directly into the navigation massage while GPS broadcasts the parameter to convert GPST into the UTC-USNO.

Coordinate reference system: GLONASS uses PZ90 (Russian acronym: Parametry Zemli 1990). PZ90 is an Earth-Center Earth-Fixed (ECEF) reference frame which is slightly different from the WGS84 (World Geodetic System 1984). WGS84 can be obtained with a rotation of -0.33 arecsecond about the Z-axis of PZ90, (Rossbach, Habrich et Zarraoa, 1996). This transformation should be performed for all the satellites positions and all the parameters in PZ90.

Signal modulation technique: The major problem in GPS/GLONASS integration is caused by different signal modulation techniques. GPS signals are modulated by Code Division Multiple Access (CDMA), while GLONASS modulation technique is Frequency Division

Multiple Access (FDMA). This modulation causes three main problems, (Keong et Lachapelle, 1999):

1. After the standard DD technique, the ambiguity parameters are no longer integer. So lots of ambiguity resolution methods cannot be applied.

2. Due to the different frequency in the FDMA modulation, time delay of each travelled signal is different from another. So receiver clock error cannot be estimated by the recursive positioning algorithm that is usually used in the CDMA modulation. The design matrix then has a rank deficiency and the normal matrix becomes singular, which means the ambiguity parameters cannot be separated from receiver clock error, (Wang et al., 2001).

3. Scale the clock error by different frequencies, causes an extra clock error.

There are different methods to overcome these problems:

1. **Clock error estimation by Pseudorange:** The first method proposes to use pseudorange to calculate the receiver clock error and substitute in the DD method. (Pratt, Burke et Misra, 1998) handled the clock bias problem in GLONASS measurements by estimating with differential pseudorange. In this method the procedure is done in two steps. In the first step, the clock error will be estimated and in the second step, this parameter will be treated as a known parameter. Clock accuracy of civil receivers specially the low cost ones, are accurate up to nanoseconds, which can cause an error about 30 cm. Another drawback of this method is the potential strong multipath effect on pseudorange, (Leick, 1998). To reduce these errors the SD GLONASS and DD GPS pseudorange can be used, (Wang et al., 2001);

2. **Clock error elimination:** There are three main methods to eliminate the clock error as follows (Leick, 1998):

- **scale to distance or Mean frequency:** This method scales the L1 frequency band into a mean frequency. The DD technique thus, can eliminate the clock error. The problem that we might encounter is the new DD ambiguity term parameter is no longer an integer linear combination of the SD technique ambiguities. So lots of popular and efficient ambiguity fixing methods cannot be used;

- **scale to common frequency:** Scaling the L1 frequencies into a common frequency is another proposed method which preserves the integer nature of the DD ambiguity parameters. But the problem is that the common frequency for GLONASS L1 is extremely short which makes the integer calculation impossible. Since all the existing ambiguity resolution methods are in centimeter level of accuracy, they cannot be used to fixing the micrometer integer ambiguities produced by common frequency method;

- **dual frequency estimation:** Using two frequencies of GLONASS is another approach. The drawback of this method is that low cost receivers do not have access to L2 as well as an accurate pseudorange which is needed to obtain accurate initial ambiguity estimation. Relatively higher level of random noise which is multiplied by factor of 2 is another drawback of this method.

3. **Reparameterization:** Due to the different carrier frequency of GLONASS some of unknown errors especially clock error are not canceled out in the standard DD method. In GPS/GLONASS combination therefore, the standard DD/SD method causes rank deficiency in the design matrix and singularity in the normal matrix. This means the ambiguity parameters cannot be separated from clock error parameters (Wang, 1998). Moreover, due to the different error sources of GPS and GLONASS

such as inter-channel hardware biases, the standard differential methods cannot guaranty a reliable solution. It has been shown by (Kozlov et Tkachenko, 1997) that the singularity of SD carrier can be removed by adding SD pseudorange observation in equations. Using SD Pseudorange has several advantages as following:

- diagonal covariance matrix;
- error elimination in the reference satellite;
- detection of the carrier cycle slip.

The existence of high level of noise in pseudorange causes a high correlation between SD ambiguities and the relative receiver clock errors. Due to the integer nature of the DD ambiguities, they can be more easily fixed. Therefore, a suitable SD/DD combination can be applied in order to obtain a combination which is less sensitive to incompatibilities. As it is shown in (Wang, Stewart et Tsakiri, 1998), the DD ambiguities obtained by estimated SD ambiguities are equal to the DD ambiguities which directly reparametrized by SD observation.

SD and DD methods in Pseudorange and carrier phase of GLONASS and GPS make a combination which is presented as the following notation, (Wang, 1998; Wang et al., 2001):

$$[a][b] - [c][d] - [e] \tag{3.56}$$

where $[a]$ is the GPS pseudo-range mode, $[b]$ is the GLONASS pseudo-range mode, $[c]$ is the GPS carrier phase mode, $[d]$ is the GLONASS carrier phase mode, $[e]$ is the DD carrier phase or DD ambiguity formulation. Relative redundancy for each model is presented in Table 3.2 in which n_e is the number of epochs in a solution, SD

is used as single difference, DD as double difference, M as mixed formulation and S as separated formulation.

Note:

- the models with M notation (mixed formulation) are reliable only when the initial phases for GPS and GLONASS are identified;

- model 1 and 12 are the models that have been implemented in commercial software applications.

- the number 12 has been identified as the optimal method based on its ambiguity resolution performance and the sensitivity level to clock error parameter. This is due to the inter system biases and initial phases elimination in this method;

Table 3.2 Mathematical models for combined GPS and GLONASS positioning
Adapted from Wang (1988)

Model numbers	**Model names**	**Relative redundancy**
1	SS-SS-S	3 n_e -2
2	SS-SD-S	3 n_e -1
3	SS-DD-S	n_e
4	SD-SS-S	2 n_e -2
5	SD-SD-S	n_e -1
6	SD-DD-S	0
7	DS-SS-S	2 n_e -2
8	DS-SD-S	n_e -1
9	DS-DD-S	0
10	SS-SS-M	3 n_e -2
11	SS-DD-M	2 n_e -1

12	SD-SS-M	2 n_e -2
13	DS-SS-M	n_e -1
14	DS-SS-M	2 n_e -2
15	DS-DD-M	n_e -1

- in general the separated DD ambiguities (GPS-GPS or GLONASS-GLONASS) have superior results compare to the mixed DD ones. That is because of the large differences between GPS and GLONASS frequencies with respect to the difference between GLONASS frequencies themselves. As a result, any remaining error can be eliminated in separated DD method more effectively than the mixed ones, (Wang, Stewart et Tsakiri, 1998);
- one of the most significant advantages of GPS and GLONASS integration, is to help to obtain fast fixed ambiguity in Precise Point Positioning (PPP) methods.

In this work, GPS only will be used for a question of time but it is clear that GLONASS measurements would benefits to the ADS solution. Some of important aspects of this improvement are as follows:

- **higher availability of satellites:** The GLONASS satellites with 64.8° inclination have more coverage around the North pole and South pole while GPS satellites with 55° inclination have less coverage around those area. The combination of measurements of these two constellations can increase the precision of the solution as well as reliability of the designed attitude determination system;

- **faster initial guess of ambiguity parameters:** In (Jokinen et al., 2012), GPS and GLONASS integration is used to obtain the float ambiguity solution and this decreased the required time for initial ambiguities with respect to GPS alone by 10.3%. It also decreases the average 3D and vertical position errors at initial calculation;

- **faster fixed ambiguity parameters:** GPS and GLONASS integration increases the ambiguity resolution speed by increasing the number of visible satellites, (Al-Shaery et al., 2012);

- **lower hardware cost:** Inexpensive mixed GPS+GLONASS single frequency receivers can replace expensive dual-frequency receivers with only C/A code processing, because results in ambiguity resolution and position quality are the same, (Kozlov et Tkachenko, 1997; Rapoport, 1997).

3.4 Conclusion

This chapter has presented different algorithms required in the project. Then, their advantages and disadvantages as well as their comparison are discussed to conclude a suitable method for each part.

As conclusion, for ambiguity resolution method, LAMBDA method seems to be more promising due to its lower computational time and higher success rate. For attitude determination part, the baseline method seems to be more promising compared to the direct method since a lot of works in literature have been done using this technique. Among baseline methods, as SVD is one of the most robust estimators for minimizing Wahba's loss function, it seems to be outstanding among other methods in the literature. For the part of the GLONASS and GPS integration, although these two constellations have several differences especially in terms of clock error elimination techniques and signal modulation technique, these problems can be overcome by the explained methods in section 3.3.

However, in this thesis this part is limited with the theoretical research that has been done in this chapter. It is shown that the GLONASS and GPS integration not only can increase the availability of the satellites, faster ambiguity initial guess and fixed solution but a high cost dual-frequency attitude determination system can be replaced by inexpensive mixed GPS+GLONASS single frequency system. In the next chapter, the baseline estimation module, its mathematical procedure and our contribution will be discussed in detail.

CHAPTER 4

ADS ALGORITHM DESIGN

The research methodology of this thesis consists in splitting the project into individual modules. The designed Attitude Determination System (ADS) consists of two main modules, baseline estimation module and attitude determination module. This chapter presents the baseline estimation as well as the attitude determination module results. First, in order to have an overall overview, each module task and their relation are presented briefly in the global ADS algorithm flowchart Figure 4.1. Then each module will be described in detailed mathematically including the algorithm procedures. Afterwards, our contributions to the work will be presented.

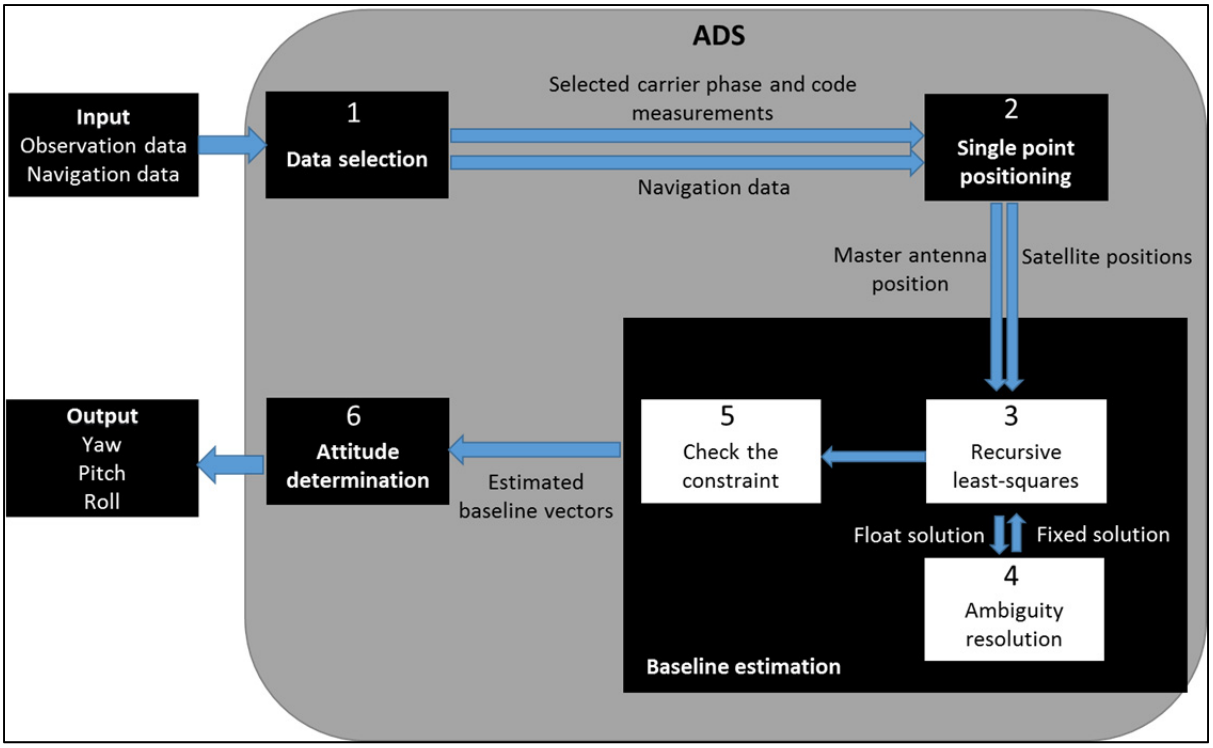

Figure 4.1 Global ADS algorithm flowchart

The inputs of the designed ADS consist of at least two observation and two navigation files in Receiver INdependent EXchange (RINEX) format. Observation file contains GPS

observables including three fundamental quantities: Time, phase, and range. The navigation file contains information about the satellites themselves such as their Keplerian parameters, satellite clock bias and drift, and satellite health. The outputs are three Euler angles, Yaw, Pitch and Roll in local frame. The following section will present them in details.

4.1 Data selection

This section presents the first module of the designed ADS algorithm which select a proper period of data within the observation file. Each GPS receiver is synchronized with GPS time, however, the U-blox receivers have clock jumps of 1 millisecond in order to compensate of their clock drift. The first part of this module checks if observations data start at the same time in the order of millisecond. If this is not the case, it will search for a common time to start taking the measurements. Epoch is defined for each set of data which corresponds with the data rate.

After the synchronization process, the proper raw measurements will be selected. An autonomous algorithm is designed that chooses the best period of the observation with respect to two algorithm parameters which can be selected by the user. The first parameter is the desired minimum number of satellites and the desired minimum number of epochs to be analysed. The algorithm will take care of finding a period in the file which contains the selected number of satellites visible during the selected minimum number of epochs. Three criterias to choose satellites are as follows:

- **elevation angle:** Satellites with the elevation angle higher than 10 ° will be selected;

- **signal to noise ratio:** Satellites with the signal to noise ratio (C/N_0) more than 30 dBHz will be selected;

- **number of satellites:** Raw measurements from an epoch will be deleted if the number of satellites which passed previous criterias in that epoch is less than four.

4.2 Single point positioning algorithm with pseudorange

After proper data selection and synchronization, the ADS algorithm estimates the master antenna position. However, this step is out of the scope of this project, but to have an estimation of master antenna position, a Single Point Positioning (SPP) algorithm developed by (Borre, 2003) is used. The SPP algorithm calculates the master antenna position without going through a time consuming algorithm in order to find ambiguities. This module calculates the satellite positions as well. The mathematical procedure of the SPP algorithm is presented as follows. First the distance between the receiver and the satellite can be written as:

$$\rho_i^j(t) = \sqrt{(X^j(t) - X_i)^2 + (Y^j(t) - Y_i)^2 + (Z^j(t) - Z_i)^2} \equiv f(X_i, Y_i, Z_i) \tag{4.1}$$

where j is the satellite number and i is the receiver number. The initialization process can be taken into account with:

$$\begin{aligned} X_i &= X_{i0} + \Delta X_i \\ Y_i &= Y_{i0} + \Delta Y_i \\ Z_i &= Z_{i0} + \Delta Z_i \end{aligned} \tag{4.2}$$

where X_{i0}, Y_{i0}, Z_{i0}, is the initial guess of receiver's position in the first iteration.
Using the Taylor series with respect to the approximate point and truncated after the linear term, Equation (4.1) becomes:

$$\begin{aligned} f(X_i, Y_i, Z_i) &= f(X_{i0} + \Delta X_i Y_{i0} + \Delta Y_i Z_{i0} + \Delta Z_i) \\ &= f(X_{i0}, Y_{i0}, Z_{i0}) + \frac{\partial f(X_{i0}, Y_{i0}, Z_{i0})}{\partial X_i}\Delta X_i + \frac{\partial f(X_{i0}, Y_{i0}, Z_{i0})}{\partial Y_i}\Delta Y \\ &\quad + \frac{\partial f(X_{i0}, Y_{i0}, Z_{i0})}{\partial Z_i}\Delta Z_i \end{aligned} \tag{4.3}$$

$$\rho_i^j(t) = \rho_{i0}^j(t) - \frac{X^j(t) - X_{i0}}{\rho_{i0}^j(t)}\Delta X_i - \frac{Y^j(t) - Y_{i0}}{\rho_{i0}^j(t)}\Delta Y_i - \frac{Z^j(t) - Z_{i0}}{\rho_{i0}^j(t)}\Delta Z_i \tag{4.4}$$

Thus by neglecting the ionospheric and tropospheric error, the code measurement Equation (2.5) can be linearized as follows:

$$R^j(t) = \rho_{i0}^j - \frac{X^j(t) - X_{i0}}{\rho_{i0}^j(t)}\Delta X_i - \frac{Y^j(t) - Y_{i0}}{\rho_{i0}^j(t)}\Delta Y_i - \frac{Z^j(t) - Z_{i0}}{\rho_{i0}^j(t)}\Delta Z_i + c\delta^j(t) - c\delta_i(t) \tag{4.5}$$

By replacing the unknown terms in one side, the final matrices can be written as:

$$AX = B \tag{4.6}$$

$$A = \begin{pmatrix} -\frac{X^1(t) - X_{i0}}{\rho_{i0}^1(t)} & -\frac{Y^1(t) - Y_{i0}}{\rho_{i0}^1(t)} & -\frac{Z^1(t) - Z_{i0}}{\rho_{i0}^1(t)} & -c \\ \vdots & \vdots & \vdots & \vdots \\ -\frac{X^j(t) - X_{i0}}{\rho_{i0}^j(t)} & -\frac{Y^j(t) - Y_{i0}}{\rho_{i0}^j(t)} & -\frac{Z^j(t) - Z_{i0}}{\rho_{i0}^j(t)} & -c \end{pmatrix} \tag{4.7}$$

$$B = \begin{pmatrix} R_i^1(t) - \rho_{i0}^1(t) - c\delta^1(t) \\ \vdots \\ R_i^n(t) - \rho_{i0}^n(t) - c\delta^n(t) \end{pmatrix} \qquad X = \begin{pmatrix} \Delta X_i \\ \Delta Y_i \\ \Delta Z_i \\ \delta_i(t) \end{pmatrix} \tag{4.8}$$

As this step is a hypothesis and not in the scope of this thesis, we would like to test the SPP algorithm and present the result here. In order to test the SPP algorithm, the Spirent GSS9000 simulator and u-blox LEA-6T receivers are used. We connected two u-blox LEA-6T receivers to two simulator RF outputs. Clock of the receivers are not synchronized together by hardware, the simulator record is in normal condition and both receivers are in stationary mode. We located two receivers with 10 meter baseline length on North direction, the true heading is 0.04°and the true elevation is 0.03°. The data rate for this test case is 1Hz. The date of the record is 13 may 2015 and the record duration is 30 minutes. The introduced SPP algorithm in this section is used to calculate the master antenna position and the result is

presented in Figure 4.2. The used reference point for the master antenna position is calculated by GNSS Solution software (Solution, 2007).

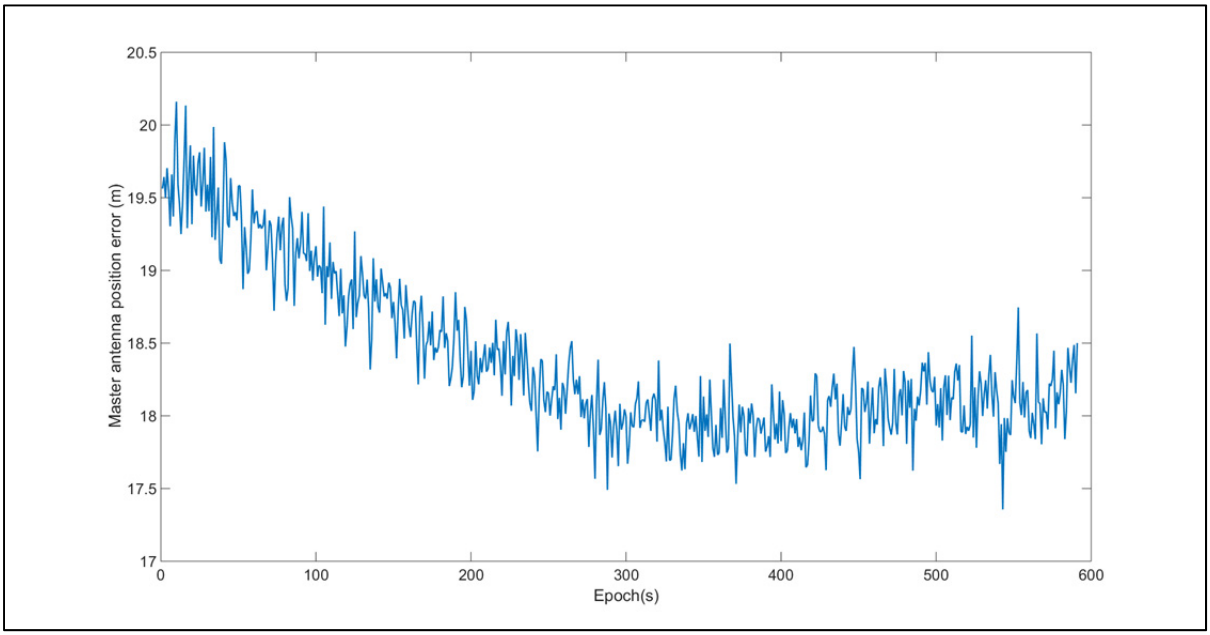

Figure 4.2 Master antenna position error by using SPP algorithm

The resulting master antenna position error in Figure 4.2 is bigger than the baseline used for this test case (10 meter) and the achieved precision in in the SPP algorithm is not enough to use in the ADS algorithm. As in the SPP algorithm the differential techniques are not used, the ionospheric and the tropospheric error as well as receiver noise can affect the pseudorange. The ionospheric and the tropospheric modelling, combining code and carrier phase measurements as well as synchronizing receivers by an external clock are among some future works for improving the single point positioning algorithm. As a result, we will continue to analyze our designed ADS by using a reference point calculated by the GNSS Solution software (Solution, 2007) for the master antenna position instead of estimated one from the SPP algorithm for real data sets in section 5.3 and 5.4.However, the satellite positions calculated in this module will be used in the next section in order to calculate the baseline vectors. The detailed of the GNSS solution software will be presented in the section 5.3 and 5.4.

4.3 Presentation of designed baseline estimation algorithm

For this section, the designed baseline estimation algorithm is presented and developed based on (Chang, Paige et Yin, 2005). One of the main advantages of this method is to reduce the computational cost of the algorithm with preserve the accuracy. All the three aspects of the algorithm implementation which are numerical reliability, computational efficiency and matrix storage efficiency have been considered. The matrix storage efficiency is addressed to optimization of the used memory by intermediate matrix calculations.

The Chang method uses both code and carrier measurements, and it does not need prior information in case of dynamic applications such as an initial baseline vector. The baseline used to test this method is ultra-short (1 meter) and the only measurement has been used is L1.

In many applications such as GPS, the measurements models are not linear and they have the following form:

$$y = f(x) + v \tag{4.9}$$

where $y \in R^m$ is a measurement vector or observed vector, f is a nonlinear function, $x \in R^n$ is an unknown parameter vector, and v is a noise vector assumed to be Identically Independently Distributed (IID). A typical approach to this estimation problem is to solve the following nonlinear least-squares system:

$$\min F(x) = \|y - f(x)\|_2^2 \tag{4.10}$$

The following sections will present optimization process to solve the previous equation.

4.3.1 General optimization problem

In order to get the solution to the equation (4.10), the Newton method is briefly introduced here. Assuming the following general problem:

$$\min f(x) \tag{4.11}$$

where *f* is a twice continuously differentiable function of measurements. This actually means that we seek a local minimizer x' i.e., $f(x') \leq f(x')$ for all *x* near x'.

Let *f* be twice continuously differentiable. If x' is a local minimizer of *f*, then $\nabla f(x')$ and moreover $\nabla^2 f(x')$ is symmetric nonnegative definite. Conversely, if $\nabla f(x') = 0$ and $\nabla^2 f(x')$ is symmetric positive definite, then x' is a local minimizer of *F*.

Let assume the initial point x_0.is available. The Taylor series expansion about x_0 gives:

$$F(x) = F(x_0) + \nabla F(x_0)^T (x - x_0) + \frac{1}{2}(x - x_0) + \frac{1}{2}(x - x_0)^T \nabla^2 F(x_0) \tag{4.12}$$

So instead of solving Equation (4.11), the following quadratic optimisation problem is used:

$$min\ M(x) = F(x_0) + \nabla F(x_0)^T (x - x_0) + \frac{1}{2}(x - x_0)^T \nabla^2 F(x_0)(x - x_0) \tag{4.13}$$

$$\nabla M(x) = \nabla F(x_0) + \nabla^2 F(x_0)(x - x_0) \nabla^2 M(x) = \nabla^2 F(x_0) \tag{4.14}$$

We assume that $\nabla^2 F(x_0)$ is symmetric positive definite, which is true if x_0 is close enough to the local minimizer, then $x_1$is a local minimum of $M(x)$if and only if:

$$\nabla M(x_1) = \nabla F(x_0) + \nabla^2 F(x_0)(x_1 - x_0) = 0 \tag{4.15}$$

$$x_1 = x_0 + \rho_0 \tag{4.16}$$

where ρ_0 referred to the search direction and it can be calculated from:

$$\nabla^2 F(x_0)\rho_0 = -\nabla F(x_0) \tag{4.17}$$

Since $\nabla^2 F(x_0)$ is symmetric positive definite ρ can be calculated by Cholesky factorization of $\nabla^2 F(x_0)$.

4.3.1.1 RLS mathematical procedure

This section presents the proposed Recursive Least-Squares (RLS) algorithm to calculate the baseline vectors. Instead of using double difference measurements RLS algorithm uses single difference and eliminates the error using the Householder transformation, (Chang, Paige et Yin, 2005). In order to calculate the baseline *x* the geometry of the problem can be illustrated as follows:

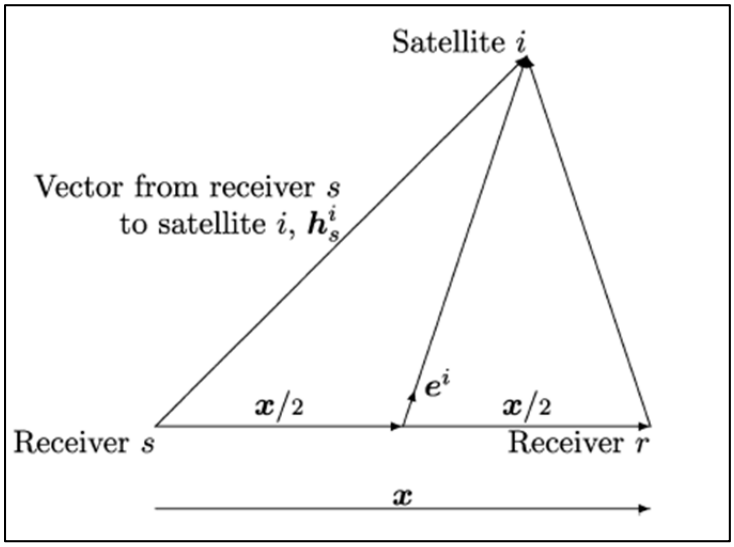

Figure 4.3 Geometry for two receivers and one satellite
Taken from Chang, Paige et Yin (2005)

$$x = h_s^i - h_r^i e^i = \frac{h_s^i - \frac{x}{2}}{\left\| h_s^i - \frac{x}{2} \right\|} = \frac{h_s^i - h_r^i}{\left\| 2h_s^i - x \right\|} \tag{4.18}$$

where h_s^i is the vector from receiver *s* to satellite *i*, e_i is the unit vector from the midpoint of the baseline to satellite *i*, ρ_s^i is the geometrical distance between the receiver and satellite. The previous Equation (4.18) can be rewritten as:

$$\begin{aligned}\left(\left\|2h^i - x\right\| e^i\right) x &= \left\|h_s^i\right\|^2 - \left\|h_r^i\right\|^2 \\ &= \left(\left\|h_s^i\right\| - \left\|h_r^i\right\|\right)\left(\left\|h_s^i\right\| + \left\|h_r^i\right\|\right) \\ &= \lambda\left(\rho_s^i - \rho_r^i\right)\left(\left\|h_s^i\right\| + \left\|h_s^i - x\right\|\right)\end{aligned} \tag{4.19}$$

We define:

$$\omega^i e^i = \frac{2h_s^i - x}{\left\|h_s^i\right\| + \left\|h_s^i - x\right\|} \tag{4.20}$$

So from the Equation (4.19) and the Equation (4.20) it can be written:

$$\lambda^{-1}\left(\omega^i e^i\right)^T x = \rho_s^i - \rho_r^i \tag{4.21}$$

From the Equation (2.14) and by combination of two errors in one we have:

$$\Delta\phi_{r,s}^j \approx \rho_s^i - \rho_r^i + \lambda\Delta N_{r,s}^j + \Delta\mu_{rs,\phi}^j \tag{4.22}$$

where $\Delta\,\mu_{rs,\emptyset}^j$ is the single difference error added all together.

Because all units are in wavelengths the Equation (4.22) is divided by λ Then by substitution of the Equation (4.21),we have:

$$\Delta\phi_{r,s}^j = \lambda^{-1}\left(\omega^i e^i\right)^T x + \Delta N_{r,s}^j + \Delta\mu_{rs,\phi}^j \tag{4.23}$$

And by applying the same procedure for code measurement we have:

$$\Delta\rho_{r,s}^j = \lambda^{-1}\left(\omega^i e^i\right)^T x + \Delta\mu_{rs,\phi}^j \tag{4.24}$$

At each epoch there are two measurements, single difference carrier phase and code measurements for each common visible satellite between two receivers. Now some vectors and matrices will be introduced in order to calculate the baseline vectors as follows:

$$\sigma = \frac{\sigma_\phi}{\sigma_\rho} \tag{4.25}$$

$$y_k^\phi = \begin{bmatrix} \phi_k^1 & \dots & \phi_k^m \end{bmatrix}^T \tag{4.26}$$

$$y_k^\rho = \begin{bmatrix} \rho_k^1 & \dots & \rho_k^m \end{bmatrix}^T \tag{4.27}$$

$$E_k = \lambda^{-1} \begin{pmatrix} (\omega_k^1 e_k^1)^T \\ \vdots \\ (\omega_k^m e_k^m)^T \end{pmatrix} \tag{4.28}$$

$$a = \begin{bmatrix} N^1 & \dots & N^m \end{bmatrix}^T \tag{4.29}$$

where $\sigma_\phi$and σ_ρ are the standard deviation of phase and code, respectively, m is the number of satellites, y_k^ϕ is the single difference of phase measurements, y_k^ρ is the single difference of the code measurements, E_k is defined as the coefficient matrix of the baseline vector and a is the single difference of the ambiguities. Then it can be written:

$$\gamma = \sqrt{1 + \sigma^2} \tag{4.30}$$

$$s = \frac{\sigma}{\gamma} \tag{4.31}$$

$$c = \frac{1}{\gamma} \tag{4.32}$$

$$F = I_{m-1} - \frac{e_{m-1} e_{m-1}^T}{m - \sqrt{m}}\text{s} \tag{4.33}$$

where σ m is the number of common visible satellite at each epoch, s and c will be used in step 4, F is the upper triangular coefficient matrix of Z. Then the baseline vector, x, can be written in a function of Z and single difference of carrier phase and code measurements as follows:

$$e = [1 \quad \dots \quad 1]^T \tag{4.34}$$

$$\bar{P} = \left[\frac{e_{m-1}}{\sqrt{m}}, F\right] \tag{4.35}$$

$$\begin{bmatrix} \bar{P}y_k^{\phi} \\ \sigma\bar{P}y_k^{\rho} \end{bmatrix} = \begin{bmatrix} \bar{P}E_k \\ \sigma\bar{P}E_k \end{bmatrix} x_k + \begin{bmatrix} F \\ 0 \end{bmatrix} z + \begin{bmatrix} \bar{P}v_k^{\phi} \\ \sigma\bar{P}v_k^{p} \end{bmatrix} \tag{4.36}$$

$$\begin{bmatrix} \bar{P}v_k^{\phi} \\ \sigma\bar{P}v_k^{p} \end{bmatrix} \approx N\left(0, \sigma_{\phi}^2 I_{2(m-1)}\right) \tag{4.37}$$

where e is a vector of 1, $\bar{P}$ is the QR factorization of the coefficient matrix of *Z*.

According to the previous equations and algorithm, here is a summary of all calculation steps. The following applies for the e first iteration:

1. Calculate h_s^i at each epoch for each selected satellite (the vector from stationary receiver to satellite);

2. Set the *x* as 0 and calculate $\omega^i e^i$ from the Equation (4.21) and E_k from the Equation (4.28);

3. Calculate the QR factorisation of $\gamma\bar{P}E_k$ and separate the Q' as the same dimension of *R* and zero matrix and name it *U* and *V* respectively;

4. Perform $y, \bar{y}$ and *g* as follows:

$$y = U\bar{P}\left(cy_k^{\phi} + s\sigma y_k^{\rho}\right) \tag{4.38}$$

$$\bar{y} = V\bar{P}\left(cy_k^{\phi} + s\sigma y_k^{\rho}\right) \tag{4.39}$$

$$g = \bar{P}\left(-sy_k^{\phi} + c\sigma y_k^{\phi}\right) \tag{4.40}$$

5. Take the QR factorization and partition as *S* and *b*:

$$Q^T \begin{bmatrix} cVF \\ -sF \end{bmatrix} = \begin{bmatrix} S_k \\ 0 \end{bmatrix} \quad (4.41)$$

$$Q^T \begin{bmatrix} \overline{y} \\ g \end{bmatrix} = \begin{bmatrix} b_k \\ \overline{b}_k \end{bmatrix} \quad (4.42)$$

6. Calculate z_k and x by back substitution:

$$S_k z_k = b_k \quad (4.43)$$

$$Rx = y - cUF\ Z_k \quad (4.44)$$

The first iteration is now completed.

Now for the next iterations, only part 3 and 5 will be changed and replaced as follows:

1. Instead of part 3 the x_{k-1} will be substituted it into the Equation (4.22);

2. Instead of part 5 the matrix with a part of upper triangular from the previous step will be replaced. By adding S_{k-1} all the previous epochs will be accumulated in order to get a better estimation and it is presented as follows:

$$Q^T \begin{bmatrix} S_{k-1} \\ cVF \\ -sF \end{bmatrix} = \begin{bmatrix} S_k \\ 0 \end{bmatrix} \quad (4.45)$$

$$Q^T \begin{bmatrix} b_{k-1} \\ \overline{y} \\ g \end{bmatrix} = \begin{bmatrix} b_k \\ \overline{b}_k \end{bmatrix} \quad (4.46)$$

The rest of steps are exactly the same i.e 1, 2, 4, 6. In order to simplify to follow the presented mathematical procedure, the algorithm flowchart is presented in Figure 4.4 and Figure 4.5.

For the first iteration, an initial value for the baseline vector is used while from the second iteration the calculated baseline vector from the previous epoch is used to calculate the baseline vector for the actual epoch Figure 4.4. As it is explained above and can be seen in

the Figure 4.5 for the first iteration, the measurements of the current epoch is used while in the other iterations an upper triangular matrix from all previous epochs is added to the current epoch matrix. The results will be analysed in the chapter 5.

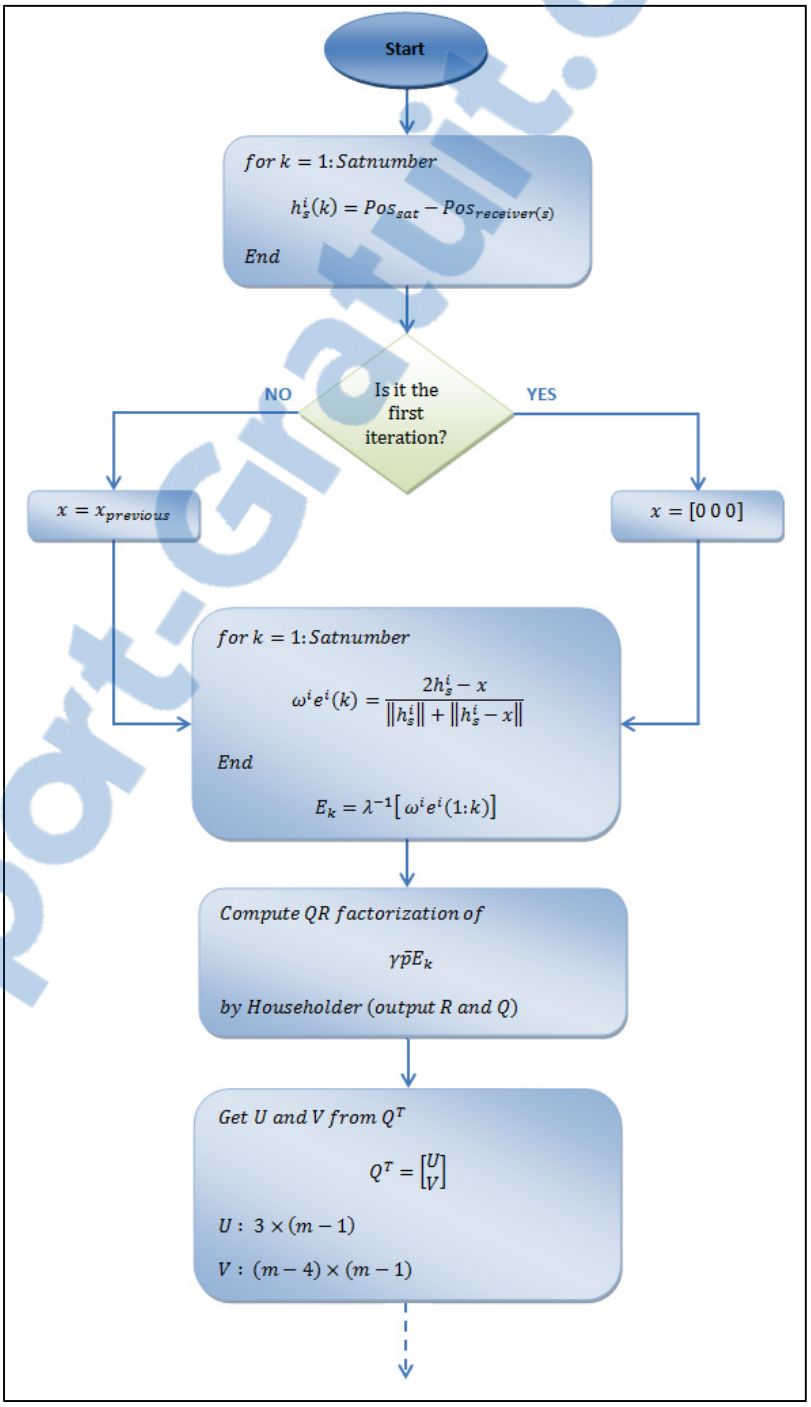

Figure 4.4 Flowchart of the proposed ADS algorithm (Part I)

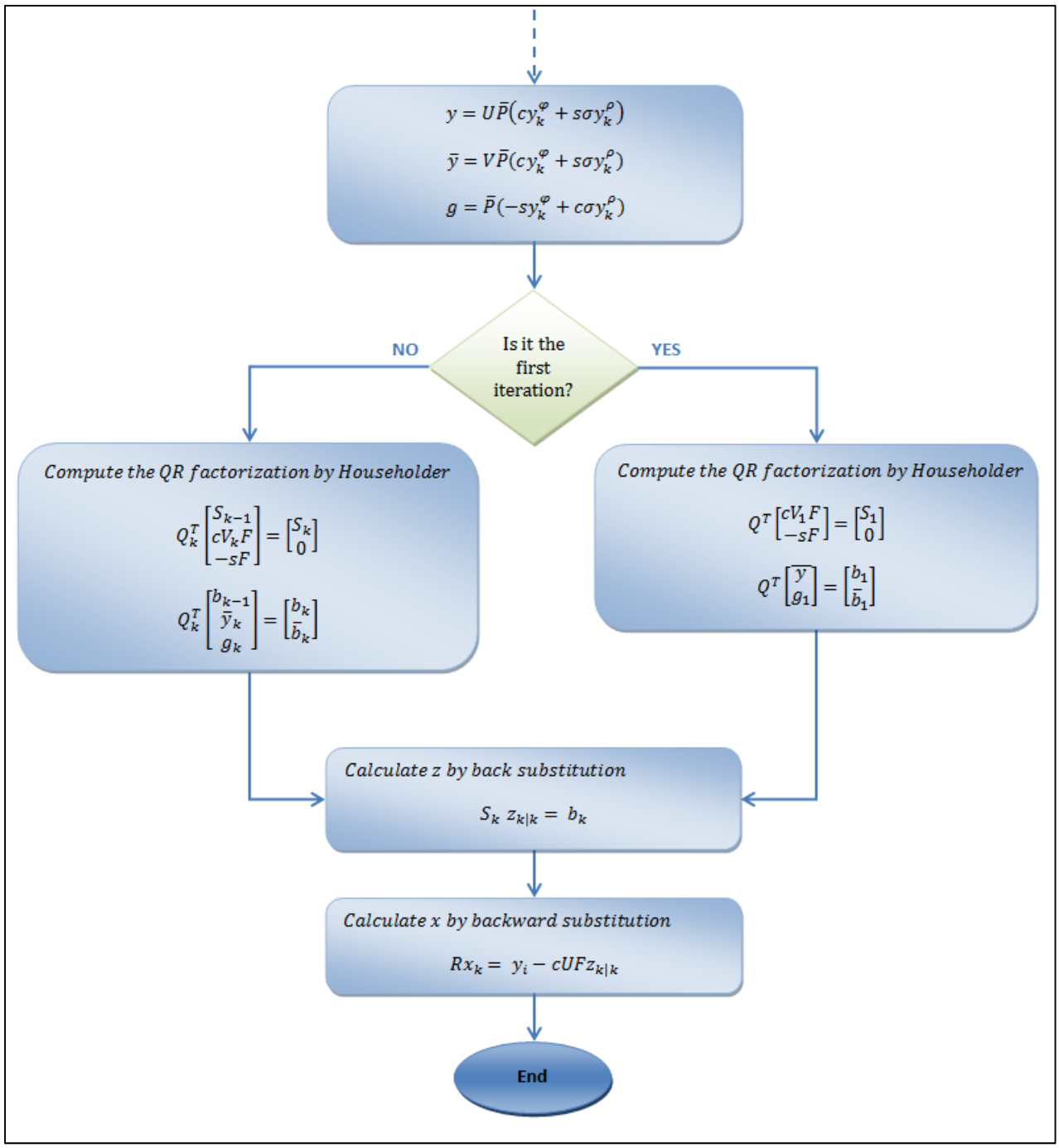

Figure 4.5 Flowchart of the proposed ADS algorithm (Part II)

4.3.2 Ambiguity resolution using LAMBDA method

The calculated ambiguities from the previous section (the RLS method) are real numbers. In order to increase the accuracy, these ambiguities need to be fixed as integer numbers. In this section the LAMBDA method will be explained and the results will be presented in the chapter 5. In the original RLS method after getting the float solution with recursive least square algorithm, the result will be substitute into the Equation (4.44). Our first contribution, is to add an efficient ambiguity resolution method to fix the ambiguity. The method that we chose for this purpose is the LAMBDA method.

Lambda method has five main steps as follows, (De Jonge et Tiberius, 1996):

1. **Shift the ambiguities to -1 and 1:** This part of the algorithm shifts (with integer steps) the center of float solution. This step is necessary before calling decorrelation routine. However, the amount of shift is saved in a variable as it should be added at the very last step back to the estimation;

2. **Decorrelation by Z-transformation:** Z transformation is used for decorrelation process. In this step first the covariance matrix of the float solution will be computed. Then the Z transformation will be calculated;

3. **Initial search space:** This routine is called before performing the search step, namely the discrete search. The purpose of this routine is to find a suitable initial size of the search space which is depends on the number of candidates you need, which should be defined at the very beginning of the algorithm;

4. **Integer minimization:** This routine solves the integer minimization problem by a discrete search over an ellipsoidal region. Now that everything is known, this routine is called to search for the integer solutions (fixed solution) which is the best integer vector close to the float solution.

5. **Z transfer back:** In this routine the fixed solution is Z-transformed back;

6. **Shift back the ambiguities:** In this routine the transformed fixed solution followed by putting back the shift that it is saved in the first routine.

4.3.3 Check the constraint

The second contribution is restriction application to the least square result, in another word, we use a-priori information to check the result. The constraint that we applied in this work, is the length of the baseline which is known.

For this purpose after fixing ambiguities, we substitute fixed ambiguities, *Z*, into the Equation (4.36). Now we can perform the least square method with a restriction. In each iteration we estimate the baseline vector, *x*, then we check the constraint. If the solution meets the condition, the algorithm will pass to the next iteration. However if it does not pass the condition, the algorithm goes back to the least square routine, so the least square function will estimate another solution. This procedure will be continued until the least square solution meet the condition. In this way we can be sure that the solution consider the hardware configuration.

4.4 Attitude determination using the SVD method

Now that the baseline vectors are calculated, the problem is to find an orthogonal matrix with determinant +1 which minimizes:

$$\frac{1}{2}\sum_{i} a_i |b_i - Ar_i|^2 \tag{4.47}$$

where b_i are unit vectors in a body frame, r_i are unit vectors in a reference frame, A is the rotation matrix and a_i are non-negative weights (in our algorithm we do not assign weights

to the attitude solution). This problem is called Wahba's loss function. We used Singular Value Decomposition (SVD) Method which is as follows:

$$B = U\Sigma V^T = Udiag[\Sigma_{11}\Sigma_{22}\Sigma_{33}]V^T \quad (4.48)$$

where U and V are orthogonal and $\Sigma_{11} \geq \Sigma_{22} \geq \Sigma_{33} \geq 0$ and the optimal attitude matrix is:

$$B = U\Sigma V^T = Udiag[\Sigma_{11}\Sigma_{22}\Sigma_{33}]V^T \quad (4.49)$$

The SVD method is the most robust estimators which minimizes Wahba's loss function. Other methods such as FOAM, QUEST, ESOQ and ESOQ2 are less robust because they solve characteristic polynomial equation to find the maximum eigenvalue. However, they are faster than the SVD method which is only preferable when the number of baseline is a lot like star sensor applications, (Markley et Mortari, 1999).

Our first contribution is to design the ADS, consisting 4 mentioned modules and 3 sub-modules. The idea of putting together these modules to meet the defined goal of the project is the first and the main contribution. Also, combining the RLS method with the LAMBDA method and applying the constraint to the solution is our second contribution. Finally, this work allows us to publish and present the following conference paper: Oliazadeh, Nasim; Landry, Rene Jr; Yeste-Ojeda, Omar A; Gagnon, Eric and Wong, Franklin 2015. «GPS-based attitude determination using RLS and LAMBDA methods». In *Localization and GNSS (ICL-GNSS), 2015 International Conference on*. p. 1-7. IEEE. doi: 10.1109/ICL-GNSS.2015.7217146.

In this chapter, the selected methods from the chapter 3 were explained mathematically and were implemented in Matlab. First a period of data is selected to be analysed. Then the SPP algorithm is used to calculate the master antenna position and satellite positions. In order to calculate the baseline vectors, a RLS algorithm is used. Then, the float solution of the ambiguities are fixed with LAMBDA method and the baselines lengths are used as a boundary of the solution. At the end, the three attitude angles are calculated using the SVD method

In the next chapter, the performance and accuracy of the designed ADS algorithm will be analysed by four different test cases. These four test cases have different goals. The two first test cases are simulation. The first test case is designed to validate the designed ADS algorithm and the second one is used to test the algorithm with simulation signals and real receivers. The other two test cases are with real data and they have been designed to address our specific application with a baseline of about 1 meter. We used different equipments and record environments to show the performance of our ADS algorithm from different aspects. Later in the chapter 5 results will be presented and discussed as well

CHAPTER 5

IMPLEMENTATION AND ANALYSIS OF THE RESULTS

In this chapter, the performance of the Attitude Determination System (ADS) is presented with simulated data in Matlab as well as with data from the GPS Spirent Simulator (test case 1 and 2). Then, the performance of the ADS with two real data sets (test case 2 and 3) is presented and analysed. At the end, all four test cases are compared and discussed. For each test case, the used antennas and receivers' type, the record scenario and configuration are presented. Then, the result of the baseline estimation and attitude determination module will be presented and discussed.

5.1 ADS performance analysis, test case 1

In order to analyze the performance of the proposed ADS and make sure that each module works properly, a set of data is simulated in Matlab in both stationary and rotating state. In order to simulate the data a set of satellite positions from (Borre, 2003) is used, which contains 250 second of 10 satellite positions with the known position of one receiver. Then, the configuration is designed similar to the configuration of the objective of this thesis as it is shown in the Figure 5.1.

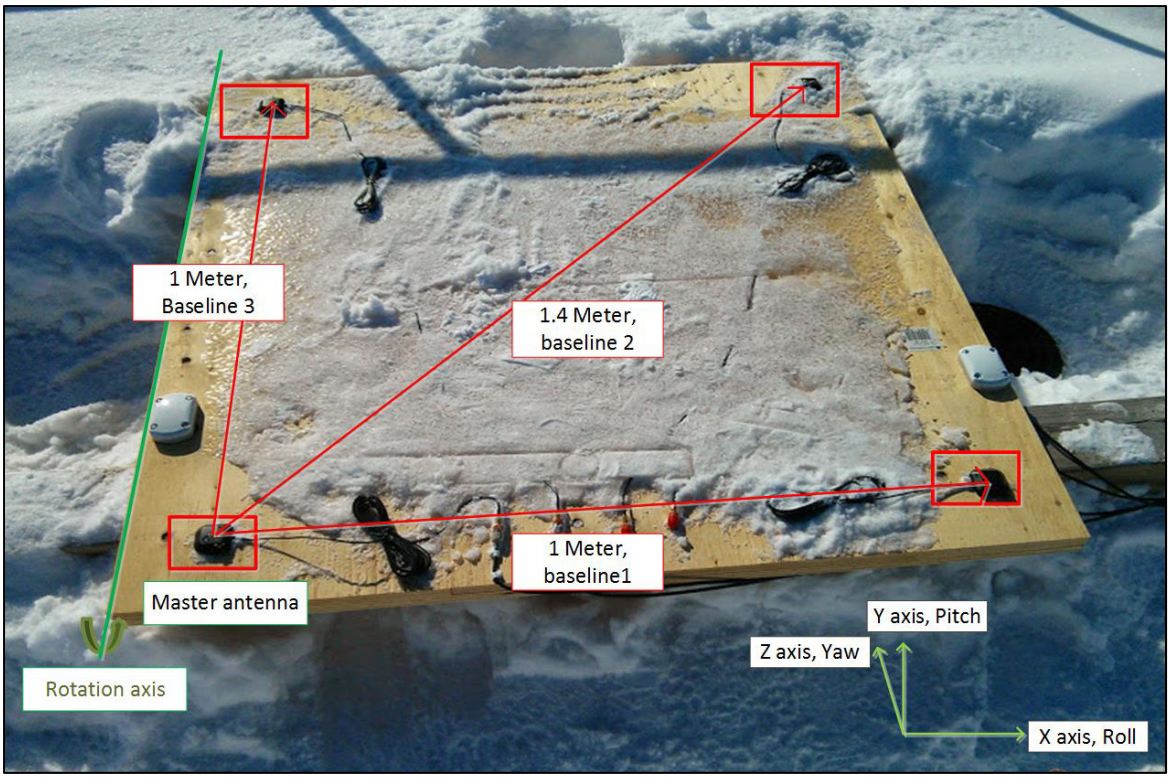

Figure 5.1 Data simulation configuration with Matlab, test case 1

By using this set of satellite positions and knowing the receiver position, the code and carrier phase measurements for each receivers are simulated in Matlab as follows:

$$\rho_r^s = \sqrt{(x^s - x_r)^2 + (y^s - y_r)^2 + (z^s - z_r)^2} + \eta_\rho \tag{5.1}$$

$$\phi_r^s = \frac{\rho_r^s}{\lambda} + \eta_\phi \tag{5.2}$$

where s is for satellite, r is for receiver, λ is at L_1wavelength, η_ρ is the code measurement noise and η_ϕ, the phase measurement noise. The measurement noise is simulated with a standard deviation of 1 m for the code measurements and 10^{-2} m for the carrier phase measurement with normal distribution (white noise model). One receiver is located at the left corner of the platform (master receiver) and three slave receivers are fixed in body frame with baseline vectors defined as $x_1 = (1,0,0)$, $x_2 = (1,1,0)$, $x_3 = (0,1,0)$ with respect to the master antenna position, (the unit is in meter).

The body frame is aligned to the navigation frame at $t = 0$. This coplanar configuration is just an example and not a requirement of our algorithm, and can be applied to any antenna configuration. The code and carrier phase measurements are simulated with the presented configuration in a stationary sate, then, a set of data is simulated when the platform is rotating.

The platform rotates counter-clockwise by 90° about the *y* axis from horizontal position to vertical position, as shown in Figure 5.1. In this simulation, it is assumed that the four receivers are synchronized with an external common clock. During the first 100 seconds, the platform is not rotating; then, it starts to rotate at 1/3° per second. In this simulation, the input data rate is 1 Hz.

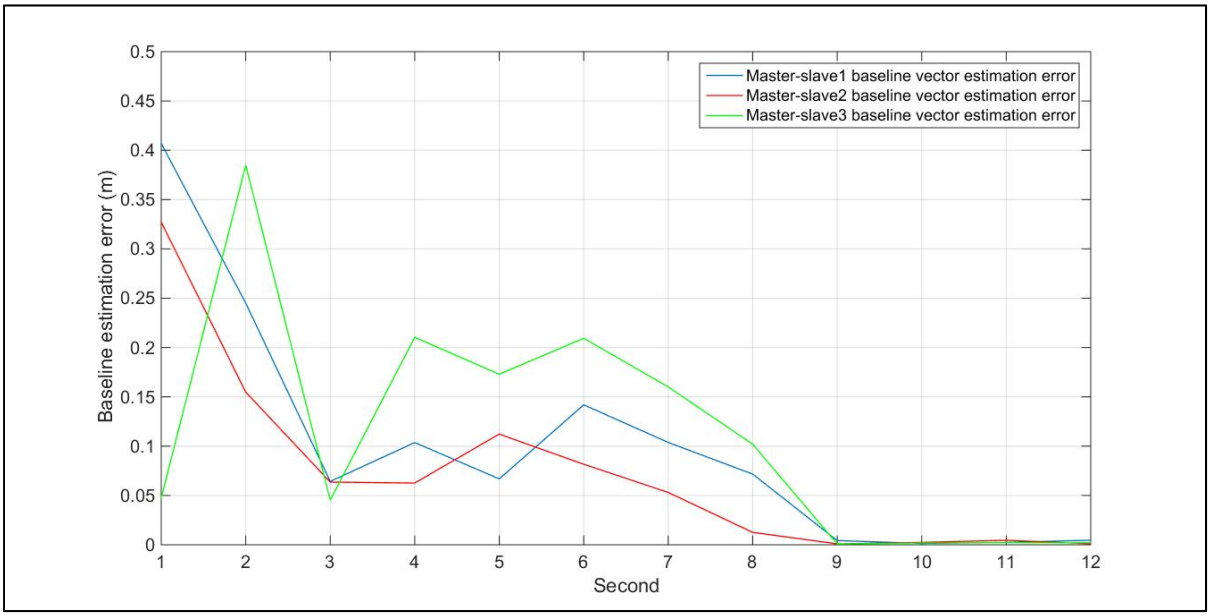

Figure 5.2 Baseline estimation error before convergence in test case 1

Figure 5.2 presents the convergence speed of the proposed ADS in the baseline estimation module for the three baselines. In order to be able to fix ambiguities with LAMBDA method, it is necessary to estimate the covariance matrix of DD ambiguities that is a square matrix with *n-1* elements which *n* is the number of satellites. In this data set, there are 10 satellites that are visible during the whole data set so that there is no rising or setting of satellites.

Because the number of satellites in this test case is 10, so the algorithm takes at least 9 second to be able to estimate the covariance matrix. This is why the proposed method requires 9 seconds to start to fix the ambiguity, as shown in Figure 5.2.

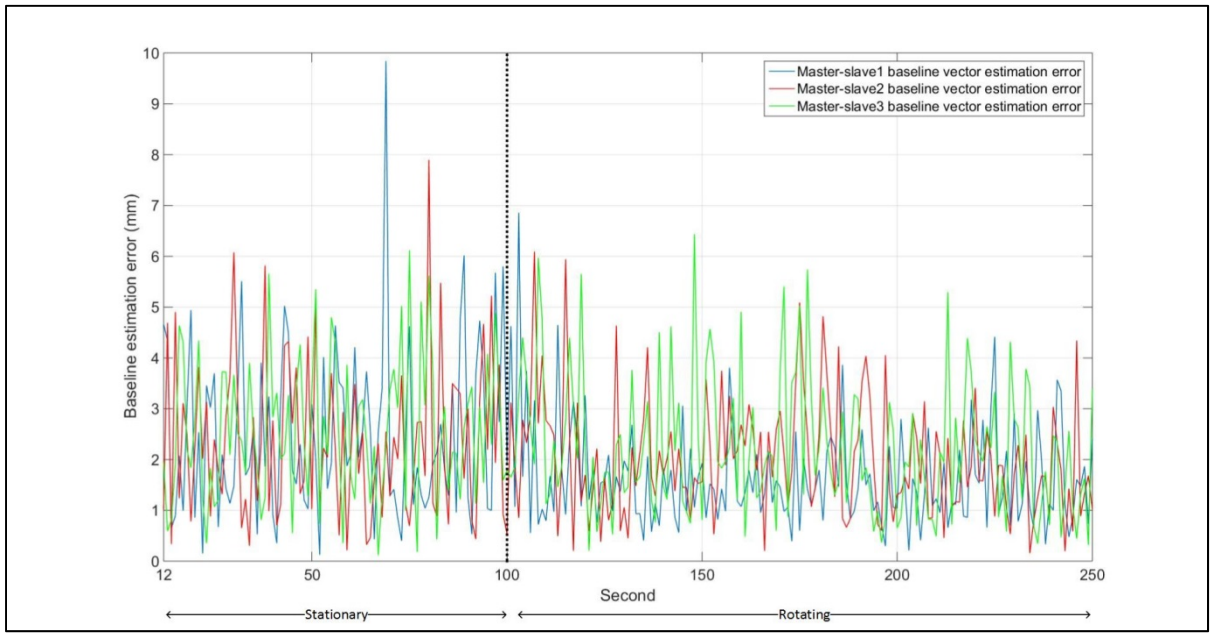

Figure 5.3 Baseline estimation error after convergence test case 1

Figure 5.3 represents the magnitude of three baseline estimation errors after convergence (from epoch 12 to epoch 250). The average errors are 2.0, 2.1, 2.4 (mm) and standard deviations are 1.4, 1.3 and 1.4 (mm) for baseline one to three respectively. The variance of the baselines estimation error for all the three baselines is presented as follows:

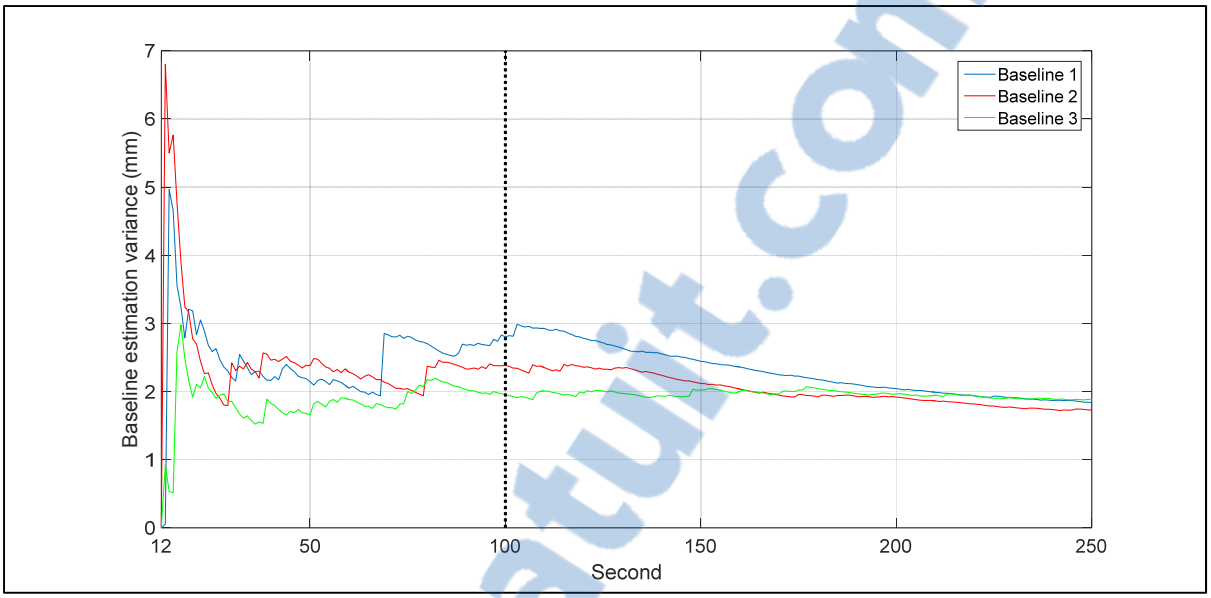

Figure 5.4 Baseline estimation variance

The variance of the estimated baseline from t=12 to t=100 (second), after the 100 second (rotation phase), is 2.83 (mm), 2.37 (mm), and 1.95 (mm) for the baseline 1 to 3 respectively while at t=250 is 1.84 (mm), 1.73 (mm) and 1.88 (mm). The variance for the third baseline remained approximately constant before and after the rotation while the variance of the estimated baseline decreased 34% and 27% for the first and the second baseline Figure 5.4, Table 5.1. The variances of the baseline estimation decreases in time and this is due to the fact that the ADS algorithm is a recursive method which improves the solution by time.

Table 5.1 Variance comparison in test case 1

	Var $_{t=12}$ (mm)	**Var $_{t=100}$ (mm)**	**Var $_{t=250}$ (mm)**
Baseline 1	4.9	2.8	1.8
Baseline 2	6.8	2.3	1.7
Baseline 3	0.9	1.9	1.8

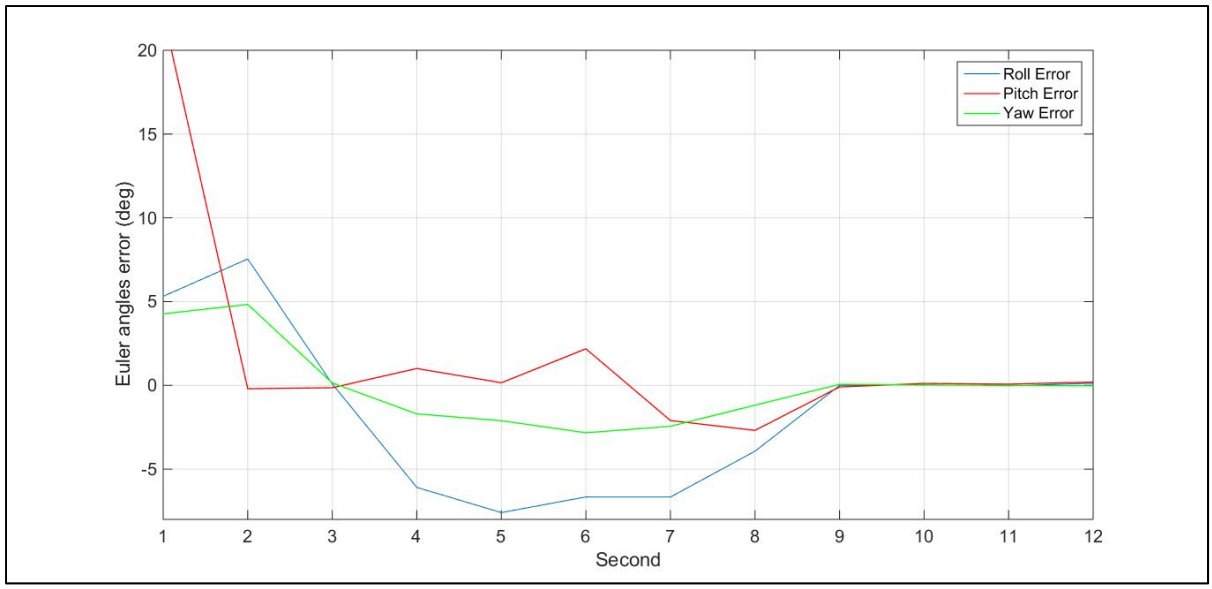

Figure 5.5 Euler angles error before convergence in test case 1

The Figure 5.5 presents the convergence time of the designed ADS for the attitude determination module. As expected, the convergence time matches the one attained when computing the baseline vectors, as no additional delay is introduced by the algorithm itself. Figure 5.6 represents the Euler angles error after the convergence. The biases from the t=12s to t=250s are -0.0094°, 0.0083°, 0.0057° and the standard deviations in the interval are 0.1201°, 0.0962° and 0.0620° for roll, pitch and yaw respectively. Euler angle's RMSE of our proposed method after convergence are 0.0621°, 0.0964° and 0.1202° for yaw, pitch and roll respectively. The computational time of ADS for this test case has an average of 50 ms.

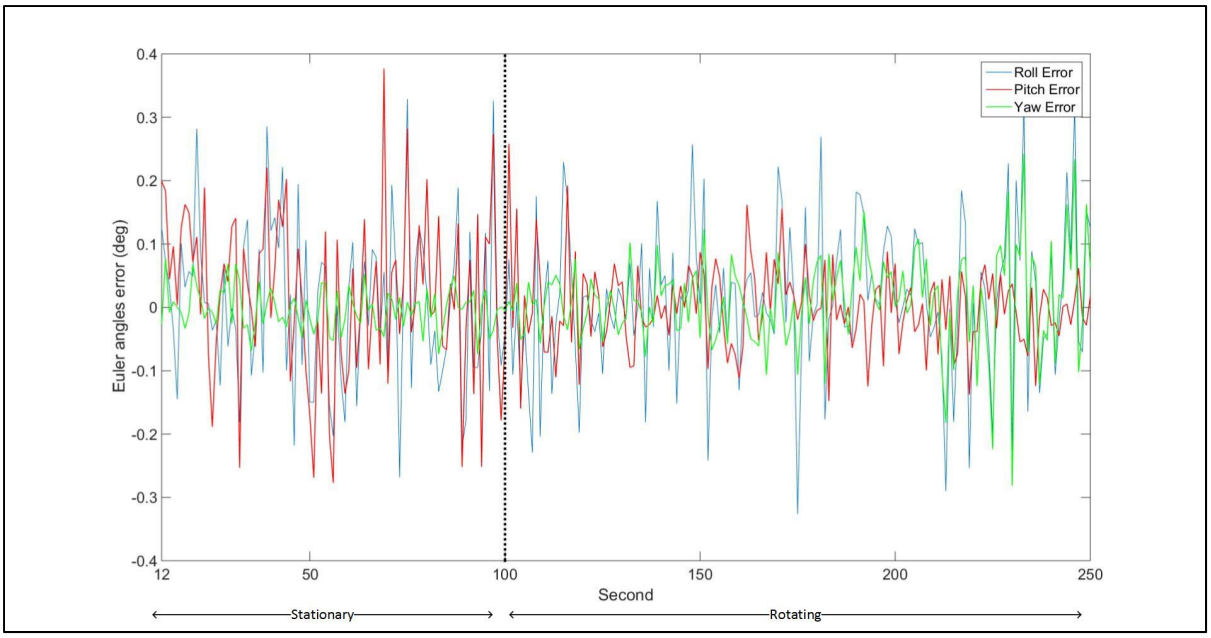

Figure 5.6 Euler angles error after convergence in test case 1

The moving variance of the yaw, pitch, and roll is as follows:

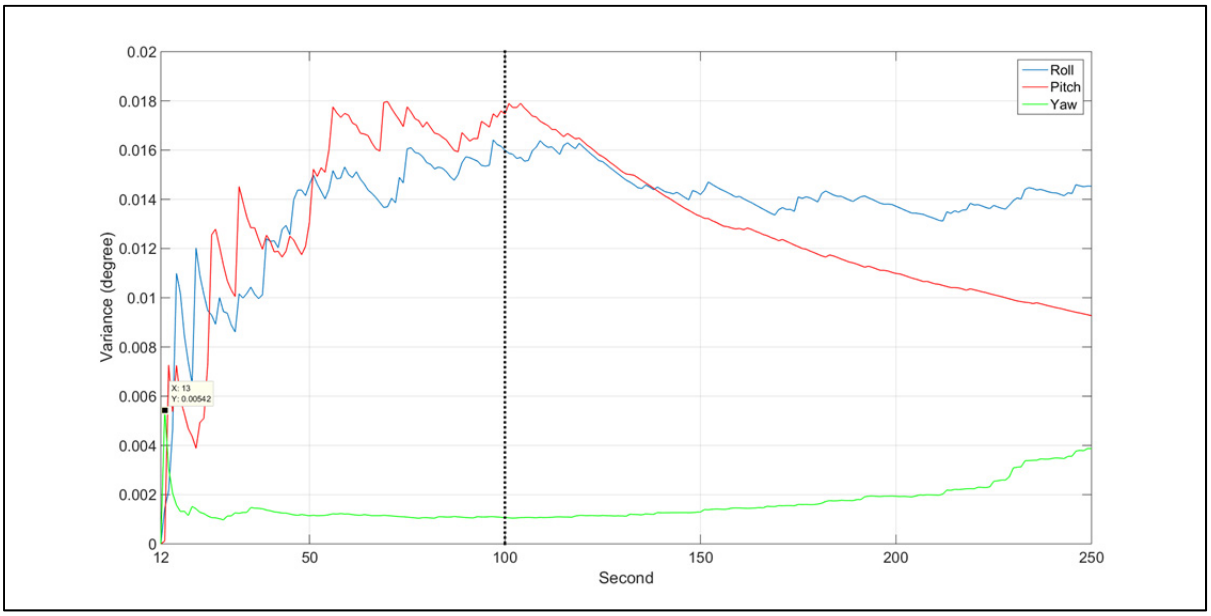

Figure 5.7 Euler angles estimation variance

The variance of the estimated roll and yaw remained approximately the same before and after the rotation while the variance of the pitch decreased by 47% before and after the rotation Figure 5.7. This is probably because that the pitch angle is the only angle that changes in this test case, so the solution improves by time.

Table 5.2 Variance comparison for Euler angles estimation

	Var $_{t=12}$ (mm)	**Var $_{t=100}$ (mm)**	**Var $_{t=250}$ (mm)**
Roll	0.01	0.015	0.014
Pitch	0.007	0.017	0.009
Yaw	0.005	0.001	0.003

The variance of the roll angle is 4.6 times more than the variance of the yaw angle while the variance of the pitch angle is 3 times more than the yaw angle as it is shown in Table 5.2.

Next, the ADS is compared to the Chang algorithm based on (Chang, Paige et Yin, 2005). The Chang algorithm was implemented in Matlab for analysis and comparison. Figure 5.8 represents the convergence time for both methods when estimating the first baseline. The results clearly show a significant performance improvement in convergence time as well as in baseline estimation error after convergence, Figure 5.9. The achieved improvement is due to the fixing the float solution of the ambiguities to integer numbers and considering the baseline length as a constrained to the solution.

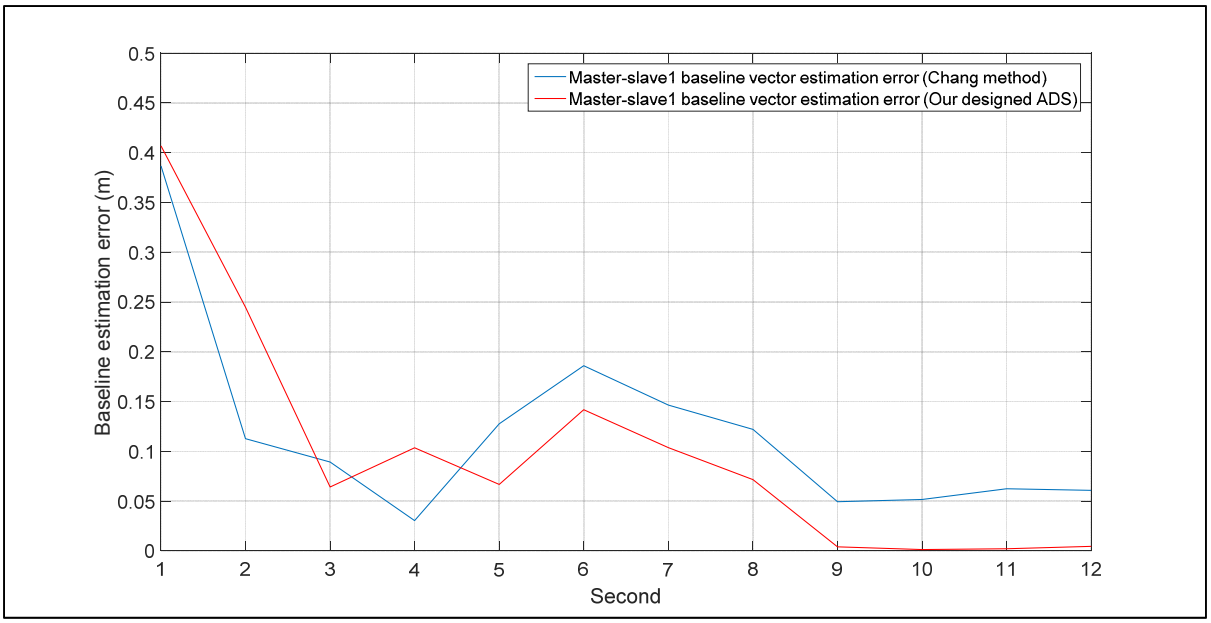

Figure 5.8 Baseline estimation error comparison before convergence comparison in test case 1

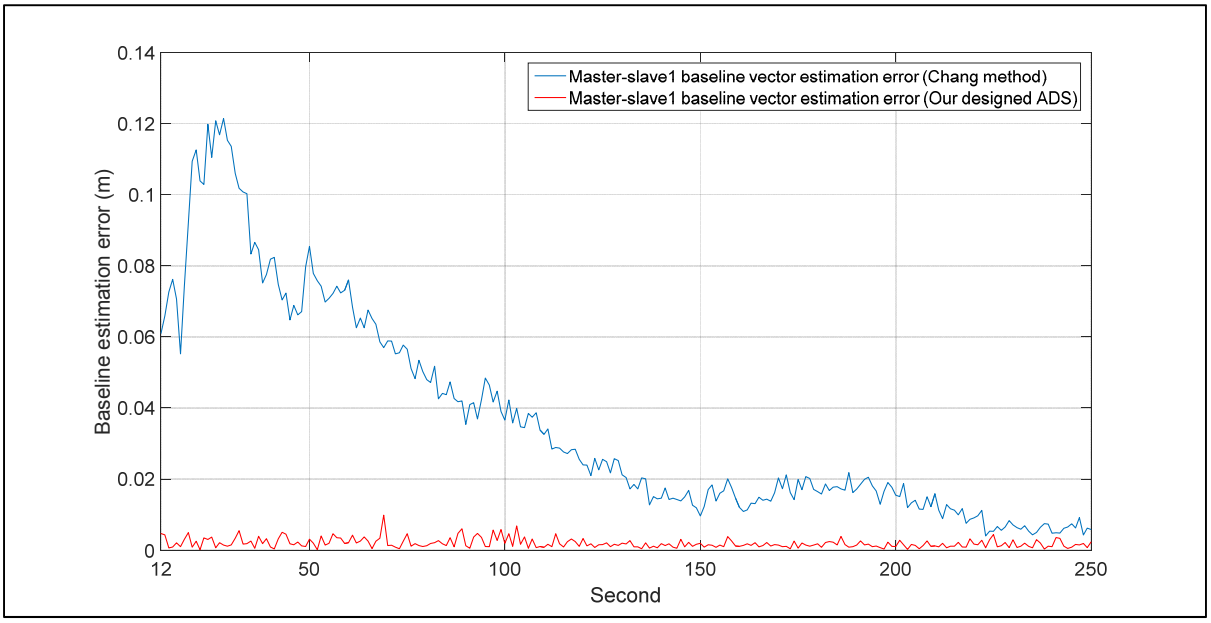

Figure 5.9 Baseline estimation error comparison after convergence in test case 1

Beside this important difference on the error, Figure 5.9 shows that the proposed ADS is more stable than the Chang method in (Chang, Paige et Yin, 2005).

Figure 5.10 and Figure 5.11 makes the same comparison of convergence time and estimation error, for the pitch angle, between the proposed ADS algorithm and the Chang method. The stability of the designed ADS can be seen in the attitude determination module as well in Figure 5.11.

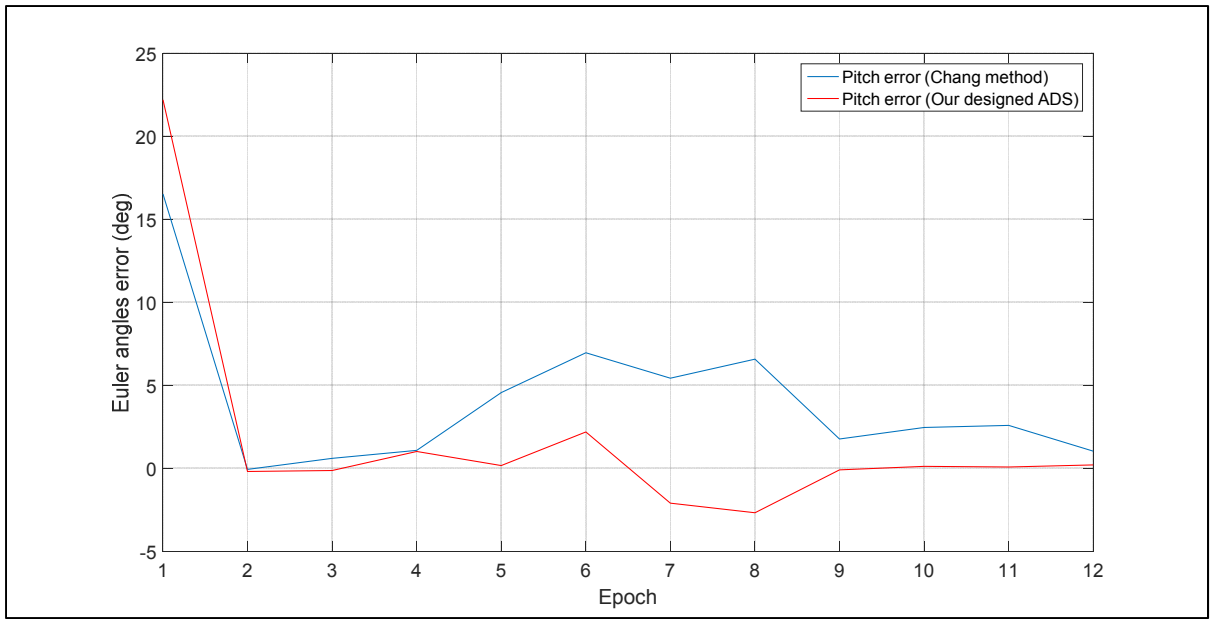

Figure 5.10 Pitch estimation error comparison before convergence in test case 1

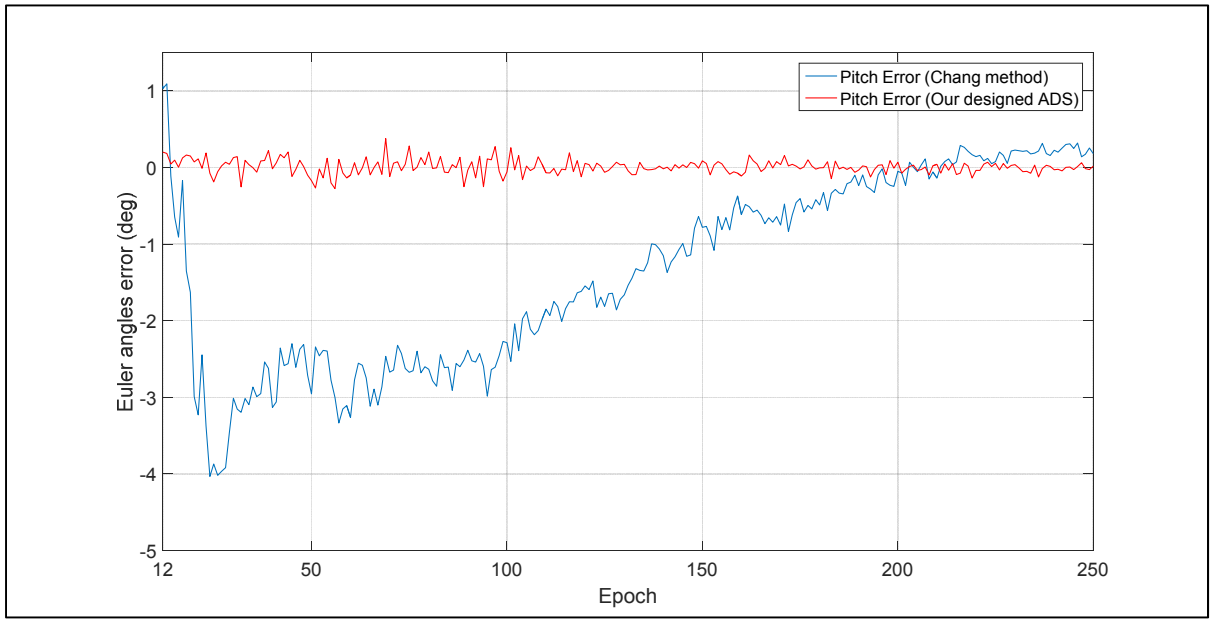

Figure 5.11 Pitch estimation error comparison after convergence in test case 1

In order to show the performance of the proposed ADS compare to other works in the literature, a comparison is also made between previous works and the designed ADS in terms of hardware cost and accuracy of the results. Figure 5.12 shows a comparison between the estimated hardware costs for the entire designed attitude determination packages with respect to their Root Mean Square Error (RMSE) per baseline length. Here, the yaw angle or heading has been chosen for comparison because it is the most common angle to take into consideration for different applications of the attitude determination systems. This figure also shows significant improvement based on a trade-off between price and accuracy. This estimated price is included all GNSS receivers and antennas which have been used in each work. The legend is explained and referred below.

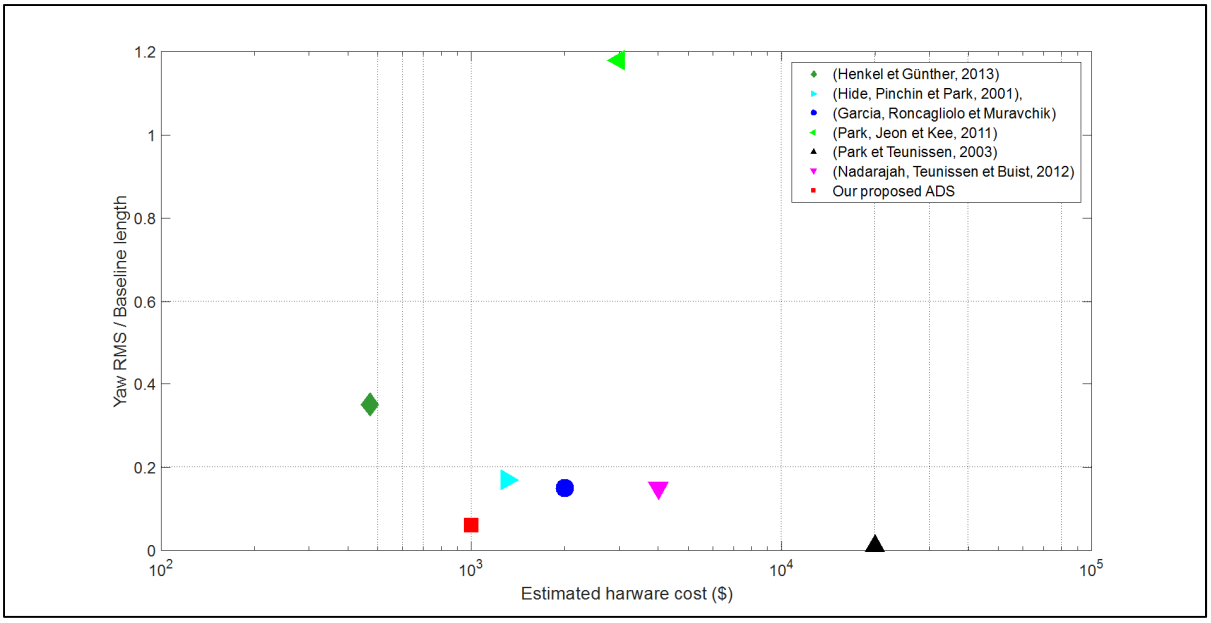

Figure 5.12 Comparison between designed ADS and previous works in literature test case 1

References in the Figure 5.12 respectively are as follows: (Henkel et Günther, 2013), (Hide, Pinchin et Park, 2001), (Garcıa, Roncagliolo et Muravchik), (Park, Jeon et Kee, 2011), (Park et Teunissen, 2003), (Nadarajah, Teunissen et Buist, 2012).

For each reference, the hardware cost of the attitude determination system is estimated based on the type of used receivers and antennas in that reference. The simulated data in this test case is designed for a low-cost attitude determination system which consists of four pairs of low cost antennas and receivers. The hardware cost of the designed ADS is estimated with four u-blox LEA 6-T receivers and four ANN-MS antennas. In the Figure 5.12, the y axis is the Root Mean Square (RMS) error of the yaw angle and the x axis is the estimated hardware cost. It is shown in that the ADS algorithm has a higher accuracy with respect to the hardware cost of the system, Figure 5.12.

5.2 ADS performance analysis, test case 2

In this test case, the GPS Spirent GSS9000 simulator and u-blox LEA-6T receivers are used. Two u-blox LEA-6T receivers are connected to two simulator RF outputs. The clock of the receivers are not synchronized together by hardware, the setup of the simulator is in normal condition and the simulator scenario is designed for two stationary receivers. In the simulator scenario, the two GPS receivers are located with 10 meter baseline length on North direction. The reason why this baseline length was chosen is to test the ADS algorithm in a favorable conditions. In subsequent test, the conditions namely baseline lengths and the record environment is getting more similar to the normal conditions in our application. The true heading is 0.04°and the true elevation is 0.03°. The rate at which the raw measurements are outputted by the receiver for this test case is 1Hz. The raw measurements used for the ADS algorithm are the code measurements and the phase measurements. The date of the simulation is 13 may 2015 and the record duration is 30 minutes. A period of the observation is selected which does not have cycle slip and the time of measurements corresponds to the same UTC 1-second epoch for both receivers[2]. The 1 second epoch is due to rate of raw measurements which is 1 Hz. In the selected period of data to be analysed, both receivers

[2] The time accuracy of the U-blox LEA-6T receiver after correcting the clock bias is ±20 ns. The maximum clock bias allowed is 1 ms. When the clock bias approaches 1 ms, the receiver delays or advances its clock by 1 ms in order to correct it. Therefore, UTC 1-second epoch are accurate in ±1ms.

detect 10 satellites in common with the mask angle of 10° and minimum C/N_0 of 30 dBHz. The added errors to the measurements are ionospheric and tropospheric errors and the simulator does not add any multipath. For the master antenna position and for the true baseline vector, the reference file generated from the simulator during the record is used. This file contains the true value of each receiver's position.

The raw measurements recorded by receivers has an average standard deviation for DD code measurements of 45 cm and the standard deviation of DD phase measurements has an average of 18.7 cm.

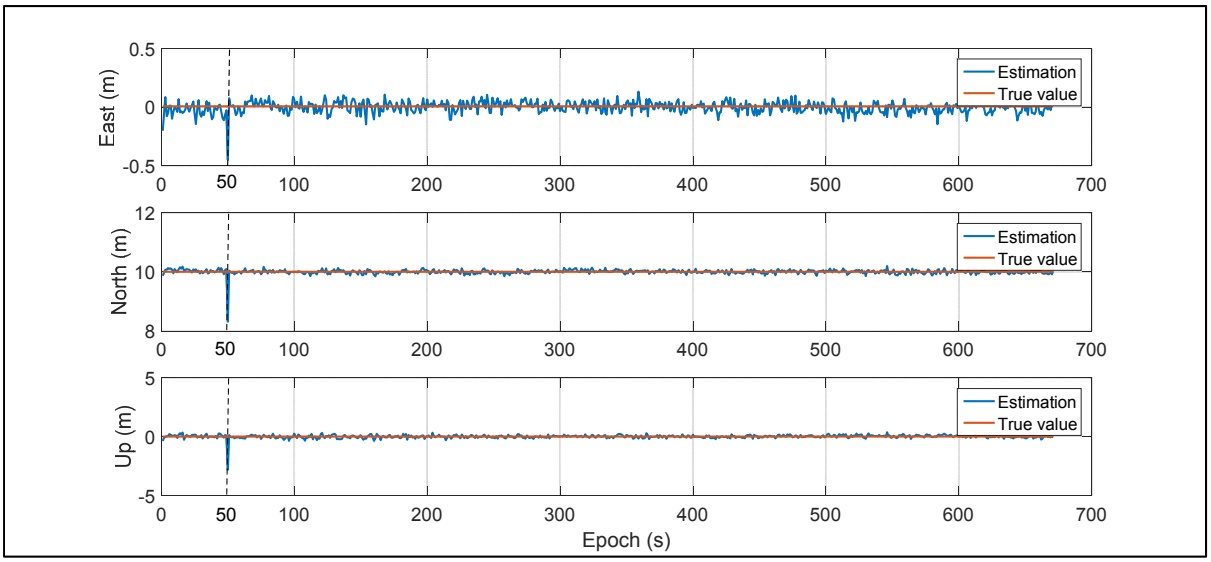

Figure 5.13 Estimated baseline components, test case 2

In order to be able to fix ambiguities, the covariance matrix of the float solution needs to be positive. So, the first 50 second is used to get a good estimation of the covariance matrix. At t=50s as shown in Figure 5.13, the LAMBDA method starts to fix the ambiguities. LAMBDA method takes time to converge to the right solution. The convergence time of the LAMBDA method depends on the quality of the raw measurements. In this test case, the convergence time of the LAMBDA method is 1 second after t=50s. The standard deviation of the estimated baseline before fixing the ambiguities is 5.4 cm, 6.4 cm and 14.2 cm for East, North, and Up respectively while they are 4.5 cm, 5.7 cm, and 11.5 cm for East, North, and

Up respectively, after fixing the ambiguities. The standard deviation of the estimated baseline after fixing the ambiguities shows an improvement of 16% for East component, 10% for North component and 19% for Up component compared to the standard deviation of the estimated baseline before fixing the ambiguities.

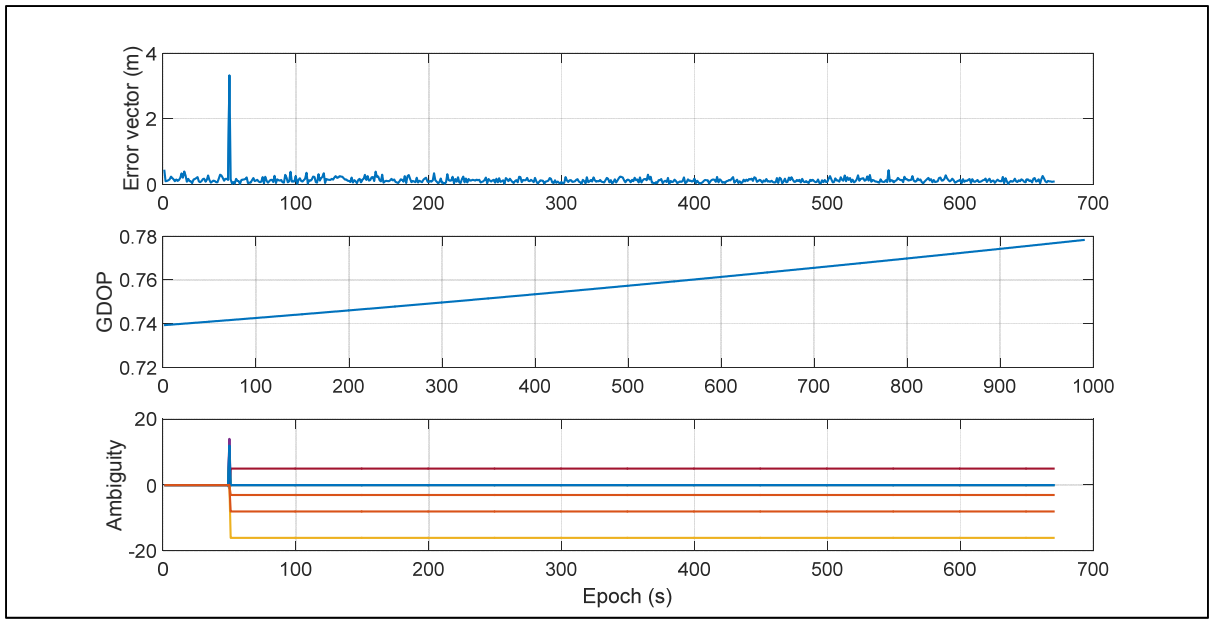

Figure 5.14 Relation between the estimation error, GDOP and the ambiguities in test case 2

In the t=50s, a jump of 3.15 m in estimated baseline is occurred due to the initial guess of the LAMBDA method Figure 5.14. Figure 5.15 and Figure 5.16 present the heading and elevation estimations after convergence of the baseline estimation.

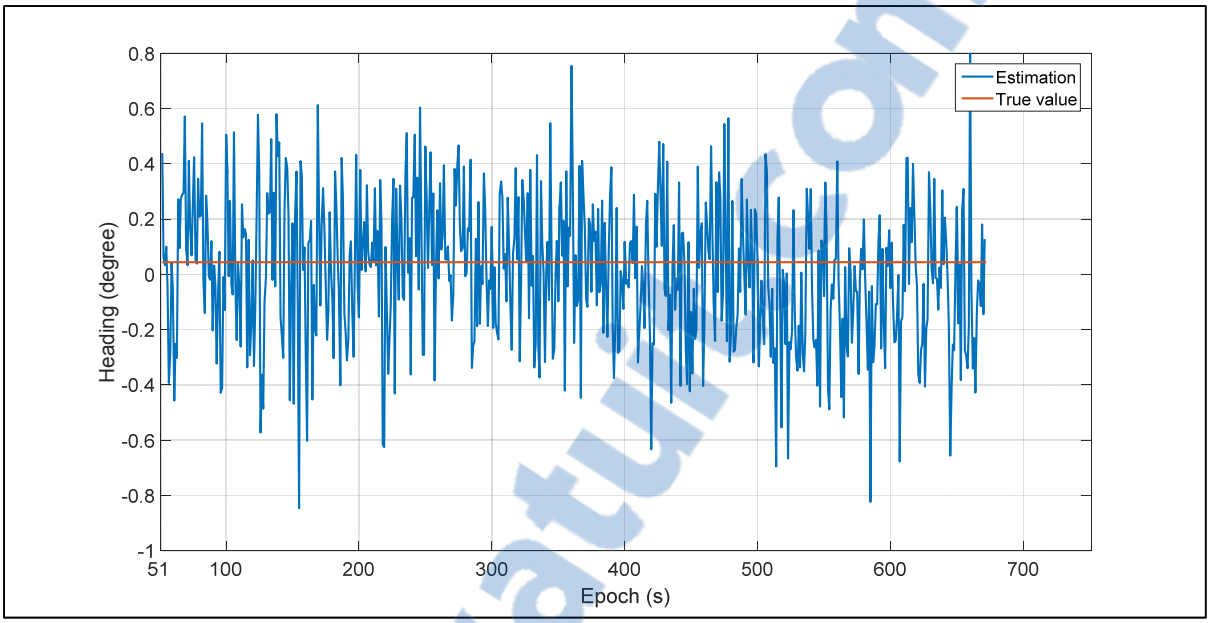

Figure 5.15 Heading estimation intest case 2

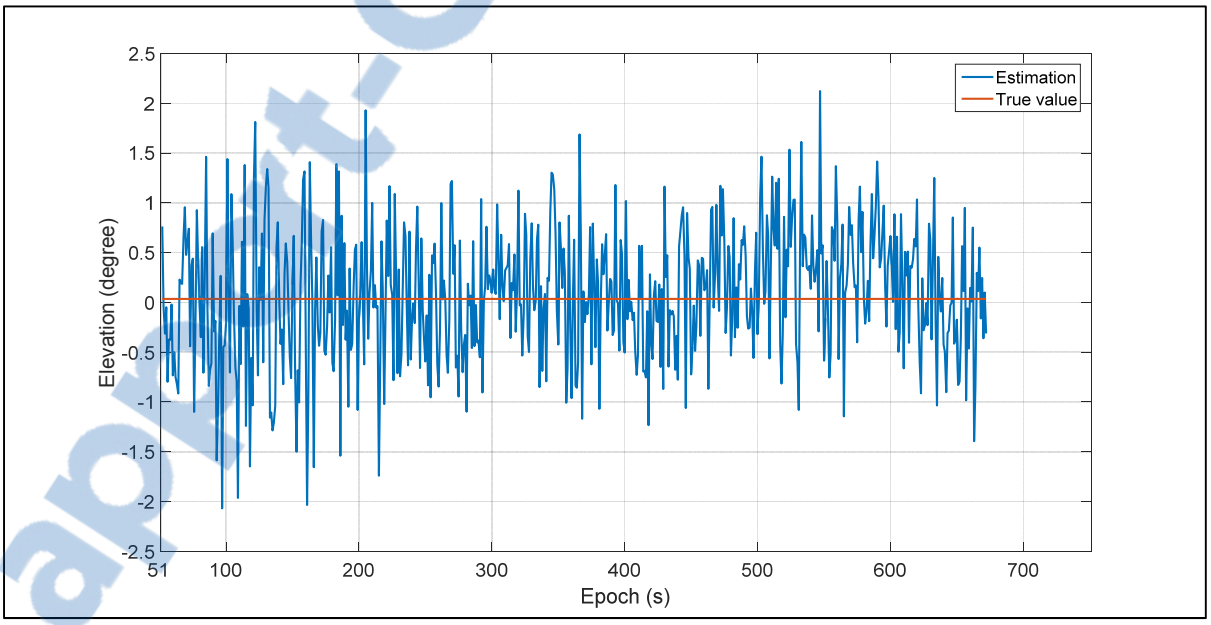

Figure 5.16 Elevation estimation in test case 2

The error of the estimated heading has an average of 0.03° (the absolute value) and has a standard deviation of 0.2°. The error for estimated elevation has an average of 0.06° with the standard deviation of 0.6° which is 3 times more than the standard deviation of the estimated

heading. This is due to the fact that the error of the heading angle contains the error of the East and North components while the elevation error contains the z component error as well. The computational time of ADS for this test case has an average of 0.16 s per epoch.

Due to the internal hardware temperature of receivers and the accuracy of the internal oscillator and other errors, there are outliers in the estimation. The outliers can be detected from the estimated solution as follows, (Goudarzi, Cocard et Santerre, 2015):

$$\left|\hat{v}_i - median\ (\hat{v}_{i-\frac{w}{2}}, \hat{v}_{i+\frac{w}{2}})\right| > n \times IQR\ (\hat{v}_{i-\frac{w}{2}}, \hat{v}_{i+\frac{w}{2}}) \tag{5.3}$$

where $\hat{v}_i$ is the residual in the time *i, w* is the length of the chosen window. The idea of using this test case is to check whether all measurements statistically are coming from the same population or not. The *w* is selected equal to 0.1 for all the analysis duration and *n* is 1 that resembles 1σ. By using the Equation (5.3), the outliers of the heading and elevation estimation can be detected and removed from the solution. Then, the least square estimator is used to fit the best line between the rests of the solutions. The number of detected outliers is 15.9 % and 16 % of the solution for heading and elevation respectively, Figure 5.17 and Figure 5.18.

The outliers are detected when the solution (here the solutions are heading and elevation estimation) has a variance greater that than 1σ during the chosen value for the window which is 64 s in this test case.

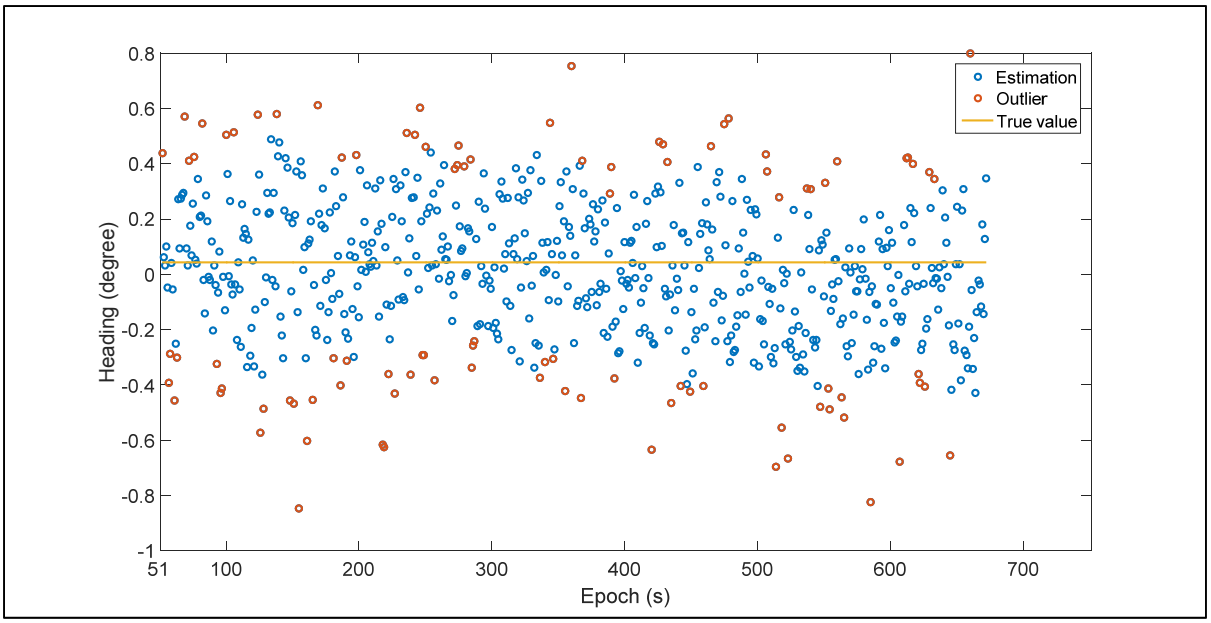

Figure 5.17 Heading estimation and the detected outliers in test case 2

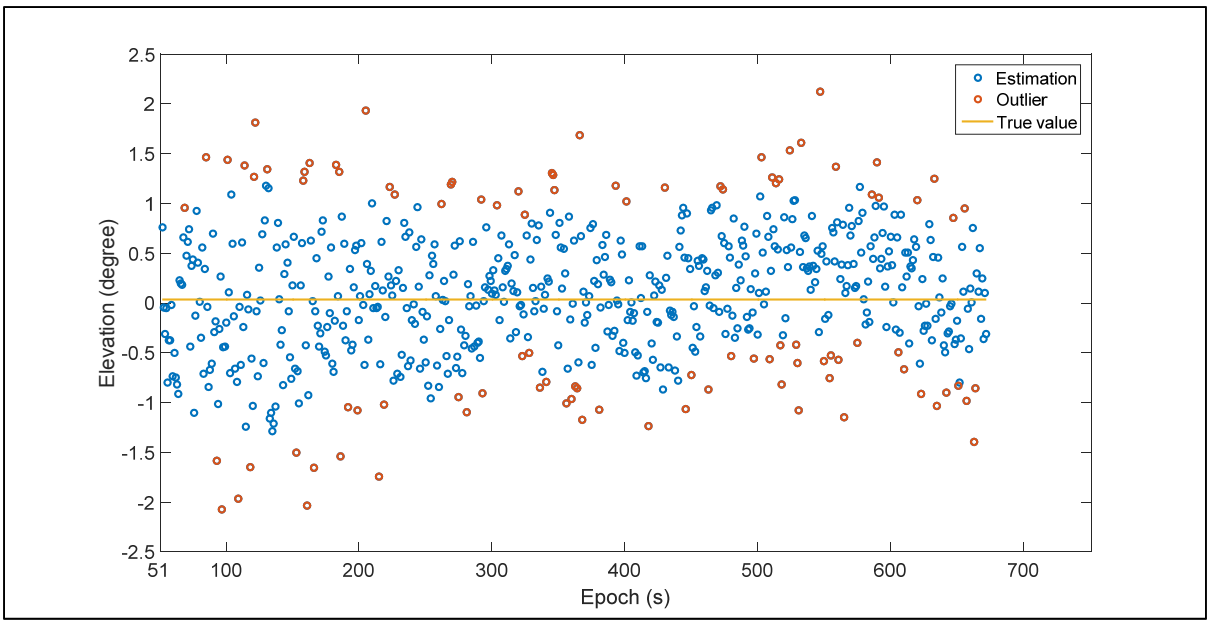

Figure 5.18 Elevation estimation and the detected outliers in test case 2

As both receivers are stationary in this test case, so the true value of the derivative of the heading and elevation is 0 and it is a straight line. After removing the detected outliers from the estimated heading and elevation, a least-squares estimator that estimates the best line

within the solution is used. Then, in order to show the improvement of the least-squares estimator, the ramp of this estimator for both heading and elevation angles are shown in the Figure 5.19 and in the Figure 5.20 The moving ramp of this estimator is getting smaller and smaller and it converges to 0 which shows that the least-squares estimation improves by time, Figure 5.19 and Figure 5.20. As it can be seen in the Figure 5.19, by removing the detected outliers, the least-squares moving ramp converge to 0 faster than the least-squares with outliers. However, the moving ramp of the least-squares for the elevation angle with and without outliers is the same, Figure 5.20.

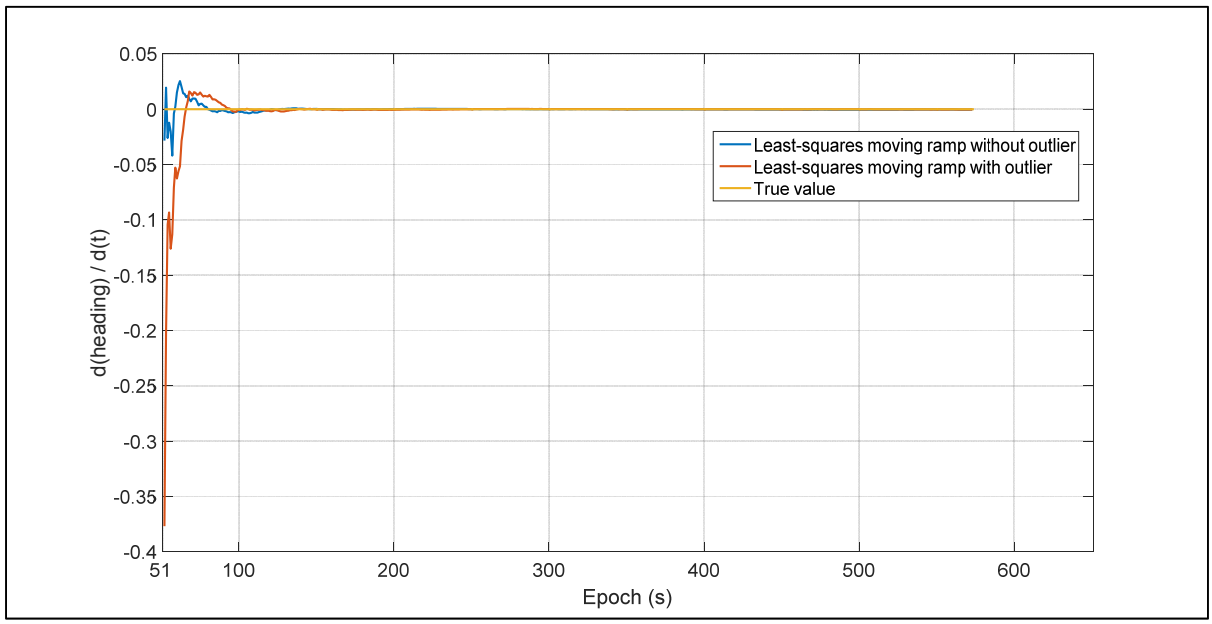

Figure 5.19 The least-squares moving ramp passed through the heading estimation

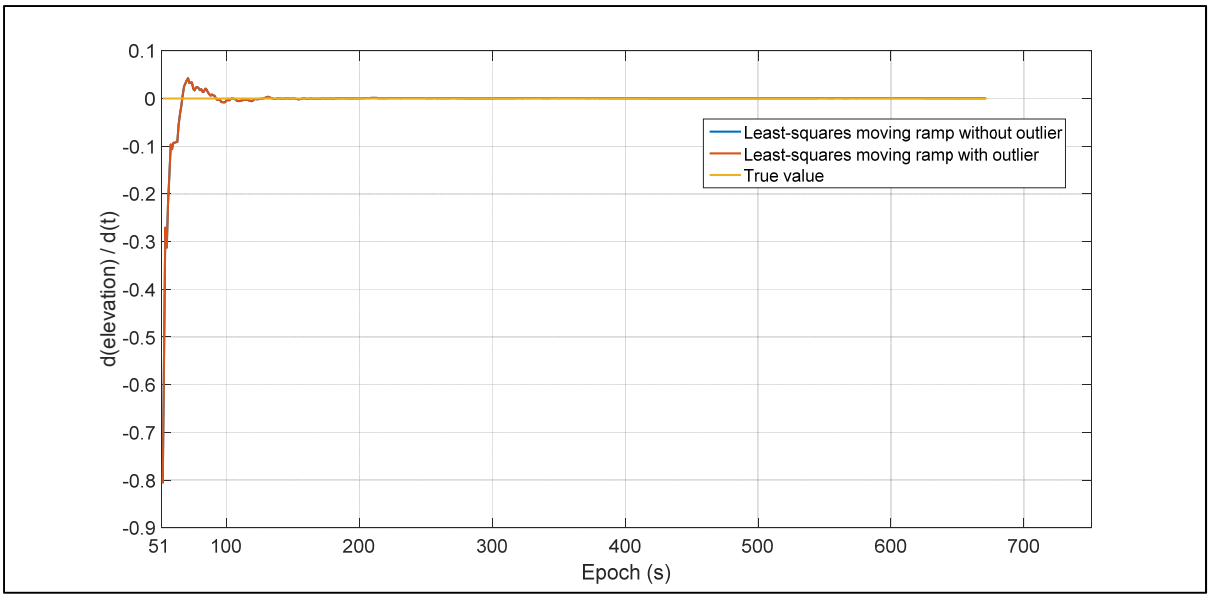

Figure 5.20 The least-squares moving ramp passed through the elevation estimation

5.3 ADS performance analysis, test case 3

In this test case, the two u-blox LEA-6T receivers are connected to the two G5Ant-4AT1 antennas. The goal of this test case is to analyze the accuracy of the baseline estimation module and its associated error in attitude determination module, so we used only two receivers (one baseline).The clock of the receivers are not synchronized together by hardware. The location of the test case is on top of ETS's roof which is a building with 5 floor (downtown Montreal) and there are several high-rise building around. The date of the record is 17 September 2015, the record duration is 15 hours and the data rate is 1 Hz. The used platform in this test case is a wood platform with the dimension of 1.2 m^2. Both receivers are stationary during the record and the distance between these two antennas is 1.13 m.

For the master antenna position and for the true baseline vector of this test case, the GNSS Solution software of Spectra Precision version 3.80.8 is used. This software uses differential positioning technique by choosing three base stations that are near the receiver location and it

creates a triangle around the receiver. This software works in post-processing mode offering centimeter precision (Solution, 2007).

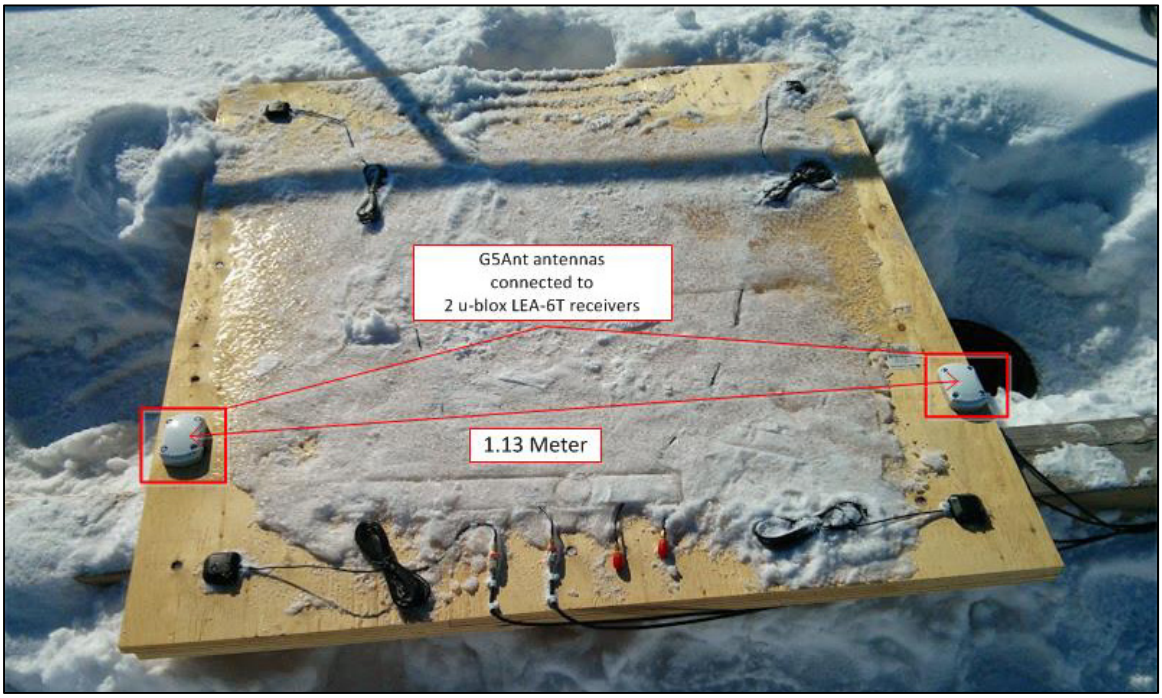

Figure 5.21 Data record configuration with two u-blox LEA-6T and two G5Ant-4AT1

Two receivers tracked 10 common satellite with 10° mask angle and minimum C/N_0 of 30 dBHz. The average standard deviation of DD code and phase measurements are 149 cm and 0.5 cm, respectively.

As it is explained in the previous test case, section 5.2, the LAMBDA algorithm needs 50 epoch to estimate the ambiguity covariance matrix so the algorithm starts to fix the ambiguities at epoch 50, similar to the previous test case. The LAMBDA starts the ambiguity resolution at t=50s and it converges at t=327s. The convergence time of the LAMBDA method in this test case is 277 second, (4.6 minutes), Figure 5.22. The potential reason for the delay of resolving the ambiguites is mainly the presence of multipath. This error increases the convergence time of the LAMBDA method and it can lead the estimation to converge to a wrong solution.

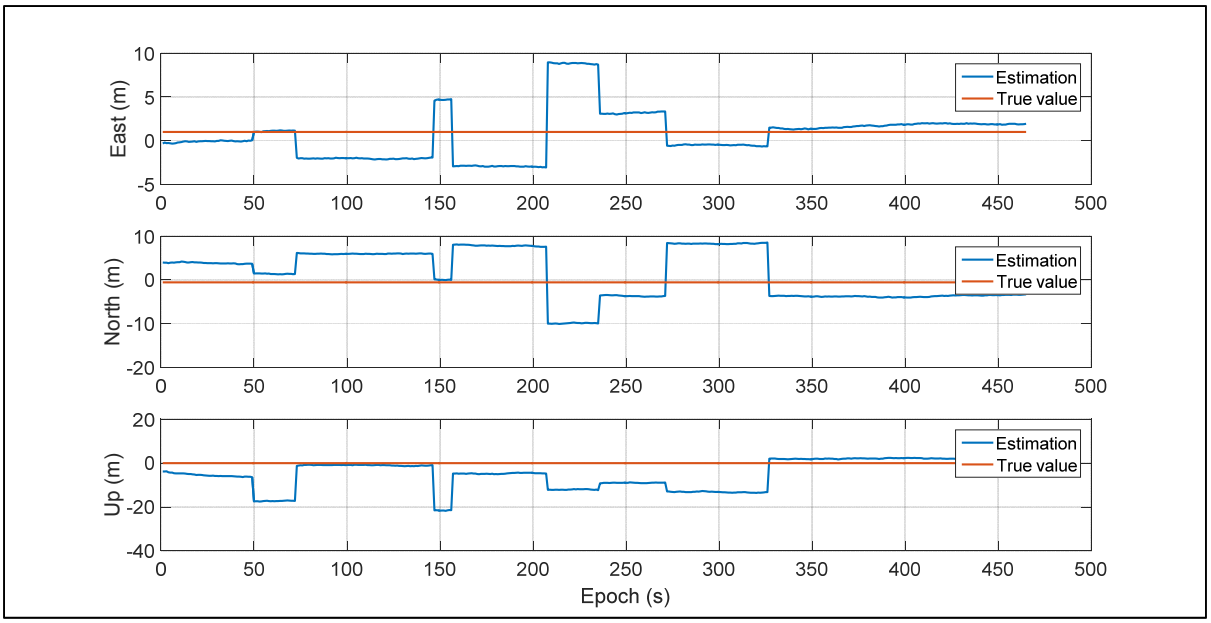

Figure 5.22 Baseline estimation in test case 3

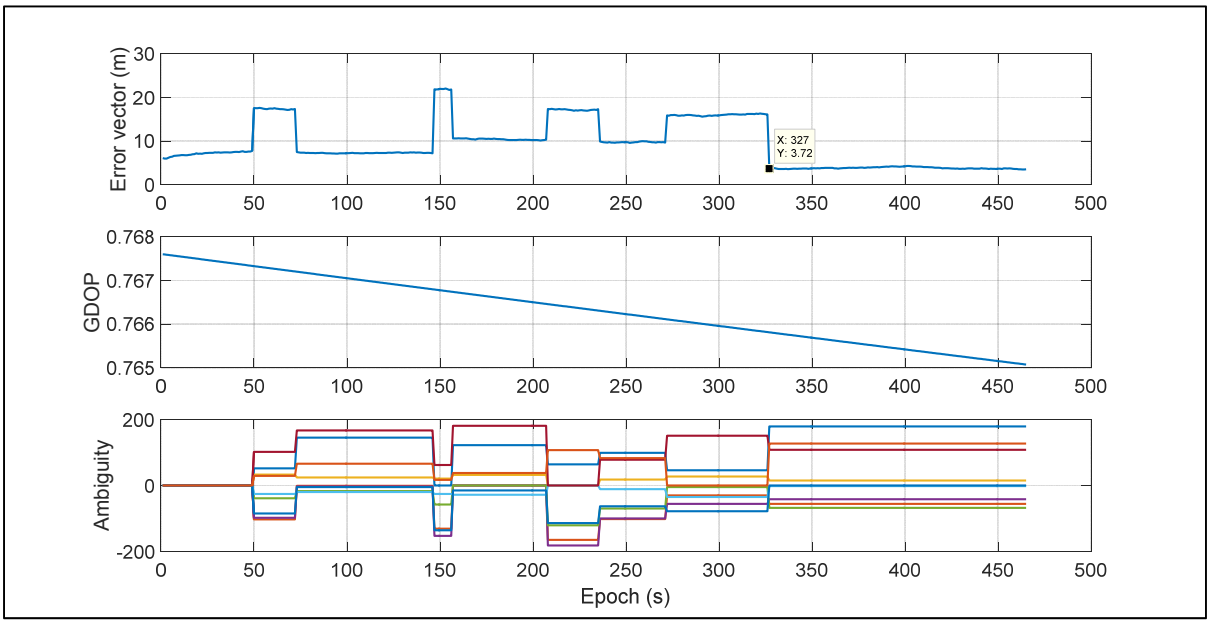

Figure 5.23 Relation between the estimation error, GDOP and the ambiguities in test case 3

The relation between GDOP, the error vector and the fixed ambiguity is shown in the Figure 5.23. In this test case, the GDOP is already good but it does not change too much mainly due to the short period of observations. The reason that the error of the estimated baseline is in

the order of meter is due to the presence of the multipath error. In the presence of the multipath error the LAMBDA method converged to a wrong solution.

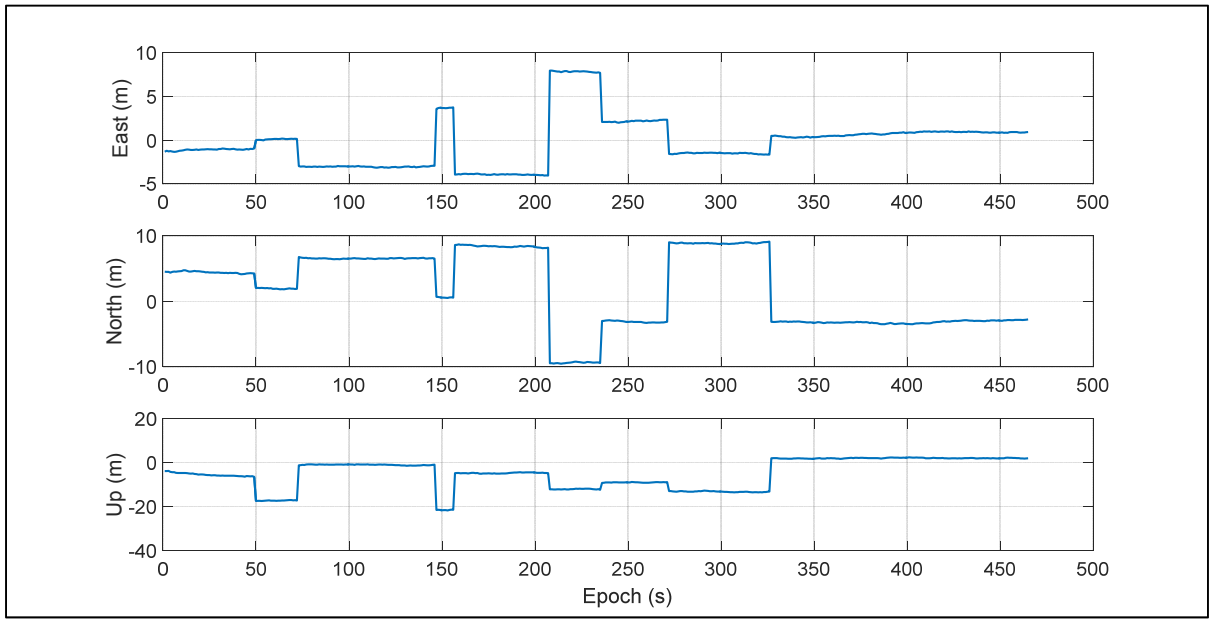

Figure 5.24 Estimation error in test case 3

The absolute value of the error for East component before the ambiguity resolution varies between 0.01m and 1.3 m, while during the ambiguity resolution varies between 0.007 m and 7.9 m. After fixing the ambiguities (t=327 sec), this range is between 0.2 m and 1.01 m. The absolute error value for the North component before ambiguity resolution (AR) varies between 2.03 m and 4.7 m. This range during the process of the ambiguity resolution is between 0.5 m and 9.5 m and after that the ambiguity resolution is solved (t=327 sec), is between 2.7 m and 3.4 m. The absolute value of the error for the Up component before the AR varies between 3.7 m and 17.4 m. This range during the AR is between 0.7 m and 21.6 m and after the ambiguity resolution (t=327 sec) is between 1.6 m and 2.4 m. After convergence of the LAMBDA method, the Up component has been improved better that the East and North components, Figure 5.24. The computational time of ADS for this test case has an average of 0.1 s per epoch.

The standard deviation of the estimated baseline before the ambiguity resolution (t=50 sec) is 10 cm, 15 cm and 73 cm for East, North and Up respectively. The standard deviations of the estimated baseline after the ambiguity resolution (t=327 sec) are 23 cm, 18 cm and 15 cm. The average of the absolute value of the positional error before fixing the ambiguities is 1.8 m, 4.42 m and 5.4 m for East, North, and Up respectively. These values after the ambiguity resolution decreases to 0.7 m, 3 m, and 2 m. An improvement of 61%, 32% and 62 % is achieved by resolving the ambiguities respectively for the East, North and Up component.

Since the achieved error in baseline estimation is more than 19 cm (the length of the carrier phase cycle), it is shown that the LAMBDA method does not converge to the right solution, however, it improved the solution. Multipath error is one of the main reasons that LAMBDA method does not converge to the right solution. The norm of the error vector of the baseline estimation solution after fixing ambiguities is 3.7 m which is more than 3 times larger than the baseline length. In this case, the attitude parameters will be estimated randomly, so it is not possible to analyze the attitude parameters (heading and elevation) for this test case.

5.4 ADS performance analysis, test case 4

In this test case four u-blox LEA-6T receivers are connected to four ANN-MS antennas. The record environment is the same as the previous test case and the data is recorded at ETS's roof which is an urban environment. The date of record is 9 January 2015 and the duration of record is 3 days. The data rate in this test case is 5Hz. Four receivers were mounted on the same square platform of the previous test case. The body frame configuration which consists of three baseline vectors are shown in the Figure 5.25. For each pair of receivers both receivers tracked 7, 6, 6 satellites for the baseline 1, 2, and 3 respectively. These satellites passed the condition of 10° for the mask angle and C/N_0 of 30 dBHz. For the master antenna position and for the true baseline vector, the GNSS Solution software is used as in the previous test cases.

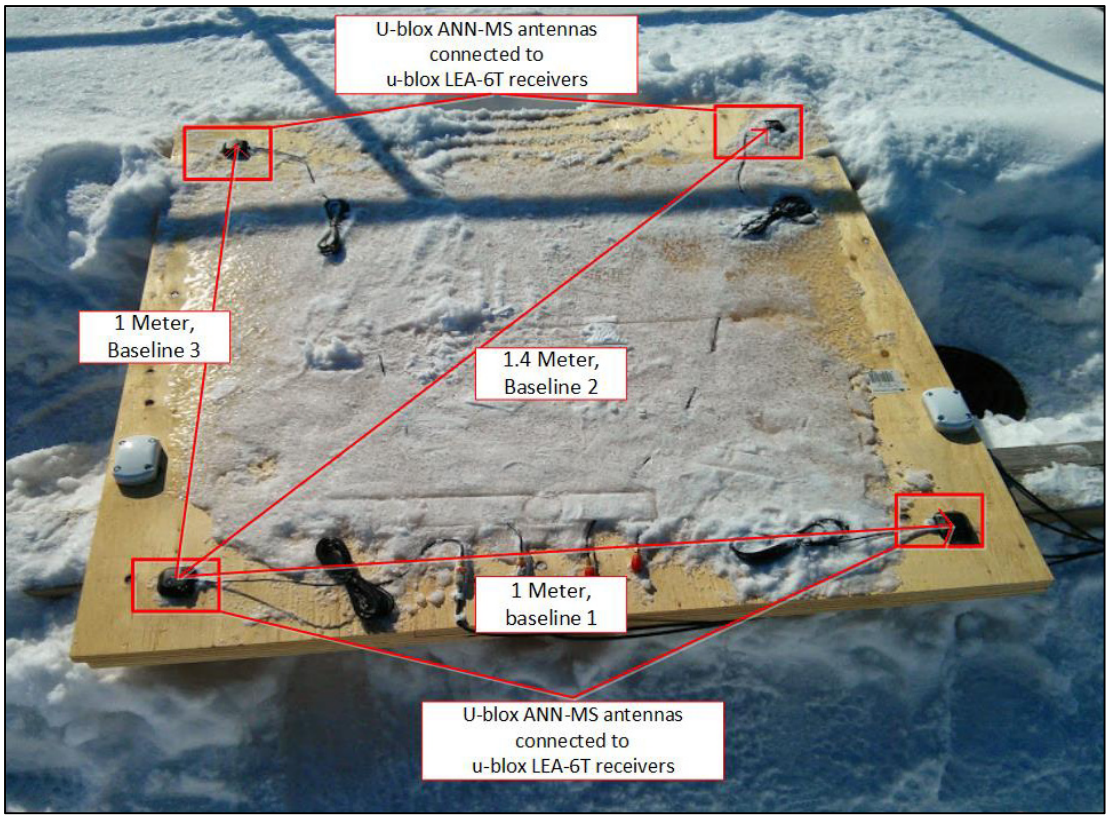

Figure 5.25 Data record configuration in test case 3

The average standard deviation of the DD code measurements for the first baseline is 2.18 m and for DD of phase measurements is 1 cm. These values for the second baseline is 2.06 m for the DD of the code measurements and 1 cm for the DD of the phase measurements. For the third baseline, the standard deviation of the DD of code measurements and phase measurements is 1.48 m and 0.6 cm respectively.

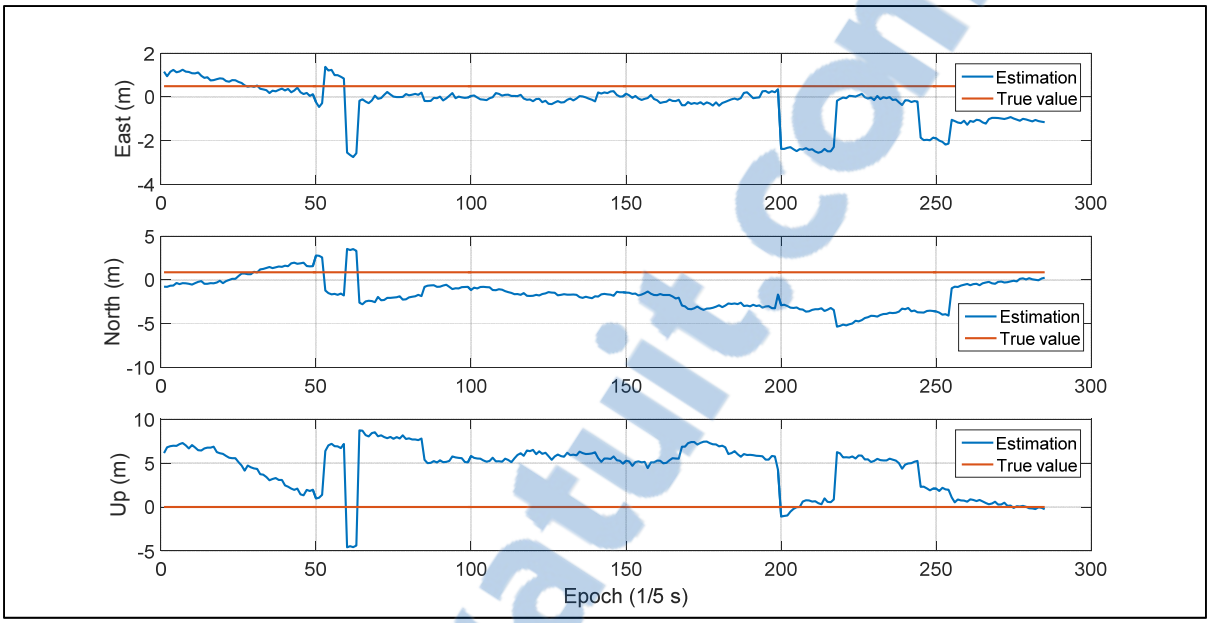

Figure 5.26 Baseline 1 estimation in test case 4

The standard deviation of the estimated baseline before the ambiguity resolution is 36 cm, 93 cm and 1.93 m for East, North and Up respectively. Here it is assumed that the ambiguities are fixed when they don't change during the time of the observation which in this test case is t=255s. The standard deviation of the estimated baseline after the ambiguity resolution and convergence decreases to 8 cm, 31 cm and 38 cm. The absolute value of the average error before the ambiguity resolution is 15 cm, 35 cm and 4.78m for East, North, and Up respectively. These values after the ambiguity resolution are1.5 m, 1.14 m, and 34 cm. The LAMBDA method was more successful to fix the ambiguities in up component according to Figure 5.26. The computational time of the ADS has an average of 0.14 s per epoch for each baseline.

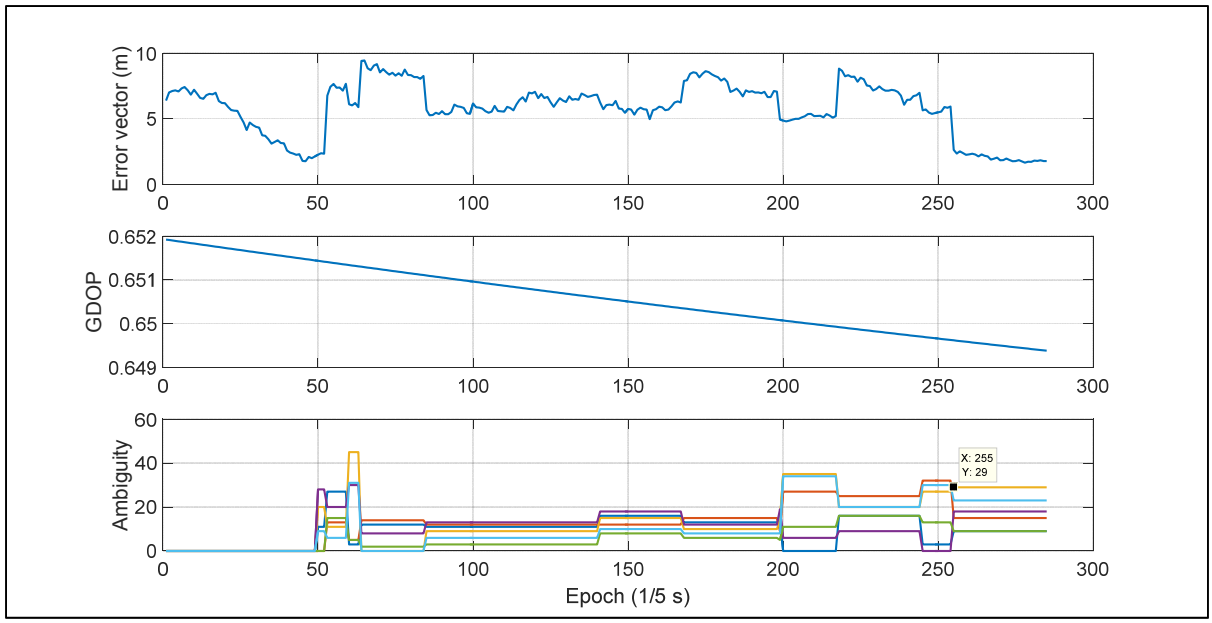

Figure 5.27 Relation between the estimation error, GDOP and the ambiguities in test case 4, baseline 1

The ADS starts to fix the ambiguities at t=50s, as it is explained in the previous test cases. The LAMBDA starts the ambiguity resolution at t=50s and it converges at t=255s. The convergence time of the LAMBDA method in this test case is 205 second, (3.4 minutes). The delay of the convergence of the ambiguities are due to the presence of the multipath error. This error not only causes delay into the convergence time but it can lead the LAMBDA method to converge to a wrong solution. Due to the higher observation rate of this test case, the convergence time is smaller than the previous test case, Figure 5.27.

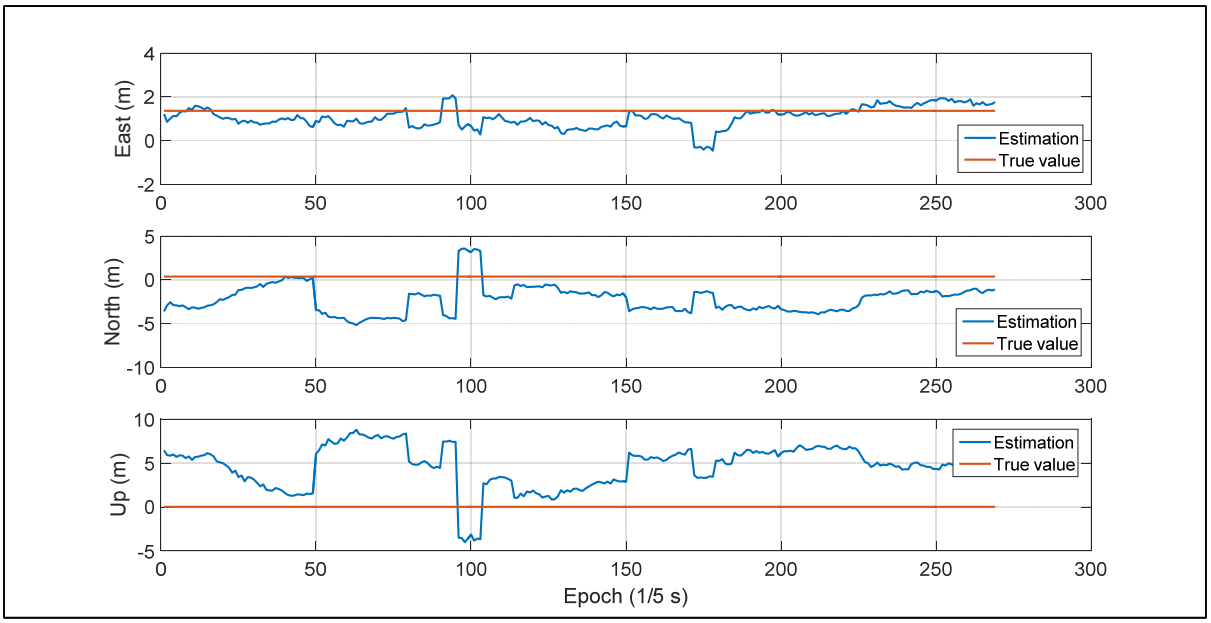

Figure 5.28 Baseline 2 estimation in test case 4

The standard deviation of the estimated baseline 2 before the ambiguity resolution is 25 cm, 1.34 m and 1.83 m for East, North and Up respectively. The standard deviation of the estimated baselines after the ambiguity resolution and convergence are 12 cm, 24 cm and 26 cm. The absolute value of the error average before the ambiguity resolution is 30 cm, 1.87 cm and 3.76 m for East, North, and Up respectively. These values after the ambiguity resolution are 35 cm, 1.82 m, and 4.67 cm, Figure 5.28.

For the second baseline, the ADS starts the ambiguity resolution at epoch 50. The LAMBDA starts to fix the ambiguities at t=50s and it converges at t=228s. The convergence time of the LAMBDA method for this baseline is 178 second, (2.9 minutes), Figure 5.29.

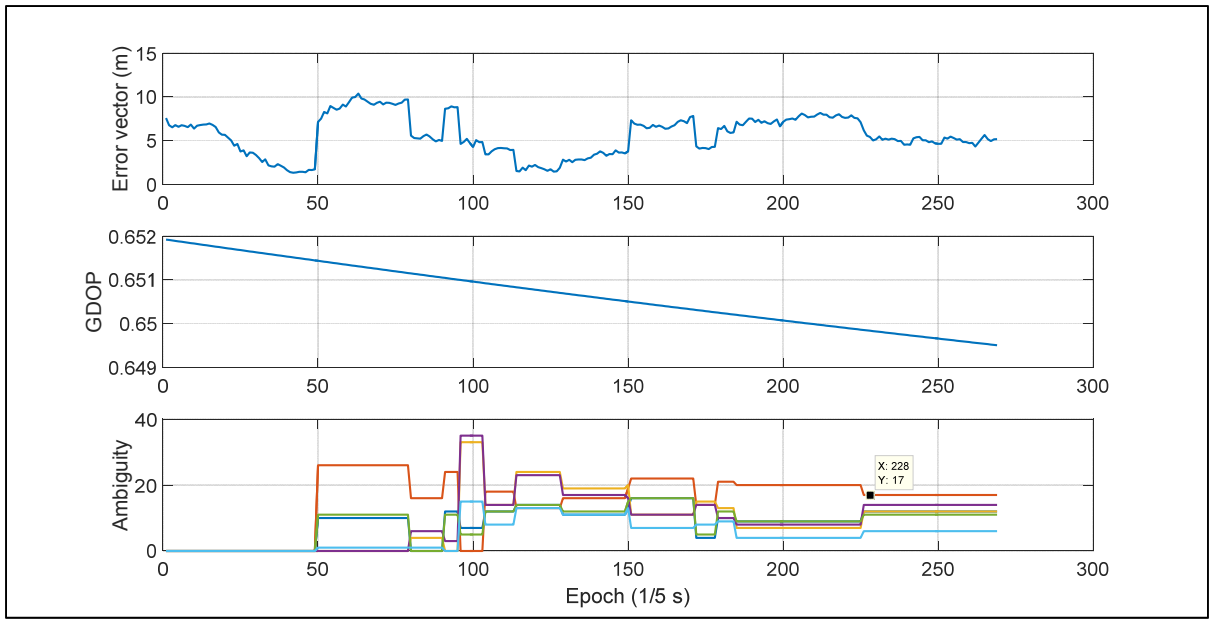

Figure 5.29 Relation between the estimation error, GDOP and the ambiguities in test case 4, baseline 2

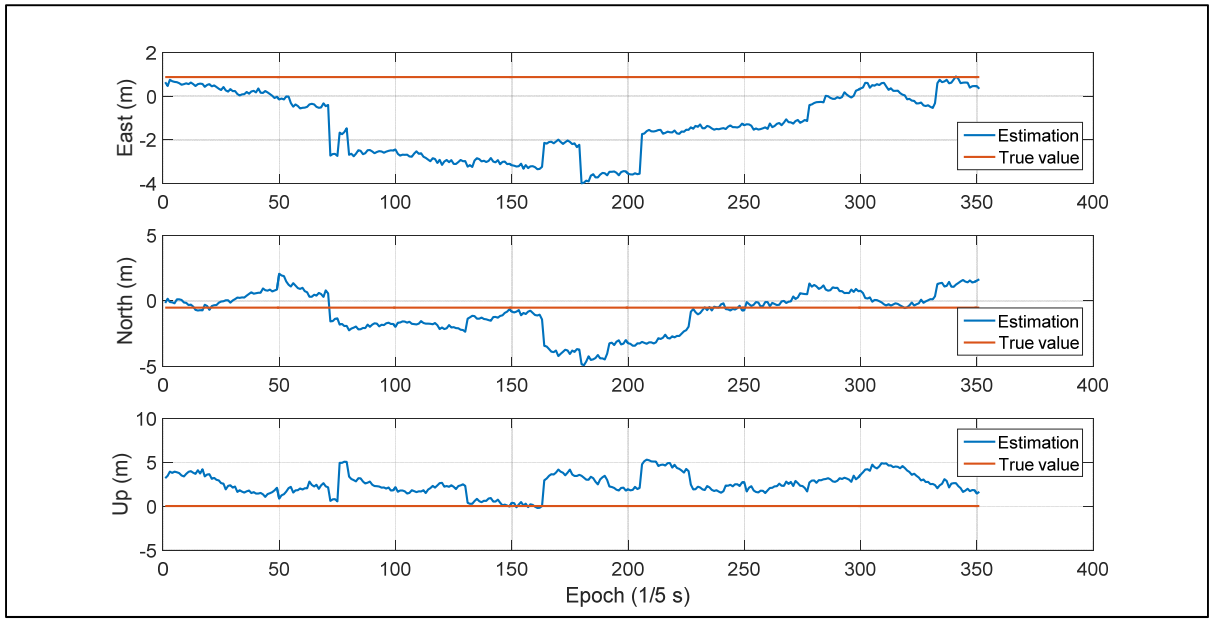

Figure 5.30 Baseline 3 estimation in test case 4

The standard deviation of the estimated baseline before the ambiguity resolution is 29 cm, 47 cm and 99 cm for East, North and Up respectively. The standard deviation of the estimated baselines after the ambiguity resolution and convergence are 14 cm, 17 cm and 46 cm.
The absolute value of the error average before fixing the ambiguities is 51 cm, 59 cm and 2.66 m for East, North, and Up respectively. These values after the ambiguity resolution are 25 cm, 1.88 m, and 2.14 m, Figure 5.30.

For the third baseline, the ADS starts to fix the ambiguities at epoch 50 as well. The LAMBDA starts the ambiguity resolution at t=50s and it converges at t=333s. The convergence time of the LAMBDA method in this baseline is 283 second, (4.7 minutes). As it is discussed before the presence of the multipath error increases the convergence time of the LAMBDA method and it can lead the LAMBDA method to converge to a wrong solution.

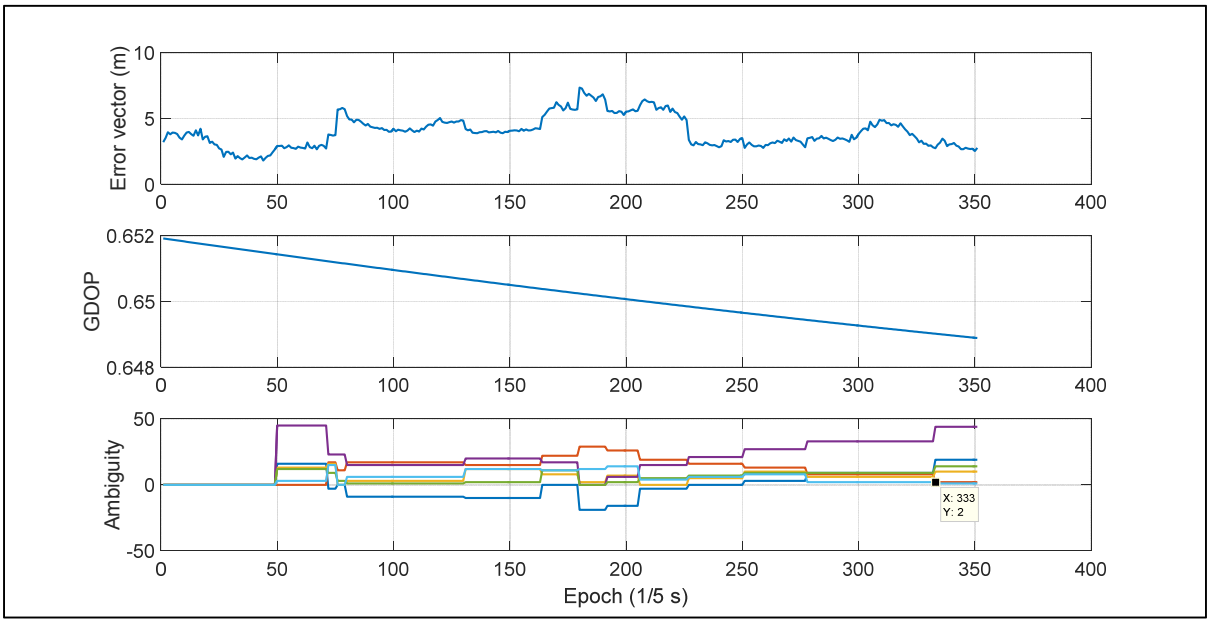

Figure 5.31 Relation between the estimation error, GDOP and the ambiguities in test case 4, baseline 3

The large discrepancy between errors of the three baselines shows that the LAMBDA method in this test case does not converge to the right solution as well. However, it improved

the norm of the solution. The norm of the error vector of the baseline estimation solution after fixing ambiguities is 1.7 m, 4.96 m, and 2.75 m for baseline 1 to three respectively. As all these errors are more than the baseline length, the attitude parameters will be estimated randomly, so it is not possible to analyze the attitude parameters (heading and elevation) for this test case.

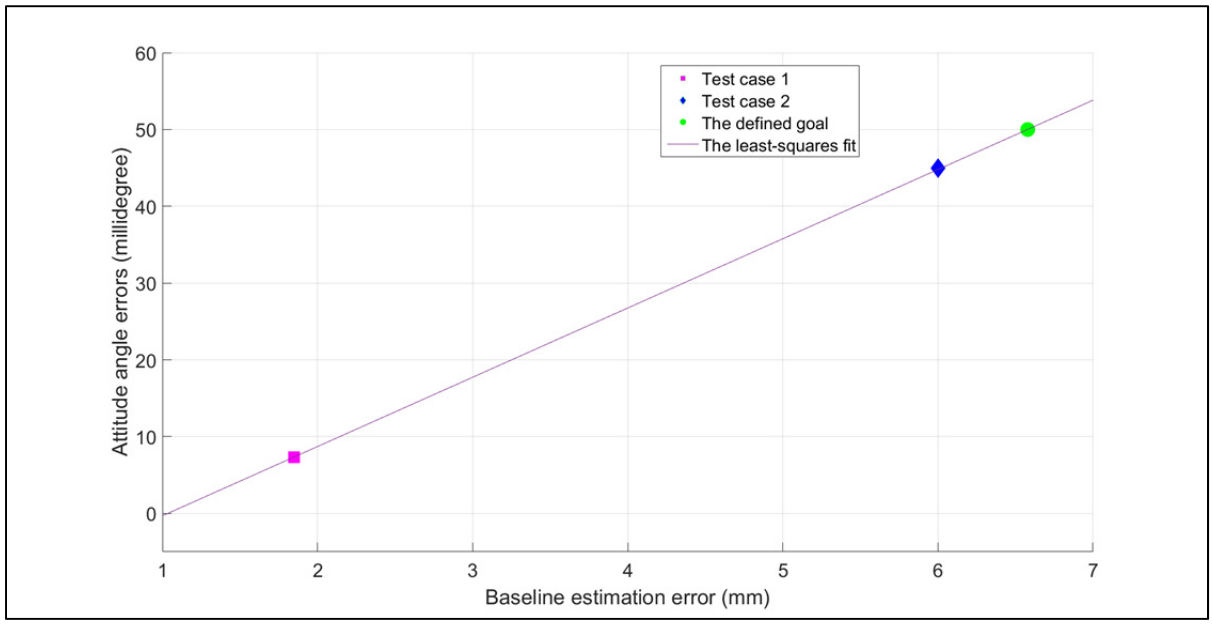

Figure 5.32 Attitude angles error versus baseline estimation error

Figure 5.32 presents the impact of the baseline estimation error on the attitude angles error for the test case 1 and test case 2. The *x* axis represents the average error of all baselines (1 m length) in the baseline estimation module and the *y* axis represents the average error of the attitude angles (yaw and pitch). A least-squares linear estimation is fitted between these two test cases, then the required accuracy in the baseline estimation module to hit the goal of this project (50m degree in attitude angles) is achieved. In order to reach the defined goal of the project, the baseline vectors need to be estimated in 6.5 mm accuracy in order to get 50m degree accuracy in yaw and pitch angle.

A summary of different test case is presented in the Table 5.3.

Table 5.3 A summary of different test cases

	Test case 1	**Test case 2**	**Test case 3**	**Test case 4**
Receiver type	Software receiver with parameters of a typical low-cost receiver	u-blox LEA-6T	u-blox LEA-6T	u-blox LEA-6T
Antenna type	-	Spirent GSS9000 simulator	G5 Ant-4AT1	ANN-MS
Number of receiver-antenna used	4	2	2	4
Record environment	Simulation in Matlab	Open sky, Out of town	ETS roof, downtown	ETS roof, downtown
Number of used satellites	9	10	10	7, 6, 6
Average GDOP	0.7	0.7	0.7	0.6
Baseline length (m)	1, 1.4, 1	10	1.13	1, 1.4, 1
Are the receivers synchronized?	Yes	No	No	No
Multipath	No	No	Yes	Yes
Antenna phase center variation	No	No	Yes	Yes
Average error for baseline estimation	B1: 2 (mm) B2: 2.1 (mm) B3: 2.4 (mm)	0.6 (cm)	3.6 (m)	B1: 2 (m) B2: 5 (m) B3: 2.7 (m)
Average error of attitude angles	Yaw: 0.005° Pitch: 0.008° Roll: 0.009°	Heading: 0.03° Elevation: 0.06°	-	-
Standard deviation of attitude angles	Yaw: 0.012° Pitch: 0.096° Roll: 0.062°	Heading: 0.2° Elevation: 0.06°	-	-

CHAPTER 6

CONCLUSION AND FUTURE WORKS

6.1 Conclusion

The main objective of this thesis is to determine the 3D attitude angles of a moving platform using four low-cost GPS receivers attached to the platform with an attitude resolution better than 50m degrees. An accuracy of 6.5 mm for the baseline estimation module is necessary to secure the localization of an object at 1km within an error of 1 meter.

In order to fulfil the research objectives, we conduct our work in four algorithm modules, Figure 6.1. The first module is the data selection. An algorithm was designed to filter the GPS raw measurements (data) based on satellites elevation angle and Carrier to Noise ratio (C/N_0). The second module is the single point positioning module. In this module the position of the master antenna as well as satellite positions are calculated using the SPP algorithm. The third module is the baseline estimation module. In order to estimate the baseline vectors, an RLS method is designed and developed by combining both code and carrier measurements. By taking advantage of the structure of the problem, the computational cost of the algorithm is reduced while preserving the accuracy. The configuration information such as the baseline length, is used as a boundary of the solution and the ambiguities are fixed with the LAMBDA method. The fourth module is the attitude determination module. In this module, the SVD method is developed which is an estimator for Wahba's loss function. A theoretical investigation is also made in order to incorporate measurements of the GLONASS, in the future, into the designed system.

Also, in accordance with and to fulfill the main objective of this research, the following research methodology is applied. A complete attitude determination system is designed and developed in Matlab. The inputs are the GPS L1 raw measurements namely code and carrier phase measurements and the output is the 3-D attitude angles. Then, the designed system is validated and tested using simulation data in Matlab and the GPS Spirent simulator. In order

to acquire the sufficient raw measurements, a platform is built and installed on ETS's roof. Four u-blox LEA 6 T receivers, four ANN-MS antennas and two G5Ant antennas are mounted on the platform. Two real data sets from the designed platform is used to analyse the ADS algorithm.

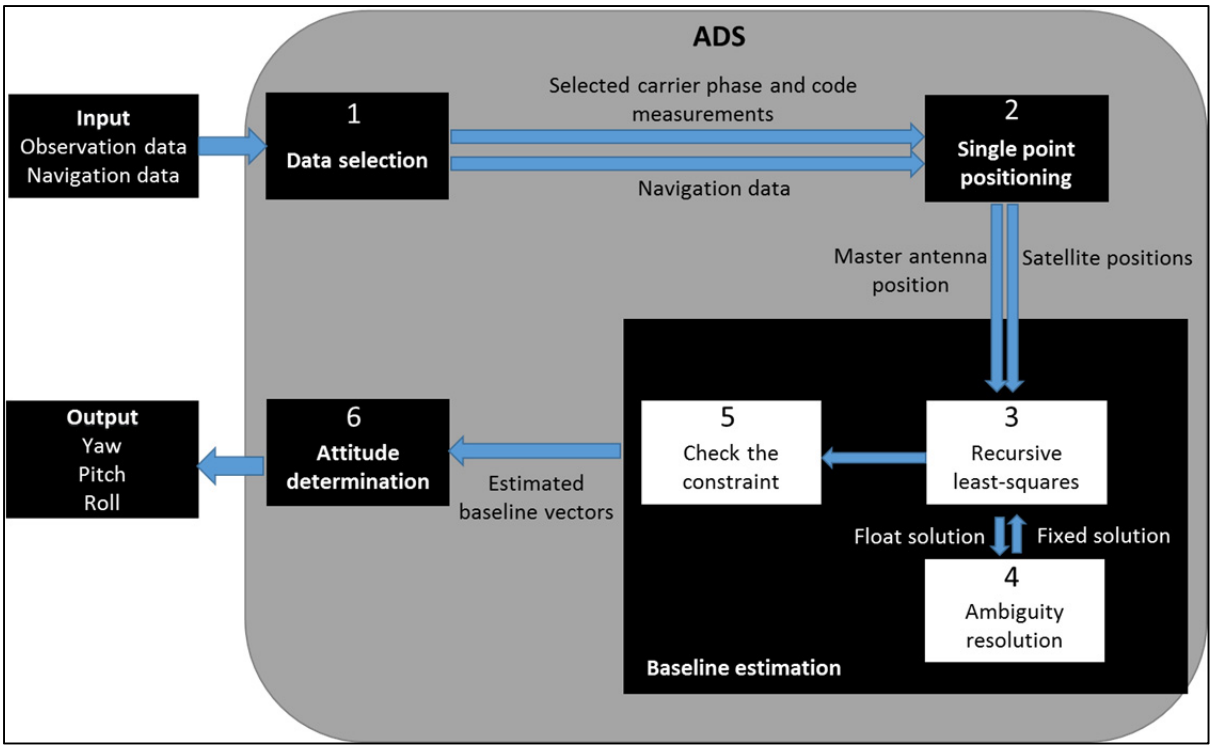

Figure 6.1 Global ADS flowchart

The objectives of this work are achieved as follows. First the ambiguity numbers are fixed by using the LAMBDA method. This method is known in literature as an efficient method with high success rate. Second, our receivers (U-Blox LEA-6T) do not allow us to synchronize the clock receiver by hardware however, an algorithm is been designed to synchronize the raw measurements within ms accuracy. In order to fulfill our third objective, the computational time of each module is been considered to choose a suitable method. Finally an investigation is done in how to overcome the difference between the GPS and the GLONASS measurements in order to incorporate these two measurements into one system.

It is shown that by synchronizing clock receivers together, a major improvement in the solution can be achieved (test case 1 and 2). In the first test case, it is shown that even though the baseline length is about 0.1 of the second test case, the achieved accuracy for the heading (yaw) angle is 6 times better and for the elevation (pitch) angle is 7.5 times more accurate than the second test case. As, in both, the second test case and the third one, receivers are not synchronized together, the major difference between these two test cases is the presence of the multipath error, antenna phase variation error and, the difference of the baseline length. On the other hand, from the first and the second test case, it is shown that the baseline length does not have a major impact into the solution accuracy and, from the literature, it is known that the antenna phase center variations error is in the millimeter scale. So the conclusion is that the major impact in the baseline estimation accuracy is the presence of the multipath. If the multipath is mitigated, the objective of this thesis can be met based on the results from test case 1 and 2. In the second test case, an accuracy of 0.03° and 0.06° for heading and elevation has been achieved without the presence of multipath. Synchronizing all clock receivers by hardware and avoid the multipath are the main limitations of this work. For the ambiguity resolution part, even though the LAMBDA method improved the solution accuracy in all test cases, but in the presence of the multipath error, it does not converge to the right solution.

For an overall, the main objective of this thesis is achieved for the first and second test cases and by overcoming the mentioned limitations, such a system can meet the main objective of this thesis for the test case 3 and 4 as well. Besides, the theoretical investigations of the GLONASS and the GPS integration showed that this integration can increase the solution accuracy, convergence time and the reliability of the system. So such a system can be a good alternative to the dual frequency expensive attitude determination systems.

6.2 Future works

In this section, some directions for the future work of this study are presented. Fixing the ambiguity parameters is a challenging work. This can be done by the LAMBDA method, as

it is used in this work, or any other popular methods in the literature as presented in the section 3.1. As ambiguity resolution methods generally are not comparable, the selection of the ambiguity resolution method for a specific application can be tricky. As a result trying 2 or 3 different ambiguity resolution methods can be useful to choose an appropriate method. Apart from that, the accuracy of the float solution of the ambiguities will decrease the convergence time of the ambiguity resolution method. A Kalman filter based algorithm with combined code and carrier phase measurements can be used to enhance the estimation of the float solution of the ambiguities, (Zhao et al., 2014).

The observation combination of several GNSS constellations can also be used to determine precisely the baseline vectors as well as the attitude angles. Due to the differences between signals from two different constellations, a complex algorithm needs to be designed. For example, in the GLONASS/GPS integration, the challenging problem is the difference of the signal modulation techniques. In this thesis, some techniques are presented to overcome this problem in order to integrate these measurements into one system. Apart from independent GNSS constellations e.g. GLONASS, BeiDou, Compass, Galileo, SBAS satellites (i.e WAAS, EGNOS, MSAS, and GAGAN) enable the user the additional corrections as well as code and carrier phase measurements. The additional observations can be used to improve the satellite availability, faster ambiguity resolution, higher accuracy solution and lower hardware cost, (Wanninger et Wallstab-Freitag, 2007).

Some improvements can be added in the designed ADS algorithm. In order to increase the absolute position accuracy in the SPP module, the master antenna position can be calculated by using both code and carrier phase measurements. Also, using differential techniques with carrier phase measurements and a reference GPS system can be used in the SPP module in order to achieve centimeter to millimetre precision of the position's user, (Delaporte, 2009). In the baseline estimation module, the estimated baseline vectors can be computed from each receiver separately. This means that each receiver can be taken as a master receiver and all the baselines can be computed from the master receiver. Then, these baseline vectors will be compared and the best least-squares fit between them will be chosen. After calculating the

baseline vectors, the configuration information can be used to force the estimated baseline solutions to be on a flat surface, which is our configuration in this thesis. In order to do that, a least-squares method can be applied to estimate the best flat surface within three estimated baseline vectors. In the hardware part of the designed ADS, synchronization of all four used receivers in the ADS with an external clock will prevent the clock jumps and cycle slip which are two of the most important and common problems in attitude determination systems.

One of the major error sources of the GPS positioning is the multipath error. In this thesis, it is shown that in the presence of the multipath error, the LAMBDA method converges to the wrong solution and the convergence time increases as well. In order to have an accurate and continues attitude determination system even near high-rise buildings, a multipath mitigation technique can be applied. One way to achieve this goal, is to apply a selection to the available satellites in order to choose only those with the fewest multipath error, (Meguro et al., 2009). Another multipath mitigation technique is to use the repetition model of the GPS signal path in one complete sidereal day. This model can be used to extract the multipath from the GPS observations, (Satirapod et Rizos, 2005). Using anti-multipath antennas is another approach to overcome the multipath error.

And finally combination of the Micro-Electro-Mechanical Systems (MEMS) and the GNSS system can increase the solution accuracy and the reliability of the system. These two systems have complementary quantities that can increase the robustness of the integrated navigation system. Such a system not only provide an accurate positioning solution but it covers those area with poor satellite availability as well, (Bistrovs et Kluga, 2015).

LIST OF REFERENCES

zAl-Shaery, A, S Zhang, S Lim et C Rizos. 2012. « A Comparative Study of Mathematical Modelling for GPS/GLONASS Real-Time Kinematic (RTK) ». In *ION GNSS*. Citeseer.

Axelrad, Penina, Christopher J Comp et Peter F Macdoran. 1996. « SNR-based multipath error correction for GPS differential phase ». *Aerospace and Electronic Systems, IEEE Transactions on,* vol. 32, n^{o} 2, p. 650-660.

Axelrad, Penina, et Lis M Ward. 1996. « Spacecraft attitude estimation using the Global Positioning System-Methodology and results for RADCAL ». *Journal of Guidance, Control, and Dynamics,* vol. 19, n^{o} 6, p. 1201-1209.

Beutler, G, DA Davidson, RB Langley, R Santerre, P Vanícek et DE Wells. 1984. « Some theoretical and practical aspects of geodetic positioning using carrier phase difference observations of GPS (Global Positioning System) satellites ». *Mitt. Satell.-Beobachtungsstn. Zimmerwald, Nr. 14, 4+ 79 pp.,* vol. 14.

Bistrovs, Vadims, et A Kluga. 2015. « Combined Information Processing from GPS and IMU using Kalman Filtering Algorithm ». *Elektronika ir Elektrotechnika,* vol. 93, n^{o} 5, p. 15-20.

Borre, Kai. 2003. « The GPS Easy Suite–Matlab code for the GPS newcomer ». *GPS solutions,* vol. 7, n^{o} 1, p. 47-51.

Campo-Cossio, Maria, Alberto Puras, Raul Arnau et Daniel Bolado. 2009. « Real-time attitude determination system based on GPS carrier phase measurements and aided by low-cost inertial sensors for high dynamic applications ». In *the Proceedings of the 13th IAIN world congress and exhibition, Stockholm, Sweden*. Vol. 2730.

Chang, Xiao-Wen, Christopher C Paige et Lan Yin. 2005. « Code and carrier phase based short baseline GPS positioning: computational aspects ». *GPs Solutions,* vol. 9, n^{o} 1, p. 72-83.

Chen, D, et Gérard Lachapelle. 1995. « A Comparison of the FASF and Least-Squares Search Algorithms for on-the-Fly Ambiguity Resolution ». *Navigation,* vol. 42, n^{o} 2, p. 371-390.

Chen, Dingsheng. 1993. « Fast Ambiguity Search Filter (FASF): A Nova1 Concept for GPS Ambiguity Resolution ». In *Proceedings of the 6th International Technical Meeting of the Satellite Division of The Institute of Navigation (ION GPS 1993)*. p. 781-787.

Cheng, Yang, et Malcolm D Shuster. 2013. « Improvement to the Implementation of the QUEST Algorithm ». *Journal of Guidance, Control, and Dynamics,* vol. 37, n° 1, p. 301-305.

Chui, Charles K. 2014. *An introduction to wavelets*, 1. Academic press.

Cocard, Marc, et Alain Geiger. 1992. « Systematic search for all possible widelanes ». In *Proceedings 6th Int. Geod. Symp. on Satellite Positioning. Columbus, Ohio*. p. 17-20.

Collins, J Paul. 1999. « An overview of GPS inter-frequency carrier phase combinations ». *Unpublished paper, retrieved May,* vol. 25, p. 2007.

Counselman, Charles C, et Sergei A Gourevitch. 1981. « Miniature interferometer terminals for earth surveying: ambiguity and multipath with Global Positioning System ». *Geoscience and Remote Sensing, IEEE Transactions on*, n° 4, p. 244-252.

Crassidis, John L, E Glenn Lightsey et F Landis Markley. 1999. « Efficient and optimal attitude determination using recursive global positioning system signal operations ». *Journal of Guidance, Control, and Dynamics,* vol. 22, n° 2, p. 193-201.

Crassidis, John L, et F Landis Markley. 1997. « New algorithm for attitude determination using Global Positioning System signals ». *Journal of Guidance, Control, and Dynamics,* vol. 20, n° 5, p. 891-896.

De Jonge, Paul, et CCJM Tiberius. 1996. « The LAMBDA method for integer ambiguity estimation: implementation aspects ». *Publications of the Delft Computing Centre, LGR-Series,* vol. 12, n° 12, p. 1-47.

Delaporte, Thomas. 2009. « Real-time kinematic software using robust Kalman filter and dual-frequency GPS signals for high precision positioning ». École de technologie supérieure.

Dierendonck, van AJ, Pat Fenton et Tom Ford. 1992. « Theory and performance of narrow correlator spacing in a GPS receiver ». *Navigation,* vol. 39, n° 3, p. 265-283.

Fenton, Pat, Bill Falkenberg, Tom Ford, Keith Ng et AJ Van Dierendonck. 1991. « NovAtel's GPS Receiver, the High Performance OEM Sensor of the Future ». In *Proc. of GPS*. Vol. 91, p. 49-58.

Force, U.S.Air. 2015. « Control segment ».

Frei, E, et G Beutler. 1989. « Some considerations concerning an adaptive, optimized technique to resolve the initial phase ambiguities ». In *Proceedings of the Fifth International Geodetic Symposium on Satellite Positioning*.

Garcıa, Javier G, Pedro A Roncagliolo et Carlos H Muravchik. « A Robust Filtering Scheme for Attitude/Rate Estimation with GNSS Signals ».

Ge, Linlin, Shaowei Han et Chris Rizos. 2002. « GPS multipath change detection in permanent GPS stations ». *Survey Review,* vol. 36, n° 283, p. 306-322.

Goudarzi, MA, M Cocard et R Santerre. 2015. « Noise behavior in CGPS position time series: the eastern North America case study ». *Journal of Geodetic Science,* vol. 5, n° 1.

Han, Shaowei, Liwen Dai et Chris Rizos. 1999. « A new data processing strategy for combined GPS/GLONASS carrier phase-based positioning ». In *Proc. ION GPS-99*. p. 1619-1627. Citeseer.

Hatch, Ron. 1989. « Ambiguity resolution in the fast lane ». *Proceedings ION GPS-89, Colorado Springs, CO*, p. 27-29.

Hatch, Ron. 1991. « Instantaneous ambiguity resolution ». In *Kinematic systems in geodesy, surveying, and remote sensing*. p. 299-308. Springer.

Henkel, P, et C Günther. 2013. « Attitude determination with low-cost GPS/INS ». In *Proc. of the 26-th Intern. Techn. Meeting of the Satellite Division of the Institute of Navigation (ION GNSS+), Nashville, TN, USA*. p. 2015-2023.

Hide, Chris, James Pinchin et David Park. 2001. « Development of a low cost multiple GPS antenna attitude system ». In *Proceedings of the 20th International Technical Meeting of the Satellite Division of The Institute of Navigation (ION GNSS 2007)*. p. 88-95.

Hofmann-Wellenhof, Bernhard, Herbert Lichtenegger et James Collins. 2013. *Global positioning system: theory and practice*. Springer Science & Business Media.

Jokinen, A, S Feng, C Milner, W Schuster, W Ochieng, C Hide, T Moore et C Hill. 2012. « Improving fixed-ambiguity precise point positioning (PPP) convergence time and accuracy by using GLONASS ». In *Proceedings of ION GNSS*. p. 3708-3727.

Joosten, Peter. 2001. « The LAMBDA-Method: MatlabTM Implementation ». *Matlab Toolbox and Manual, Mathematical Geodesy and Positioning, TU Delft*.

Keong, JiunHan, et Gérard Lachapelle. 1999. « Heading and Pitch Determination Using GPS/GLONASS with a Common Clock ». In *Presented at ION GPS99 Conference*. Vol. 1.

Kim, Donghyun, et Richard B Langley. 1999. « An optimized least-squares technique for improving ambiguity resolution and computational efficiency ». In *Proceedings of the*

12th International Technical Meeting of the Satellite Division of the Institute of Navigation (ION GPS'99).

Kim, Donghyun, et Richard B Langley. 2000. « A search space optimization technique for improving ambiguity resolution and computational efficiency ». *Earth, planets and space,* vol. 52, n° 10, p. 807-812.

Kozlov, Dmitry, et Michael Tkachenko. 1997. « Instant RTK cm with Low Cost GPS+ GLONASS [TM] C/A Receivers ». In *PROCEEDINGS OF ION GPS*. Vol. 10, p. 1559-1570. INSTITUTE OF NAVIGATION.

Landau, Herbert, et Hans-Jurgen Euler. 1992. « On-the-fly ambiguity resolution for precise differential positioning ». In *Proceedings of the 5th International Technical Meeting of the Satellite Division of the Institute of Navigation (ION GPS 1992)*. p. 607-613.

Leick, Alfred. 1998. « GLONASS satellite surveying ». *Journal of Surveying Engineering,* vol. 124, n° 2, p. 91-99.

Li, Y, K Zhang, C Roberts et M Murata. 2004. « On-the-fly GPS-based attitude determination using single-and double-differenced carrier phase measurements ». *GPS Solutions,* vol. 8, n° 2, p. 93-102.

Lu, Gang. 1995. *Development of a GPS multi-antenna system for attitude determination*. Citeseer.

Marais, Juliette, Marion Berbineau et Marc Heddebaut. 2005. « Land mobile GNSS availability and multipath evaluation tool ». *Vehicular Technology, IEEE Transactions on,* vol. 54, n° 5, p. 1697-1704.

Markley, F Landis. 1988. « Attitude determination using vector observations and the singular value decomposition ». *The Journal of the Astronautical Sciences,* vol. 36, n° 3, p. 245-258.

Markley, F Landis. 1993. « Attitude determination using vector observations: a fast optimal matrix algorithm ». *Journal of the Astronautical Sciences,* vol. 41, n° 2, p. 261-280.

Markley, F Landis, et Daniele Mortari. 1999. « How to estimate attitude from vector observations ». In *Proceedings of the AAS/AIAA Astrodynamics Specialist Conference*. Vol. 103, p. 1979-1996.

Meguro, Jun-ichi, Taishi Murata, Jun-ichi Takiguchi, Yoshiharu Amano et Takumi Hashizume. 2009. « GPS multipath mitigation for urban area using omnidirectional infrared camera ». *Intelligent Transportation Systems, IEEE Transactions on,* vol. 10, n° 1, p. 22-30.

Mortari, Daniele. 1997a. « ESOQ-2 single-point algorithm for fast optimal spacecraft attitude determination ». *Advances in the Astronautical Sciences,* vol. 95, p. 817-826.

Mortari, Daniele. 1997b. « ESOQ: A closed-form solution to the Wahba problem ». *Journal of the Astronautical Sciences,* vol. 45, n° 2, p. 195-204.

Nadarajah, Nandakumaran, Peter JG Teunissen et Peter J Buist. 2012. « Attitude determination of LEO satellites using an array of GNSS sensors ». In *Information Fusion (FUSION), 2012 15th International Conference on*. p. 1066-1072. IEEE.

Nadarajah, Nandakumaran, Peter JG Teunissen, Peter J Buist et Peter Steigenberger. 2012. « First results of instantaneous GPS/Galileo/COMPASS attitude determination ». In *Satellite Navigation Technologies and European Workshop on GNSS Signals and Signal Processing,(NAVITEC), 2012 6th ESA Workshop on*. p. 1-8. IEEE.

Park, Byungwoon, Sanghoon Jeon et Changdon Kee. 2011. « A closed-form method for the attitude determination using GNSS Doppler measurements ». *International Journal of Control, Automation and Systems,* vol. 9, n° 4, p. 701-708.

Park, Chansik, Ilsun Kim, Jang Gyu Lee et Gryu-In Jee. 1996. « Efficient ambiguity resolution using constraint equation ». In *Position Location and Navigation Symposium, 1996., IEEE 1996*. p. 277-284. IEEE.

Park, Chansik, et PJG Teunissen. 2003. « A new carrier phase ambiguity estimation for GNSS attitude determination systems ». In *Proceedings of international GPS/GNSS symposium, Tokyo*. Vol. 8.

Pratt, M, B Burke et P Misra. 1998. « Single-epoch integer ambiguity resolution with GPS-GLONASS L1-L2 Data ». In *PROCEEDINGS OF ION GPS*. Vol. 11, p. 389-398. INSTITUTE OF NAVIGATION.

Psiaki, Mark L. 2006. « Batch algorithm for global-positioning-system attitude determination and integer ambiguity resolution ». *Journal of guidance, control, and dynamics,* vol. 29, n° 5, p. 1070-1079.

Rapoport, Lev. 1997. « General purpose kinematic/static GPS/GLONASS postprocessing engine ». In *Proceedings of the 10th International Technical Meeting of the Satellite Division of The Institute of Navigation (ION GPS 1997)*. p. 1757-1765.

Remondi, Benjamin W. 1991. « Pseudo-kinematic GPS Results Using the Ambiguity Function Method ». *Navigation,* vol. 38, n° 1, p. 17-36.

Rossbach, Udo, Heinz Habrich et Nestor Zarraoa. 1996. « Transformation parameters between PZ-90 and WGS 84 ». In *Proceedings of the 9th International Technical*

Meeting of the Satellite Division of The Institute of Navigation (ION GPS 1996). p. 279-285.

Satirapod, Chalermchon, et Chris Rizos. 2005. « Multipath mitigation by wavelet analysis for GPS base station applications ». *Survey Review,* vol. 38, n° 295, p. 2-10.

Scaccia, Milena. 2011. *Numerical Algorithms for Attitude Determination Using GPS*.

Solution, GNSS. 2007. « GNSS solution software ». *Version 3.00. 07, Magellan Navigation Company Copy right*.

Tamazin, Mohamed Essam Hassan Roshdy. 2011. « Benefits of combined GPS/GLONASS processing for high sensitivity receivers ». In *Masters Abstracts International*. Vol. 50.

Teunissen, Peter. 2004. « GPS and integer estimation ». *Nieuw Archief Voor Wiskunde,* vol. 5, p. 48-53.

Teunissen, Peter JG. 1995. « The least-squares ambiguity decorrelation adjustment: a method for fast GPS integer ambiguity estimation ». *Journal of Geodesy,* vol. 70, n° 1-2, p. 65-82.

Teunissen, Peter JG. 1999. « An optimality property of the integer least-squares estimator ». *Journal of Geodesy,* vol. 73, n° 11, p. 587-593.

Teunissen, Peter JG, Gabriele Giorgi et Peter J Buist. 2011. « Testing of a new single-frequency GNSS carrier phase attitude determination method: land, ship and aircraft experiments ». *GPS solutions,* vol. 15, n° 1, p. 15-28.

Teunissen, PJG. 1997. « A canonical theory for short GPS baselines. Part I: The baseline precision ». *Journal of Geodesy,* vol. 71, n° 6, p. 320-336.

Vaillon, L, B Taffet, J Degeselle, L Giulicchi et A Pasetti. 2000. « Attitude determination using GPS: Multipath reduction through GPS antenna design ». In *Spacecraft Guidance, Navigation and Control Systems*. Vol. 425, p. 355.

Verhagen, Sandra. 2004. « Integer ambiguity validation: An open problem? ». *GPS solutions,* vol. 8, n° 1, p. 36-43.

Verhagen, Sandra, et Peter JG Teunissen. 2006. « New global navigation satellite system ambiguity resolution method compared to existing approaches ». *Journal of Guidance, Control, and Dynamics,* vol. 29, n° 4, p. 981-991.

Wang, Bo, Lingjuan Miao, Shunting Wang et Jun Shen. 2009a. « A constrained LAMBDA method for GPS attitude determination ». *GPS solutions,* vol. 13, n° 2, p. 97-107.

Wang, Bo, Lingjuan Miao, Shunting Wang et Jun Shen. 2009b. « An integer ambiguity resolution method for the global positioning system (GPS)-based land vehicle attitude determination ». *Measurement Science and Technology,* vol. 20, n° 7, p. 075108.

Wang, J, MP Stewart et M Tsakiri. 1998. « A discrimination test procedure for ambiguity resolution on-the-fly ». *Journal of Geodesy,* vol. 72, n° 11, p. 644-653.

Wang, J, MP Stewart et M Tsakiri. 2000. « A comparative study of the integer ambiguity validation procedures ». *Earth, planets and space,* vol. 52, n° 10, p. 813-817.

Wang, Jinling. 1998. « Mathematical models for combined GPS and GLONASS positioning ». In *Proceedings of the 11th International Technical Meeting of the Satellite Division of The Institute of Navigation (ION GPS 1998)*. p. 1333-1344.

Wang, Jinling, Chris Rizos, Mike P Stewart et Alfred Leick. 2001. « GPS and GLONASS integration: modeling and ambiguity resolution issues ». *GPS solutions,* vol. 5, n° 1, p. 55-64.

Wanninger, Lambert, et Stephan Wallstab-Freitag. 2007. « Combined processing of GPS, GLONASS, and SBAS code phase and carrier phase measurements ». In *Proceedings of ION GNSS*. p. 866-875.

Wei, Ziqing. 1986. *Positioning with NAVSTAR, the global positioning system*. Department of Geodetic Science and Surveying, The Ohio State University.

Xu, Guochang. 2007. *GPS: theory, algorithms and applications*. Springer Science & Business Media.

Yoon, SungPil, et John B Lundberg. 2002. « An integer ambiguity resolution algorithm for real-time GPS attitude determination ». *Applied Mathematics and Computation,* vol. 129, n° 1, p. 21-41.

Zanetti, Renato, Thomas Ainscough, John Christian et P Spanos. 2012. *Q Method Extended Kalman Filter*. NASA Technical Reports.

Zhao, Sihao, Xiaowei Cui, Feng Guan et Mingquan Lu. 2014. « A Kalman Filter-Based Short Baseline RTK Algorithm for Single-Frequency Combination of GPS and BDS ». *Sensors,* vol. 14, n° 8, p. 15415-15433.

Zheng, Guijin. 2010. *Methods for enhancing carrier phase GNSS positioning and attitude determination performance*.